The Effect of Vegetation Zones on Adjacent Clear Channel Flow

Peter Mark Hirschowitz

A dissertation submitted to the Faculty of Engineering and the Built Environment, University of the Witwatersrand, Johannesburg, in fulfilment of the requirements for the degree of Master of Science in Engineering

Johannesburg, 2006

Declaration

I declare that this Dissertation is my own unaided work. It is being submitted for the degree of Master of Science in Engineering in the University of the Witwatersrand, Johannesburg. It has not been submitted before for any degree or examination in any other University

day of 2007

Abstract

Methods are proposed to take account of the effect of emergent vegetation (which covers only part of the channel bed) on conveyance and depth-averaged velocity in open channels. For emergent vegetation strips parallel to the flow direction, discharge can be predicted separately for each vegetated or non-vegetated zone. The equations of Kaiser (1985) and Nuding (1991, 1994) can predict the influence of the vegetation on conveyance within the non-vegetated zone via the composite roughness formula of Pavlovski (1931). In order to predict the lateral distribution of depth-averaged velocity within the non-vegetated zone, the equations of Nuding (1991, 1994) have been modified to take account of the relation between non-vegetated zone width, apparent shear stress on the vegetation interface and the maximum velocity which will occur. For more complex geometries, two-dimensional numerical hydraulic models using existing software and existing relations for the prediction of eddy viscosity are recommended.

Acknowledgements

This project was funded by both the National Research Foundation and the Water Research Commission (as part of Water Research Commission Project K5/1508). I am indebted to my supervisor Prof. C.S. James and my colleague Mrs A.A. Jordanova for ongoing advice and assistance. My thanks also go to Mrs W. Midgley for administrative support. I would also like to thank the laboratory staff of the School of Civil and Environmental Engineering for their assistance in setting up laboratory experiments.

CONTENTS

Page

LIST OF FIGURES

Figure **Page**

LIST OF TABLES

LIST OF SYMBOLS AND ABBREVIATIONS

Flowrates

Discharge: .... Q
Non-vegetated zone discharge: .... Qc
Vegetation zone discharge: .... Q_v

General

Constant of Mertens (1989): c
Constant of Pasche (2004): .... C_P
Constant power of bed friction factor: .... z
Cross-sectional flow area: .... A
Constant numerical solution parameter: .... m
Density: .... ρ
Drag coefficient: .... C_D
Energy slope: .... S
Flow depth: .... D
Gravitational acceleration: .... g
Half inside and half outside: .... H
Hydraulic radius of the non-vegetated zone: .... R_{nv}
Hydraulic radius of the vegetated zone: .... R_V
Hydraulic radius: .... R
Inside: I
Interface height, or the flow depth at the vegetation interface: .... h_t
Length l
Longitudinal distance: x
Nuding's (1991, 1994) empirical constant: .... K
Parameter defined in terms of Equation (110) .... a
Porous medium permeability .... K_d
Substrate Transmissivity: .... T
Total head: .... H
Vegetation parameters of Pasche and Rouvé (1985): .... Ω, c_t
Weight of water per unit volume: .... γ
Wetted perimeter .... P

Hydraulic Resistance

Composite Manning's resistance coefficient for the non-vegetated zone: .... n_{comp}

Darcy-Weisbach friction factor .... λ
Darcy-Weisbach friction factor for the channel bed: .... λ_b
Composite friction factor for the non-vegetated zone: .... λ_{comp}
Apparent friction factor of the vegetation interface: .... λ_v
Friction factor due to the vegetation structure: .... λ_{T0}
Friction factor due to the interaction: .... λ_I
Equivalent sand grain roughness for the interface: .... k_t

Roughness component due to the vegetation itself:......................$k_{Veg\ Arrangement}$
Equivalent sand grain roughness of a fully vegetated channel:............ $k_{Veg\ Zone}$
Chézy resistance coefficient: C
Equivalent Sand Grain Roughness: ....k_s
Manning's Resistance coefficient:... n
Manning's resistance coefficient for the bed:..n_b
Manning's resistance coefficient for the vegetation interface:.......................n_v
Resistance parameter of James et al. (2001):..F

Lateral distances

Contributing width:..bm
Lateral distance from the vegetation interface:... Y
Lateral distance over which 50% of the velocity change occurs:... $D_{50\%}$
Lateral distance over which 90% of the velocity change occurs:... $D_{90\%}$
Lateral distance step:...Δy
Lateral distance:.. y
Non-vegetated half width plus contributing width: ....bf
Non-vegetated zone (half) width: ....bfo
Transition width for 62% of velocity change within non-vegetated zone:.. Bm
Transition width for 62% of velocity change within the vegetation zone:....Bs
Transition width within a narrow non-vegetated zone: ....TW Narrow
Transition width within a wide non-vegetated zone:......................... TW Wide
Transition width within the non-vegetated zone:...TW
Vegetation zone (half) width: .... Bv

Shear force, shear stress and shear velocity

Apparent shear stress on the vegetation interface:... τ_v
Apparent shear velocity on the vegetation interface:...................................u_v*
Bed shear stress:...τ_b
Shear force applied at the bed:.. F_b
Shear force applied at the vegetation interface:.. F_v
Shear force applied at the sidewall: ....F_w
Shear Stress:.. τ
Shear stress due to vegetation...τ_{v0}
Sidewall average shear stress:.. τ_w

Turbulence and eddy viscosity

Eddy Viscosity Parameters used by River2D hydraulic modelling software:ε_1, ε_2 and ε_3
Horizontal large scale: .... HLS
Mixing coefficient:..f
Mixing Length: l
Stem wake length:.. a_{nl}
Stem wake width:..a_{nb}
Sub-depth scale:...SDS

Transverse eddy viscosity divided by rate of change of velocity with lateral distance: .... ε_3
Transverse eddy viscosity: .... ε_t

Vegetation geometry (see also lateral distances)

Longitudinal (half) spacing: .... ax
Transverse (half) spacing: .... ay
Vegetation diameter: .... dp

Velocities

Depth averaged velocity magnitude: .... Velocity, V, V(y)
Dimensionless maximum velocity: .... $V_{DL\ max}$
Dimensionless velocity magnitude: .... V_{DL}
Local depth average velocity in the longitudinal direction: vx
Local depth average velocity in the transverse direction: .... vy
Maximum velocity: .... V_{max}
Square root of the ratio of velocity in a fully vegetated channel to velocity with bed resistance only: .... J
Total velocity defect: .... u_{total}
Velocity defect: .... u
Velocity magnitude at the vegetation interface: .... V_{int}
Velocity predicted by the equation of Nuding (1991, 1994): .... V_{nb}
Velocity predicted in a fully vegetated channel: .... $V_{VegZone}$
Velocity with bed resistance only: .... V_{inf}

PART 1: Introduction and Background

1 Introduction

Vegetation has a greater hydraulic effect than any other biotic component of a river ecosystem. Prediction of the effect of vegetation is therefore essential for meaningful hydraulic predictions. Vegetation strips parallel to the flow direction commonly occur in rivers. Vegetation which grows in this way may include trees, bushes, grasses and reeds, and may form either vegetated bank strips or long, thin islands of vegetation. In this situation, it is the characteristics of the individual zones with and without vegetation, as well as the lateral interaction between them that determine velocities and water levels. While existing methods for predicting the average velocity magnitude and hydraulic resistance within vegetation (Freeman et al. (2002), Järvelä (2004), Jordanova et al. (2006) and Kutija and Hong (1996)) appear to be acceptable, considerable uncertainty surrounds the prediction of the lateral interaction. The specific situation considered in this project is where the vegetation comprising these strips grows out of the water (which is termed emergent vegetation). The effect of these vegetation strips on velocity distribution within the river is not well understood.

In addition to longitudinal strips, vegetation also occurs in the form of irregular shapes and patches. However, even in such cases, lateral interactions are an important aspect of the flow patterns, and this will be treated as an extension of the methods used for longitudinal strips.

This project is motivated principally by the need for prediction of velocity distributions for ecological studies. The biological importance of interface zones (such as that between a vegetated strip and clear-channel zone) has been recognised. "The length of interface … may give an index of the potential for the exchange of animals and resources between habitats. In fact, the contact zone between habitat types may constitute a unique habitat type in itself … Quantifying habitat juxtaposition, extent of edges and habitat connectivity may provide habitat-based measures of ecosystem function in streams," (Bovee, 1996).

The investigation of these lateral hydraulic interactions between vegetated and non-vegetated zones, and the provision of a set of tools for the prediction of stage-discharge relations and depth-averaged lateral profiles of velocity magnitude within non-vegetated zones as a result of this lateral interaction are the objectives of this project. It is hypothesised that the magnitude of depth-averaged water velocity in the non-vegetated zones of open channels adjacent to strips of emergent vegetation can be estimated (with sufficient accuracy for the determination of ecological suitability) based on physical characteristics of the vegetation and the friction characteristics of the channel bed. Note that (as is common in ecohydraulics), throughout this report, the term velocity is used to represent velocity magnitude or speed of flow. Predictions are based on a combination of empirical relations based on laboratory data, theoretical analyses and two-dimensional numerical modelling.

The report will include a review of existing prediction methods (for stage-discharge relations in chapter 4 and for lateral velocity distributions in chapter 7.) It also includes an examination of available laboratory data (in chapter 5). New laboratory experiments were performed specifically to examine the effect of the widths of the vegetated and non vegetated zones on the velocity profiles produced, with relatively wide non-vegetated zones. Based on a comparison of existing methods with laboratory data, the velocity distribution equation of Nuding (1991, 1994) is selected as a basis for further refinement. In particular, the relations are modified to account for the effect of the width of the non-vegetated zone and limitations observed on the maximum velocity attained. Finally, the use of two-dimensional numerical hydraulic modelling software River2D (Steffler and Blackburn, 2002) for predictions with more complex geometries is examined.

2 Ecological Importance of Velocity

2.1 River Hydraulics and Ecology

Ultimately, the aim of river hydraulics is to be able to predict the interaction between river flow and the broader ecosystem (including human social and economic systems) of which it is a part. Predictions may include water levels and water quality, morphological changes and changes in the river life, such as the species composition, health and population sizes of organisms which will be present.

Such predictions can be used for various purposes, including:

- The determination of a river's in-stream flow requirements, in order to attain a specified future state, with a defined risk of deterioration from the desired state.

- The design of man-made changes to the river, including

    - structures
    - rehabilitation works
    - creation of river or wetland areas to be used for purposes such as water purification
    - changes in the use of the river channel or floodplain

    The present and future effects of any design choice must be taken into account.

- The evaluation of the ecological integrity and importance of specific reaches or features of a river in terms of the potential broader effects of ecological changes.

- The evaluation of the effects of broader changes which may affect the river, for example catchment land use changes or climate change.

2.2 Velocity for Ecological Studies

In order to determine the knowledge which we need of velocities, we need to understand how velocity affects various ecosystem components. Velocity itself is an important attribute for many species. This report therefore first considers requirements in terms of velocity itself. Estimates of velocity are also required for prediction of other physical variables, including substrate type and sediment concentration (through sediment transport analyses), presence and types of debris, concentrations of chemicals, pollutants and sediment (through diffusion-dispersion analyses), water temperature and depth.

There have been a great number of studies considering the velocity requirements of various organisms, particularly macro-invertebrates and fish. A compilation of these requirements would form a useful study in itself. This section presents an example of a simplified assessment of the effect of velocity prediction errors on the usable area within defined velocity ranges.

The case used is a cross-section of the Okavango River, named site D by McCarthy (1992). This site provides a good example of the effect of longitudinal zones of bank vegetation. At the time of measurement, the water surface width was 26m and the flow depth was 3.8m. McCarthy (pers. comm.) measured the velocity profiles away from one bank. To his results, the curves representing a 10% over-estimation and a 10% under-estimation of velocity have been added. The resulting plot is shown in Figure 2-1. Next, using only the preferred velocity ranges given by various authors, the usable width within each range was determined from the velocity profile. This was done both for the measured profile and for the assumed error profile. The results are indicated in Table 2-1. They indicate that an error of only 10% in velocity estimation may cause an error in usable area of up to almost 200%, depending on the specific range of velocities considered suitable. Thus, even though most organisms can tolerate a relatively wide range of velocities, a small change in velocity can completely alter the estimation of usable area. This gives a clear indication that accurate determination of velocity profiles is important for meaningful estimation of habitat availability. However, these results perhaps over-emphasise the importance of precision, since it is clear from the publications listed in Table 2-1 that suitability is not defined in terms of definite ranges with sharp boundaries. Rather, there is considerable tolerance of a range of velocities, and gradual changes in suitability measures with changing velocity. However, reasonable accuracy in the prediction of velocity remains important.

Table 2-1: Effect of Velocity Prediction Errors on Habitat Availability

Velocity Range	For	Source	Suitable Width per bank(m) at McCarthy (1992) Site D				
(m/s)			Measured Velocity	Velocity Over-estimated by 10%	Error in suitable width (%)	Velocity Under-estimated by 10%	Error in suitable width (%)
<0.9	Hippopotami	Gore et al. (1992)	13	6.5	-50	13	0
0.3-0.7	In-stream Vegetation Species Richness	Nilsson (1987)	2.4	1.6	-33	3	25
0.2-0.3	In-stream Vegetation Cover	Nilsson (1987)	0.3	0.3	0	0.5	67
0.75-1.25	Invertebrate Diversity	Gore (1978)	7.7	8.6	12	1	-87
0.4-1.0	Ophiogomphus morrisoni	Gore (1978)	10.2	10.2	0	9.8	-4
<0.3	Rhagovelia sp.	Gore (1978)	2.4	2.4	0	2.7	13
0.6-1.2	Physa gyrina	Gore (1978)	9.2	9.35	2	8.6	-7
0.5-1.4	Rhithrogena hageni	Gore (1978)	9.7	9.7	0	9.3	-4
<0.9	Taxa of Invertebrates used as water quality indicators	Gore et al. (2001)	13	7	-46	13	0
0.1-0.6	Macro-invertebrate Diversity in streams of slope less than 0.005	Gore et al. (2001)	2.2	2.1	-5	2.8	27
0.4-0.8	One fish species	Lamouroux et al. (1999)	3.3	2	-39	9.8	197
>0.8	Two fish species	Lamouroux et al. (1999)	6.8	8.2	21	0	-100
0.1-0.9	Rock Catfish (Older)	Niehaus et al. e (1997).	11.4	11.4	0	11.4	0
0-0.2	Clanwilliam Yellowfish Larvae	Cambray, J.. Et al. (1998)	2.1	2.1	0	2.2	5
>0.7	Periphyton Maximum Growth Rate	Biggs (1996)	8.4	9	7	7.2	-14
0.2-0.3	Periphyton Permanent Mass	Biggs (1996)	0.3	0.3	0	0.5	67
<0.3	General categorisation for use in fish studies	Kleynhans (1999)	2.4	2.4	0	2.7	13
>0.3	General categorisation for use in fish studies	Kleynhans (1999)	10.6	10.6	0	10.3	-3
Absolute Maximum Error (%)					50		197

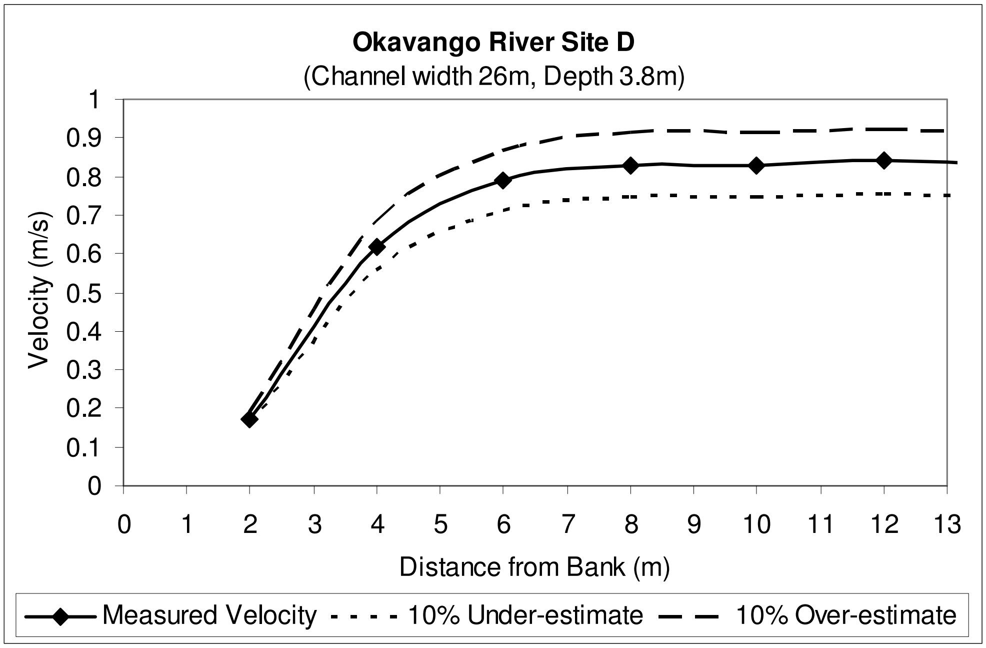

Figure 2-1: Example of Lateral Velocity Distribution (measured by McCarthy, pers. comm.) with 10% Error lines added

3 Flow Patterns and Turbulence Effects

3.1 Introduction

Studies of the interaction between non-vegetated and vegetated zones have recognised that flow velocities are slower in the vegetated zone than in the non-vegetated zone, and that momentum and energy transfer between these zones across the interface, dominates the flow. (This effect is described by Choi and Kang (2006), Rimkus and Vaikasas (2001), Sand-Jensen and Pedersen (1999), Thornton et al. (2000) and Tsujimoto and Shimizu (1994).) The effect can be considered at three levels of detail: patterns of turbulence, velocity distributions and conveyance information. Hydraulically, these three descriptions are mutually interdependent. Turbulence creates the momentum transfer which determines velocity profiles; however, it is the differences in velocity which create the turbulence patterns in the first place. Conveyance is a measure of flow energy dissipated. Energy is dissipated through turbulence associated with velocity differences. Hydraulic resistance relates conveyance to the depth and cross-section average velocity within which patterns of velocity distribution and turbulence occur. As explained previously, velocity and depth are the hydraulic parameters most commonly used to relate hydraulics to biological requirements. Turbulence will therefore only be considered in a descriptive way, in order to understand and better predict velocity profiles. Patterns and existing models of the turbulence produced in this situation will therefore be described briefly. As velocity is probably the most important parameter, the prediction of lateral velocity profiles is the main focus of this study. Resistance can be estimated using some formula for combining the resistance co-efficients of different zones, or directly from velocity profiles, and both of these possible methods will be considered.

3.2 Turbulent Structure

Nadaoka and Yagi (1998) provide a clear description of the turbulence associated with the velocity differences between longitudinal zones with and without vegetation. They suggest that the turbulence in a partially vegetated channel has two distinct components: "3D turbulence having length scales less than the water depth [which they term SDS turbulence] and horizontal two-dimensional (2D) eddies with much larger length scales [which they term HLS turbulence]." Nezu and Onitsuka (2001) emphasise the importance of the interaction between these turbulent structures: "The structure of partly vegetated open channel flows is complicated … because there is a close interaction between the cross-sectional characteristics such as secondary currents and horizontal characteristics such as free-surface coherent vortices."

Nadaoka and Yagi (1998) also describe the sources and energy losses for both types of turbulence. HLS turbulence is generated by the transverse velocity profile of the vegetation, and is attenuated mainly by vegetation drag and bottom friction. SDS turbulence is generated both from the breakdown of larger HLS eddies, and from wave-breaking and wind energy.

The measured length and time period of the HLS eddies can be seen to scale approximately with other dimensions. In the experimental study of Nadaoka and Yagi (1998), for a depth of 0.044m in a 0.4m wide flume, the horizontal eddies had a period of 3.8s and a length of approximately 0.2m. For a depth of 0.060m in a 0.96m wide flume, the horizontal eddies had a period of 6.4s and a length of approximately 2m. The turbulent energy spectrum presented by Pasche and Rouvé (1985), with a maximum depth of 0.255m in a 1m wide flume has a major peak with a period of approximately 10s and a much smaller peak with a period of approximately 5.9s.

3.3 Models

Following their description of the turbulence structure discussed above, Nadaoka and Yagi (1998) propose a model in which sub-depth scale (SDS) and horizontal large scale (HLS) turbulence are treated separately. The total turbulent kinetic energy is divided between these two types. The smaller-scale SDS turbulence is modelled in three dimensions. "It is assumed that all of the energy dissipated by both bottom friction and vegetation drag is converted to SDS turbulent kinetic energy." HLS turbulence is modelled in two dimensions by a depth integrated formulation. The formation of the HLS eddies is explained in terms of the vorticity fluctuations shown by the model. The combined model, called the SDS-2DH model, "can directly describe the effects of flow geometry, such as vegetation layer width, on large-scale eddy development." It also correctly predicts the velocity and turbulence profiles measured in two sets of experiments in laboratory flumes.

Attempts have been also been made to use conventional turbulence models to model the turbulence produced by vegetation strips. Both Tsujimoto et al. (1991, as referred to by Tsujimoto, undated) and Naot et al. (1996) proposed the use of a k-ε turbulence model to model the turbulence. However, they note that "the effect of form drag [of the vegetation] is taken into account not only in the momentum equation … but also in the k- and ε- equations." Because of this, their model contains two additional numerical constants. Their model thus seems to require more data than conventional models for calibration.

De Lemos and da Silva (2002) show that it is possible to model the turbulence structure while maintaining a simple formulation of the vegetation layer and the interface. They consider the vegetation as a porous layer, through which flow is defined in terms of porosity and Darcy permeability. The difficulty with this approach is that any change in the physical vegetation structure affects both of these parameters, and the effect must be calculated from a known relation. Thus, when the influence of porosity on velocity distribution is modelled, this cannot be directly related to vegetation density, since vegetation density also has a large effect on permeability. Nonetheless, their approach could be a useful simplification when coupled with analysis of flow through the vegetated region, from which permeability can be calculated.

Their results suggest that vegetation characteristics (porosity and permeability) affect the velocity in the clear channel in the region where this velocity becomes independent of distance from vegetation. This is in agreement with the experimental results for narrow channels presented by James et al. (2001), which could not previously be explained theoretically. Their analysis is based on computational modelling, for which considerable resources and exact geometries are required. A more general analysis, which will enable calculation of depth averaged velocities and river stage with more limited data, is therefore required.

3.4 Similarity of Flow Patterns with Vegetation Strips to those observed in Compound Channels

Flow in channels with lateral zones with and without vegetation has often been compared to compound channel flows, and similar methods of analysis suggested for both. "Turbulent structures in partly vegetated open-channel flows may be somewhat similar to those in two-stage compound channel flows," Nezu and Onitsuka (2001). Comments on compound channels provide a striking echo of the description of flow in partially vegetated channels by Nadaoka and Yagi (1998) given above: "Transverse shear flow may become unstable in a wide and shallow open channel, leading to large-scale transverse turbulent motions with a horizontal length scale significantly greater than the water depth. … Small-scale turbulence motion is generated by the bed friction forces" Chu et al. (1991).

Indeed, since both vegetation strips and compound channels frequently occur together (in the case of bank or floodplain vegetation, as illustrated in Figure 3-1.), and since both produce similar flow patterns, it is frequently impossible to distinguish between these two effects. Laboratory experiments such as those of

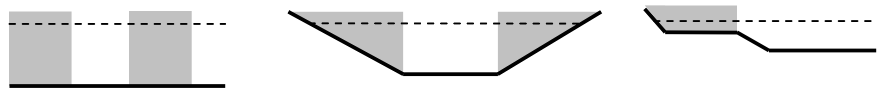

Idealised In-channel Vegetation

Idealised Bank Vegetation Layout

Idealised Floodplain Vegetation Layout

All diagrams are river cross-sections.
Grey areas represent vegetation.
Dashed line represents the water surface.

Figure 3-1: Idealised cross-sections with in-channel, bank and floodplain vegetation

Table 3-1: Applicability of various methods to simple and compound channels

Method	**Developed for**	**Applicability according to Helmiö (2004)**	
		to simple channels	**to compound channels**
Bertram (1985) in Nuding (1991)	Vegetated banks	Forms the basis of the Method of Mertens (1989) in Nuding (1991), which is not applicable. Therefore probably also not applicable.	Possibly
Mertens (1989) in Nuding (1991)	Vegetated banks	Not applicable (Helmiö, 2004)	Over-estimated friction factor (Stephan, 1993 in Helmiö, 2004)
Nuding (1991, 1994)	Vegetated banks and in-channel vegetation	Applicable (Helmiö, 2004)	Relatively accurate (Stephan, 1993 in Helmiö, 2004)
Pasche and Rouvé, (1985)	Vegetated floodplains	Not applicable (Helmiö, 2004)	Relatively accurate (Stephan, 1993 in Helmiö, 2004)
Ikeda et al. (1991, 1994) and Tsujimoto and Kitamura, (1994)	In-channel vegetation	Applicable (Developed for this)	Unlikely to be applicable
Kaiser (1984) in Nuding (1991)	In-channel vegetation	Developed for this situation	Unlikely to be applicable

Harris et al. (2003), Mertens (1989) as described by Helmiö (2002) or Pasche and Rouvé (1985) frequently combine these effects by placing vegetation along raised areas at the side of the channel. Similar floodplain vegetation is present in field studies such as those of the River Severn by Darby and Thorne (1996) and of the Rhine by Helmiö (2004).

Some of the methods to be discussed in this project were therefore developed to analyse each situation (vegetated banks, vegetated floodplains and in-channel vegetation) as listed in Table 3-1. Helmiö (2004) assessed the applicability of various methods to various channel types (using the findings of Stephan (1993) for assessing applicability to compound channels.) Her suggestions, together with some of my own comments on this issue are also included in Table 3-1. Methods such as that of Nuding (1991, 1994) which are applicable to both compound and simple channels are more flexible than those which consider the effect of in-channel vegetation only. They can be applied directly to the situation where there is vegetation on the bed itself, by substituting appropriate values for interface depth and hydraulic radius within the vegetation.

Note, however, that since this report focuses on the vegetation effect, all laboratory experiments analysed here have a constant bed elevation across the section, so that compound channel effects do not apply, and the vegetation effect can be isolated.

3.5 Implications for the Prediction of Velocity Profiles

While the prediction of turbulence is not an aim of this study, from the models discussed above, two important pointers emerge for the prediction of velocity and resistance. The first follows from the description of Nadaoka and Yagi (1998). Transfer of momentum occurs through large horizontal eddies, which may cover most of the transition zone. Rooseboom (1992) showed that for a circular eddy, Prandtl's shear stress formula:

$$\tau = \rho \cdot l^2 (\partial V/\partial y)^2 \quad (1)$$

applies. Comparing this with the definition of eddy viscosity:

$$\tau = \rho \cdot \varepsilon_T (\partial V/\partial y) \quad (2)$$

It is clear that the transverse eddy viscosity (ε_T) is proportional to the rate of lateral change in velocity $(\partial V/\partial y)$. This will assist in the selection of velocity distribution functions, depending on the eddy viscosity formulation on which they are based. The second pointer is the applicability of the simplification of de Lemos and da Silva (2002). Both velocity distribution and resistance can be modelled simply in terms of a single characteristic average velocity or resistance within each zone. This approach will be used both for equations describing the lateral velocity profiles, and for two-dimensional hydraulic models.

Since prediction of velocity profiles is the major focus of this investigation, consideration of selected methods for velocity prediction form the major focus of this report. These methods will be described in chapters 7 and 8, compared to laboratory data presented in Chapters 5and 6 and used in two-dimensional hydraulic models as described in Chapter 11.

Each of the velocity profiles which have been proposed assume that the individual effect of each zone (vegetated or non-vegetated) is known when the other zone is not present. In other words, a channel with no vegetation, and a certain depth and slope is assumed to exhibit a known downstream flow velocity V_{inf}, corresponding to resistance λ_b. Similarly, a fully vegetated channel is assumed, at the same depth and slope, to exhibit a known average downstream flow velocity $V_{VegZone}$, corresponding to a vegetation resistance which may be expressed in terms of various parameters.

Velocity profiles are derived by assuming certain relationships for the turbulent transfer of momentum between these two zones of known characteristics.

Part II: Conveyance in a Channel with Longitudinal Vegetation Strips

4 Conveyance Estimation Methods

Channel conveyance defines the relationship between discharge and the dissipation of flow energy (or friction slope) according to the relation:

$$Q = Conveyance \cdot \sqrt{S} \qquad (3)$$

Where: Q is the discharge and S is the energy slope (or flow energy dissipated per unit length).

Hydraulic resistance equations relate conveyance to flow geometry (as determined by bed and water surface elevations) through resistance coefficients. For example, the Darcy-Weisbach resistance equation can be formulated as:

$$Conveyance = \cdot\sqrt{8 \cdot g}\, A^{3/2} \cdot P^{-1/2} \cdot \lambda^{-1/2} \qquad (4)$$

Where: A is the cross-sectional flow area.

P is the wetted perimeter.

λ is the Darcy-Weisbach friction factor.

Thus, if bed geometry, water surface elevation and discharge are known at a certain position, a resistance equation is used to predict the corresponding energy dissipation occurring between this position and another defined position. This estimate of energy dissipation is then used to predict water surface elevation or depth at the second position.

This chapter will consider methods for estimating the conveyance of channels with longitudinal strips of emergent vegetation.

4.1 Sub-division

‘

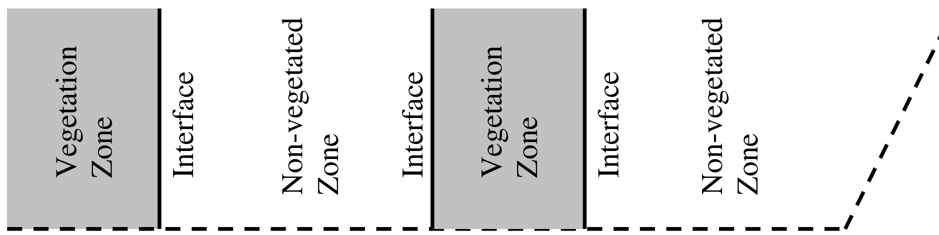

Figure 4-1: Schematic Cross-section Representation of Vegetation and Non-vegetated Zones

Overall channel conveyance may be considered by dividing the channel laterally into separate zones, and estimating the discharge for each individually. Conventional composite roughness formulae divide the channel into areas of different resistance, separated by planes of zero shear. This is the approach suggested by Masterman and Thorne (1994) for partially vegetated channels. However, this ignores the physical vertical boundary between vegetated and non-vegetated zones, at which an abrupt change in shear stress occurs, indicted as the interface in Figure 4-1. Most authors have therefore preferred to divide the channel at the physical location of the vegetation interface. Each zone conveys a certain discharge, which must be predicted depending on the flow depth and slope, the zone characteristics, and the interaction with adjacent zones. Individual discharges are summed to obtain a total discharge. This can be specified where desired in terms of a resistance parameter, which can be calculated using a resistance equation as a function of slope, depth and discharge.

4.2 Vegetated Zones

“The flow contribution of the vegetated zones … is usually small,” (James and Makoa, in press), so the relative accuracy of its magnitude is less important. It has therefore been suggested that vegetated zone discharge may be estimated by simply assuming the un-affected velocity $V_{VegZone}$ throughout this region, and neglecting the interaction. This simplification is suggested by Nuding (1991, 1994) and James et al. (2001) and James and Makoa (in press).

Where a lateral velocity profile has been derived within the vegetation zone, this can be integrated across the width of the zone to give the zonal discharge. One such equation is that of Ikeda et al. (1991, 1994) and Tsujimoto & Kitamura (1994), which will be presented in section 7.4. This velocity distribution equation will be integrated in Appendix D to give equation (39) on page 67 for the vegetation zone discharge. This procedure is considerably more complex than that assuming a constant velocity, and is only as accurate as the velocity distribution equation used. The simpler assumption of a constant velocity is therefore preferred.

4.3 Non-vegetated Zones

Momentum transfer between adjacent zones can have a major effect on the resistance of non-vegetated zones. As for vegetated zones, the total discharge within a non-vegetated zone can be derived by integration of the velocity distribution. These integrations will be presented in section 4.5.

The alternative is to apply one of the methods which have been developed for summing the resistances of different portions of the wetted perimeter of a composite channel. In this case, the vegetation interface (represented by solid lines in Figure 4-1) and bed (represented by dashed lines in Figure 4-1) must be considered as separate portions of the non-vegetated zone boundary, each having its own specified resistance co-efficient. To apply this, in addition to a specified bed resistance, a composite roughness formula must be selected, and an effective resistance must be specified for the interface between the vegetated and non-vegetated zones. This will be considered in Section 4.4.

Regarding formula selection, James and Makoa (in press) tested various composite roughness formulae, and recommended either the composite roughness formula of Horton (1933), or that of Pavlovski (1931). Nuding (1994) also suggests that either of these formulae may be used, but the application formula adopted by Nuding (1994) was that of Pavlovski (1931). Selection must also depend on the assumptions used. "Horton … assumed that velocities in [all areas] are … equal," (James and Makoa, in press). This is clearly not the case, since the main factor causing the resistance is the interaction of zones of different velocity. The formula of Horton is therefore not recommended. "Pavlovski … assumed that the total boundary shear force for the whole cross-section is the sum of the … shear forces [for each area] calculated separately," (James and Makoa, in press). Although simplifying the effect of the interaction between zones, this assumption would appear to be a somewhat more realistic approximation, and the method of Pavlovski (1931) is therefore suggested. (Note that vegetation drag forces do not occur within the non-vegetated zone, but are reflected in the apparent interface shear.)

In terms of Manning's resistance coefficient, the method of Pavlovski (1931) is expressed by:

$$n_{comp} = \left[\left(n_v^2 \cdot h_T + n_b^2 \cdot bfo\right) / \left(h_T + bfo\right)\right]^{1/2} \tag{5}$$

Where: n_v is the equivalent Manning's resistance coefficient for the vegetation interface

h_T is the interface height, or the flow depth at the interface.

n_b is the Manning's resistance coefficient for the bed

bfo is the non-vegetated zone (half) width as defined in Figure 4-2 on page 33.

n_{comp} is the total composite Manning's resistance coefficient for the non-vegetated zone.

This may be formulated in terms of the Darcy-Weisbach friction factor (λ) through the relationship between Manning's n and Darcy-Weisbach (λ):

$$\lambda = 8 \cdot g \cdot n^2 / R^{1/3} \tag{6}$$

Where: R is the hydraulic radius.

Noting that λ and n^2 are proportional to each other, λ may replace n^2 in Equation (5), leading to:

$$\lambda_{Comp} = (\lambda_v \cdot h_T + \lambda_b \cdot bfo)/(h_T + bfo) \quad (7)$$

Where: λ_{comp} is the total composite friction factor for the non-vegetated zone.

λ_v is the apparent friction factor of the vegetation interface.

λ_b is the Darcy-Weisbach friction factor for the bed

This composite roughness can be used to relate discharge to energy slope, and to water surface elevation (through hydraulic radius and cross-sectional area). This is done using a hydraulic resistance equation such as the Darcy-Weisbach equation:

$$Q = A\sqrt{8gRS/\lambda_{comp}} \quad (8)$$

Where: Q is the discharge

A is the cross-sectional flow area

R is the hydraulic radius

S is the energy slope

λ_{comp} is the composite roughness

The only remaining requirement is an estimate of the apparent friction factor (λ_v) for the vegetation interface.

4.4 Estimation of a friction factor for the vegetation interface

The interface friction factor clearly depends on the characteristics of the two zones, and some relation is needed for its specification. Nuding (1991) presents four previous methods for the estimation of this resistance co-efficient. Comparison with laboratory data indicates that in these methods, zone widths and vegetation spacing should be taken as indicated in Figure 4-2 and Figure 4-3 respectively. Nuding (1991) also presents objections to each of these methods, and proposes his own method. To the best of my knowledge, two of these relations have not previously been presented in English, and the third is presented in a manner that is difficult to follow. I will therefore present the full set of equations for each of these methods.

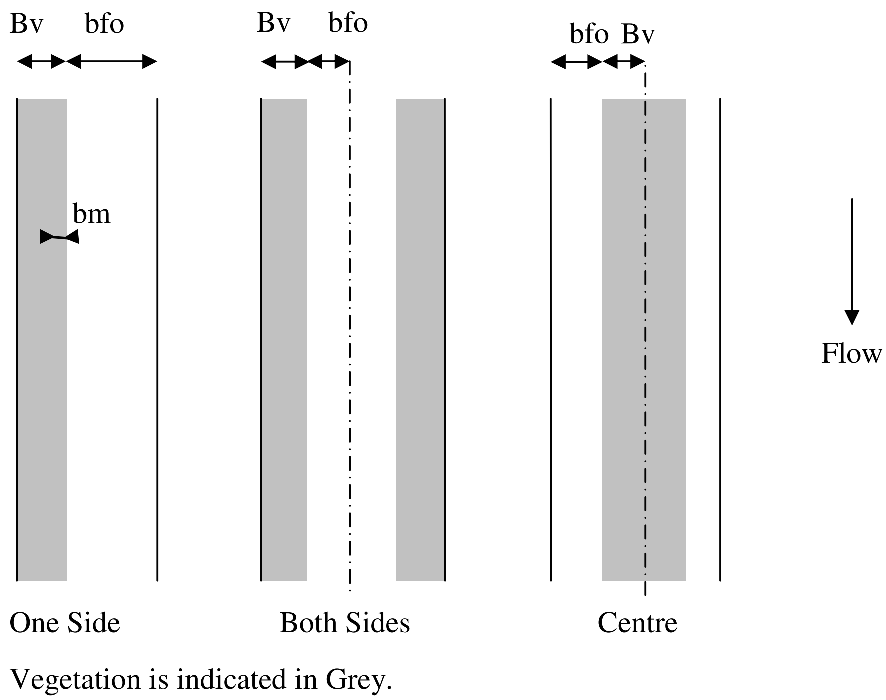

Figure 4-2: Vegetation Locations and Width Definitions

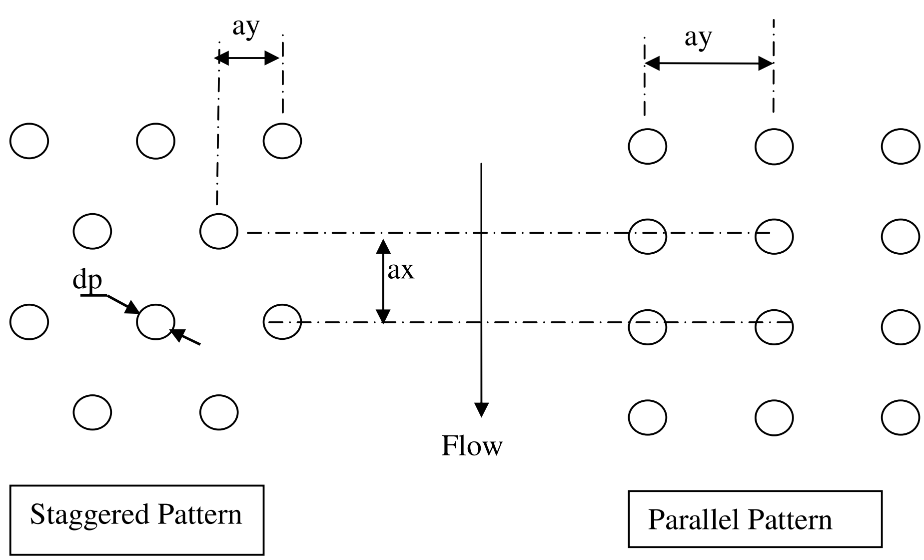

Figure 4-3: Vegetation Patterns and Spacing

4.4.1 Method of Pasche and Rouvé (1985)

This is the first method presented by Nuding (1991), and is also presented by Pasche and Rouvé (1985) and Pasche et al. (2004). This method suggests the following equations for the interface friction factor λ_v (with some symbols changed to my own): Two slightly different versions are presented by different authors. The formulation presented by Nuding (1994) will be used in further analysis. This is:

$$1/\sqrt{\lambda_V} = -2.03 \cdot \log\left[0.072 \cdot \Omega \cdot \frac{bm}{bfo}\right] \tag{9}$$

$$\Omega = \left[0.071 \cdot a_{NL}/a_x\right]^{3.29} \cdot \left[a_{NB}/a_y\right]^{0.95} \tag{10}$$

$$a_{NL} = 128.87 \cdot C_D \cdot dp \Bigg/ \left[1 + 2 \cdot g \cdot a_{NL} \cdot S \big/ V_{\text{int}}^2\right]^{2.14} \tag{11}$$

$$a_{NB} = 0.24 \cdot a_{NL}^{0.59} \cdot (C_D \cdot dp)^{0.41} \tag{12}$$

$$bm = \frac{V_{VegZone}^2}{8 \cdot g \cdot S}\left(0.068 e^{0.56 \cdot c_T - 0.056}\right) \tag{13}$$

$$c_T = 2.85 - 3.27 \cdot \log \Omega \tag{14}$$

Where: λ_v is the Darcy-Weisbach friction factor for the interface.
Ω is described as a vegetation parameter.
bm is a width within the vegetation zone contributing to the transition.
bfo is the full or half-width of the non-vegetated zone as indicated in Figure 4-2.
a_{NL} is the stem wake length.
a_{NB} is the stem wake width.
a_{NL} is the stem wake length.
C_D is the drag coefficient of a single stem.
dp is the stem diameter.
g is the constant of gravitational acceleration.
S is the Energy Slope.
V_{int} is the velocity at the vegetation interface between the vegetated and non-vegetated zones.
a_x and a_y are the longitudinal and transverse stem spacings respectively. (See Figure 4-3.)

c_T is a dimensionless interface velocity (non-dimensionalised by dividing by interface shear velocity).

$V_{VegZone}$ is the velocity within a fully vegetated channel of the same vegetation.

In the version presented by Pasche et al. (2004), Equation (9) is replaced by:

$$1/\sqrt{\lambda_V} = -2 \cdot \log\left[0.07 \cdot \Omega \cdot \left(\frac{C_P \cdot bm}{bfo}\right)^{1.07}\right] \tag{15}$$

Where C_P is a constant equal to 1.7 for compact cross-sections where "the flow velocity varies significantly over the channel cross-section due to the channel shape" and equal to 1 for partitioned cross-sections where "the flow velocity [at] all points [across] a cross-section can be approximated by the mean velocity."

Note that equation (9) is implicit in a_{NL}, and must be solved iteratively. Equation (13) for bm was originally stated in terms of an equivalent friction factor, but velocity has been substituted. As noted by Nuding (1991), the velocity V_{int} at the vegetation interface is needed as an input for this method, being used in equation (11) for wake length. However, this velocity would usually be unknown. In order to apply this method, the relations of Ikeda et al. (1991, 1994) and Tsujimoto and Kitamura (1994) (which will be described in section 7.4) were used to give the following expression for the velocity at the interface (V_{int}):

$$V_{\text{int}} = \sqrt{V_{\text{inf}} \cdot V_{VegZone}} \tag{16}$$

Where V_{inf} is the velocity with bed resistance only.

Nuding (1991) also notes the unnecessary complexity of this method. He also notes that the linear proportionality between contributing width bm and interface depth suggested is not in agreement with the results of Kaiser (1984). He also notes that these equations were based only on narrow vegetation zone widths.

4.4.2 Method of Bertram (1985)

This is the second method presented by Nuding (1991).

$$\frac{1}{\sqrt{\lambda_v}} = 2.035 \cdot \log(4 \times 3.046 \cdot Interface\ Depth / k_t) \qquad (17)$$

$$k_t = 0.77 \cdot bm \cdot \sqrt[3]{V_{VegZone} / V_{\inf}} + k_{VegArrangement} \qquad (18)$$

$$k_{VegArrangement} = 1.2 - 1.5 \cdot dp \qquad (19)$$

Where: $k_{Veg\ Arrangement}$ is a roughness component due to the vegetation itself.
dp is the stem diameter as before.
k_t is the equivalent sand grain roughness for the interface.
$V_{VegZone}$ is the velocity within a fully vegetated channel, as before.
V_{inf} is the velocity produced by flow over the channel bed in the absence of vegetation.
$k_{VegZone}$ is the equivalent sand grain roughness of a fully vegetated channel.
bm is a width within the vegetation zone contributing to the transition, as before. Where the transition zone is not at a constant depth, this should be taken as a hydraulic radius rather than a width. Nuding (1991) gives no indication how Bertram calculated bm, but one of the other methods will be applied.

These equations are considerably simpler than those of Pasche and Rouvé (1985) However, the following objections raised by Nuding (1991) appear valid:

- There is no physical basis for the addition of roughness heights.
- Since this method is based on experiments with a sloping vegetated bank, the mutual influence of the embankment and the vegetation are inseparable.
- The formulation of roughness component $k_{Veg\ Arrangement}$ based on tests of a few arrangements is unsatisfactory
- The procedure depends on widespread use of relations derived from one set of experiments

4.4.3 Method of Mertens (1989)

This method is based on the method of Bertram (1985), but gives the following expression for k_t:

$$k_t = c \cdot bm + 1.5 \cdot dp \qquad (20)$$

c is an empirically determined co-efficient, depending on the vegetation itself. Values of c are not stated by Nuding (1991). Without this value, the method cannot be applied. Nuding (1991) states that this equation is purely empirical, and would not apply to sparse shrubs.

This is also the only method to explicitly consider the interaction with vegetation on both sides of a non-vegetated zone, although it may be applied with vegetation on one side only.

4.4.4 Method of Kaiser (1984)

According to Nuding (1991), Kaiser (1984) suggests the following relations:

$$\lambda_v = \lambda_{T0} + \lambda_I \qquad (21)$$

Where: λ_v is the friction factor of the interface as before

λ_{T0} is the friction factor due to the vegetation structure. Values between 0.06 and 0.10 are suggested.

λ_I is a friction factor due to the interaction. For channels where both zones with and without vegetation are wide (Non-vegetated zone width bfo > 1.5m and vegetated zone width Bv > bm), it may be calculated according to:

$$\lambda_I = 0.18 \cdot \log\left[0.0135m \cdot V_{\inf}^2 \Big/ \left(h_T \cdot V_{VegZone}^2\right)\right] \qquad (22)$$

Where: $V_{VegZone}$ is the velocity within a fully vegetated channel of the same vegetation as before

$V_{\inf}$ is the velocity expected with bed resistance only, and no vegetation.

h_T is the depth at the interface as before.

Note that the distance 0.0135 is specified in metres (m)

Where either zone width is less than the limits stated above, Kaiser (1984) suggests that this will reduce the effect of the interaction. However, Nuding (1991) does not present equations for calculating this reduction.

Nuding (1991) notes that these are only provisional equations based on experiments using only two arrangements of vegetation.

4.4.5 Method of Nuding (1991, 1994)

Having reviewed the existing methods, Nuding (1991, 1994) proceeded to develop his own relations. In addition to resistance, these relations include a velocity profile, which will be presented in section 7.3. The velocity distribution equation requires prior knowledge of the interface shear stress, which can be obtained using the method for estimation of the interface friction factor, which will be presented here.

Nuding's (1991, 1994) method for estimation of the interface friction factor requires two steps: estimation of a contributing transition width bm within the vegetation, and calculation of the friction factor.

Transition width bm:
For regularly arranged elements (presumably in rows parallel to the flow direction), he suggests the following estimate:
bm is the smallest of:

- The lateral spacing of the vegetation ay. Note that for a staggered vegetation pattern, which has frequently been used in laboratory experiments, it is not immediately obvious how the lateral spacing should be measured. Consideration of various experimental results, as discussed in section 7.5, indicates that for a staggered vegetation arrangement, ay is as indicated in Figure 4-3 on page 33.
- The wake width a_{NB}, which is calculated as $3.2\sqrt{a_x \cdot d_p}$, (23)

where a_x is the longitudinal spacing of the vegetation and d_p is the vegetation diameter.

- The actual thickness of the vegetation strip

but that bm must be a minimum of 0.15 times the flow depth at the interface between the vegetation and the clear channel.

For brushwood, Nuding suggests that the transverse vegetation spacing (ay) can only be used as bm if it is greater than 0.3 times the flow depth at the interface. He also suggests an equation for computing the wake width bm based on a combination of vertical and horizontal vegetation elements.

The **Interface Friction Factor** is calculated according to the equation:

$$\frac{1}{\sqrt{\lambda_{\mathrm{v}}}} = \frac{0.518}{\log\left(\frac{V_{\inf}}{V_{VegZone}}\right)} \cdot \sqrt{\frac{h_T}{R_v}} \cdot \sqrt{\frac{bfo}{bm}} \qquad (24)$$

Where: $V_{VegZone}$ is the velocity within a fully vegetated channel of the same vegetation as before

$V_{\inf}$ is the velocity expected with bed resistance only, and no vegetation as before

h_T is the depth at the interface as before

R_v is the hydraulic radius of the Vegetation Zone.

Note that where the vegetated and non-vegetated zones are at the same bed level, $h_T = R_v$, so the factor $\sqrt{\frac{h_T}{R_v}}$ may be omitted.

4.4.6 Comparison of Predicted Interface Friction Factors with Data of James et al (2001)

James et al. (2001) presented laboratory flume experiments in which the resistance and velocity were measured for various configurations of vegetation strips. Their readings will be used in this report for the analysis of lateral depth averaged velocity profiles. The experimental procedures and data of James et al. (2001) are presented in Chapter 5 of this report as a background to the investigation of velocity profiles. Experimental conditions are listed in Appendix A. (Note that of the experiments listed in Appendix A, interface friction factors were given only for tests 38 to 41 and 50 to 57, and only these tests are used here.) Their results in terms of the friction factor (λ_v) for the vegetation interface will be considered here. They obtained this friction factor using two methods:

- The magnitude of bed shear stress was "measured using [a] pitot-static tube as a Preston tube and using the calibration relationships of Patel (1965) to relate shear stress to dynamic pressure head," James et al. (2001). This shear stress was then integrated across each non-vegetated zone to give a total bed shear force. "The shear force at the interface was calculated from a balance of forces for uniform flow." This force was then converted to a Darcy-Weisbach friction factor (λ_v) for the vegetation interfaces using the definition of the friction factor.

- A side wall correction procedure was also used to separate the bed and interface friction factors, as described by James and Makoa, in press.

"The average value of [interface Darcy-Weisbach friction factor] determined by the force balance (0.233) agrees remarkably closely with that determined by the side-wall correction procedure (0.243)," James and Makoa (in press). They further noted that this did not show "any discernable trend with flow condition". The methods above can be checked by application to their experimental conditions. For each test, the parameters necessary for calculation of the interface friction factor, as well as the friction factor itself were calculated according to the equations given above.

The results obtained are indicated in Figure 4-4. In looking at the comparison, it is most helpful to look at the actual values, as well as the two obvious trends.

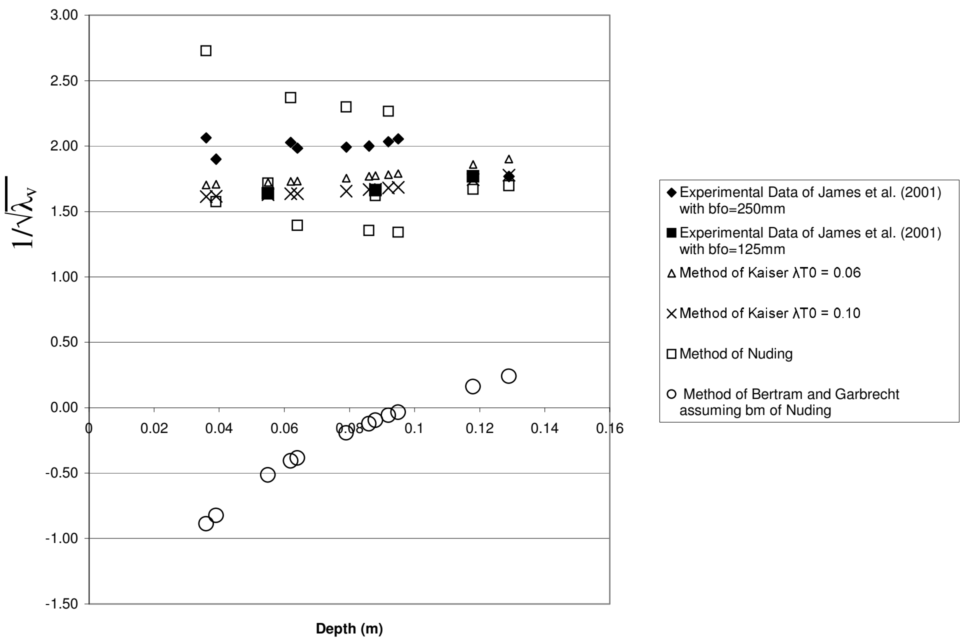

Figure 4-4: Interface Friction predictions against data of James et al. (2001)

The method of Pasche and Rouvé (1985) could not be applied since, using the interface velocity given by equation (16), equation (14) gives a negative value for c_T, so that equation (13) in turn gives a negative value for bm. This merely confirms the assertion made by Helmiö (2004) that this method is applicable only for compound channels, for which it has been found to perform adequately. "Stephan [1993] compared the methods to measurements in a compound channel having a single floodplain, finding that the … methods of Pasche and Nuding were relatively accurate," Helmiö (2004).

The method of Bertram (1985) as presented by Nuding (1991) is clearly un-realistic (even suggesting negative friction factors for certain experiments), and cannot be considered. Again, this merely serves as confirmation of the assertion in Table 3-1 that this method is probably not applicable to simple channels.

This leaves two possible methods – that of Kaiser (1985) and that of Nuding (1991, 1994). It is clear that both of these methods give close to the actual values obtained, regardless of the value selected for λ_{T0}, although the method of Nuding has a somewhat greater spread of values. The method of Kaiser also correctly predicts that depth has a very small influence on the interface resistance.

Also note that the three experimental runs which used the 125mm clear channel half-width had a lower interface resistance than those with the 250mm clear channel half-width. This is not predicted by any equation, and points to the need to account for clear channel width.

4.5 Discharge by Integration of Lateral Velocity Distributions

Before any of these composite roughness methods can be recommended, it is worth considering the alternative suggested in section 4.3 – the integration of lateral velocity distributions as a method to predict discharge and hence account for resistance. Because lateral velocity distributions have not yet been presented, extensive reference will have to be made to material in later chapters.

The lateral velocity distribution equations of Ikeda et al. (1991, 1994) and Tsujimoto & Kitamura (1994) will be presented in section 7.4. Their velocity distribution equation is integrated in Appendix D to give equation (39) on page 67 for the vegetation zone discharge and equation (38) on page 67 for the non-vegetated zone discharge. However, since this method does not accurately predict the lateral distribution of velocity (section 7.5), the discharge equations derived by integrating the velocity distributions cannot be accurate.

The equation to be recommended in this report (for the lateral distribution of velocity in the non-vegetated zone) is that of Nuding (1991, 1994), modified as described in sections 8.4 and 8.5. This velocity distribution equation is given as equation (106) on page 101. The integration of this equation to derive a relation between discharge, depth and energy slope is performed in Appendix D. The following expression for the non-vegetated zone discharge is derived:

$$Q_c = V_{\max} \cdot D \cdot (bfo - TW) + \frac{3 \cdot K \cdot u_v^* \cdot D}{2\log\left(V_{\max} / V_{VegZone}\right)} \left[TW \sqrt{\frac{TW}{bm}} + bm \right] \quad (25)$$

Where: V_{max} is the maximum velocity, which may be predicted according to the method presented in section 8.4, using equations (105) and (140) on page 124.

D is the flow depth

bfo is the clear channel (half) width as indicated in Figure 4-2 on page 33.

K is an empirical constant, equal to 2.2 according to Nuding (1991, 1994).

bm is Nuding's transition width within the vegetation, calculated as described in section 4.4.5 on page 38.

u_v* is the apparent shear velocity on the vegetation interface, predicted as described in section 8.5.

TW is the transition width within the non-vegetated zone (as depicted in Figure 5-1 on page 50). This will be taken as TW Wide for a wide non-vegetated zone or TW Narrow for a narrow non-vegetated zone. TW Wide can be calculated by Equation (101) on page 99. The criterion for the distinction between a wide and narrow channel is:

> A channel is narrow when bf / TW Wide < 1.29, where bf is the non-vegetated zone half-width as indicated in Figure 4-2 on page 33 plus the contributing width bm.

For a narrow channel, TW Narrow can be calculated by the procedure given in section 8.5.3 on pages 106 to 110.

4.6 Comparison of Results

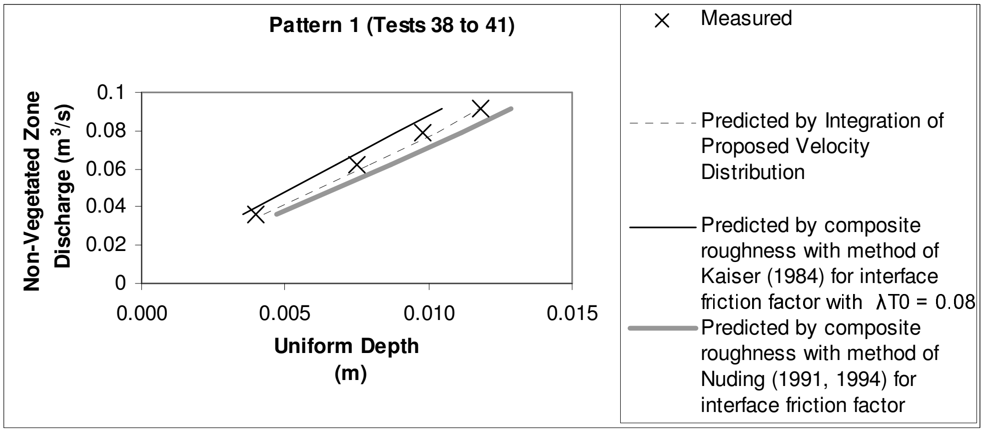

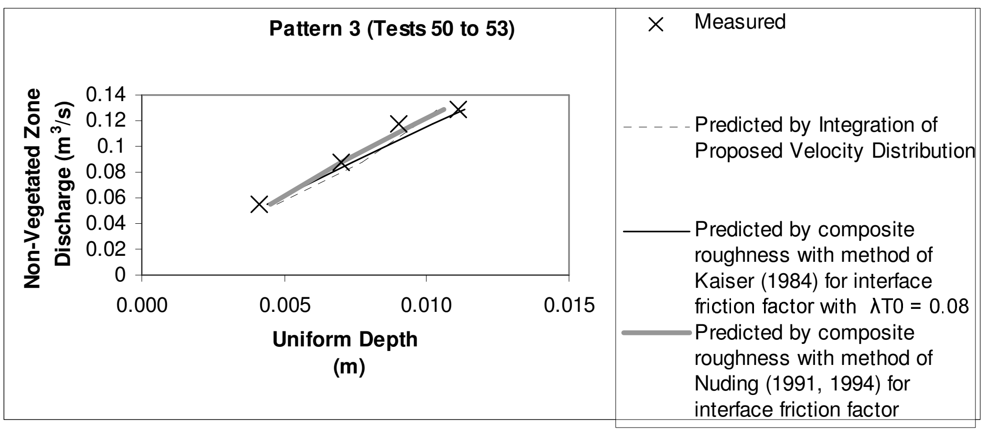

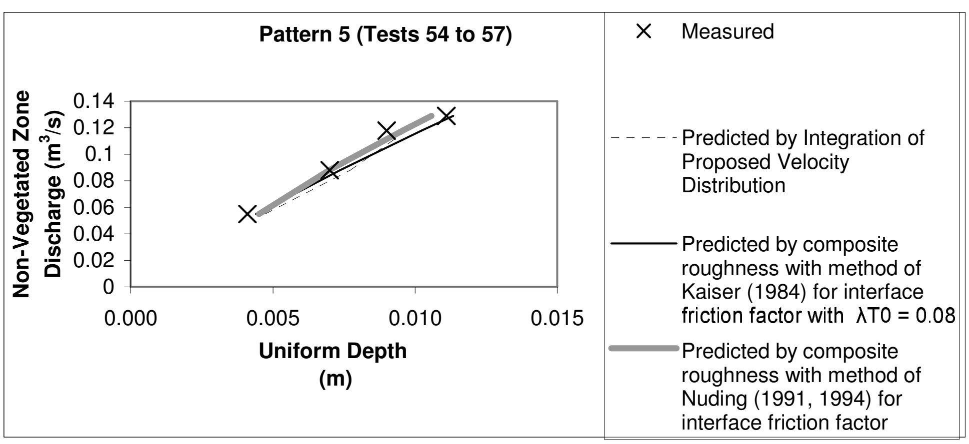

Figure 4-5: Comparison of Predicted and Measured Non-Vegetated Zone Uniform Depth-Discharge Relations for Vegetation Strips

Measured relations between (uniform depth) and (non-vegetated zone discharge) are compared to predictions using both velocity integration and composite roughness formulae in Figure 4-5. The comparison is performed for the same tests by James et al. (2001) for which a comparison of interface friction factors was presented in section 4.4.6. It is clear that there is little difference between predictions using the velocity integration and the composite roughness methods. All methods reproduce the measured stage-discharge relations well. The velocity integration assumes a constant flow depth and bed resistance across the channel. This idealised situation will seldom be applicable in practice. Numerical integration of the velocity distribution is also possible, and will be more flexible in taking variations of depth and bed resistance into account. However, this would be highly computational, and would still have little advantage over the composite roughness methods. Composite roughness methods can describe changes in geometry and hydraulic resistance across the non-vegetated zone. Either composite roughness method is therefore preferred to the velocity integration. The recommendation is therefore as outlined in the following section:

4.7 Recommended Methods

In order to derive the conveyance of a channel with lateral vegetation strips, a water surface elevation and energy slope will have to be assumed. Discharge can then be calculated separately for each zone.

For the vegetation zone, a reasonable approximation is to assume a constant velocity equal to the velocity that would be present in a fully vegetated channel. This velocity may be estimated by existing methods appropriate to the type of vegetation present. The methods mentioned in the introduction to this report (Freeman et al. (2002), Järvelä (2004), Jordanova et al. (2006) and Kutija and Hong (1996)) are relevant.

For the non-vegetated zone, a conventional resistance equation (such as equation 8) can be used to relate energy slope, discharge and water surface elevation The composite roughness coefficient to be used in this resistance equation can be derived using the composite roughness formula of Pavlovski (1931) (equation 7 on page 32). This relies on a defined bed resistance and a defined apparent resistance of the vegetation interface. The apparent resistance of the vegetation interface can be estimated using either the method of Kaiser (1985) or that of Nuding (1991, 1994). These methods were discussed in sections 4.4.4 on page 37 and 4.4.5 on page 38 respectively.

Next, the discharge estimated for each zone can be added to derive the total discharge for the channel. Discharges can be predicted for several different water surface elevations and corresponding energy slopes. These can be combined into a stage-discharge curve.

Where a particular range of flow depths is specified for a particular ecological study, the discharge required to produce these flow depths can thus be determined.

Part III: Lateral Velocity Distributions Adjacent to Vegetation Strips

5 Available Velocity Distribution Data

5.1 Description

The data used in this project are all derived from flume studies. In these studies, the controlled environment and idealised characteristics of a laboratory flume allow relationships between relatively few variables to be investigated without the variability in other factors which is present in natural channels.

Table 5-1: Range of Conditions for Published Experimental Data

Source	**No. of Tests**	**Flume Width (m)**	**Depth (mm)**		**Slope**		**Vegetation (Half) Spacing** (ay x ax) (mm)
			Min	**Max**	**Min**	**Max**	
Tsujimoto and Kitamura (1992) in Nadaoka & Yagi (1998) an in Xiaohui and Li (2002)	3	0.4	43.8	45.7	0.001 65	0.001 70	Unknown
Ikeda et al. (1991) and Ikeda et al. (1994)	4	0.96	30	85	0.001 22	0.003 13	50 x 50
Nagdi and Sharpe (2000) in James et al (2001)	8	1	32	91.2	0.00 107		12.5x25
Makoa (2001) in James et al (2001)	28	1	36	150	0.00 107		12.5x25

In all experiments used, vegetation was simulated by regular arrays of vertical cylindrical rods. All experiments were conducted in rectangular channels. With reference to Figure 3-1 on page 24, in order to isolate the effect of vegetation, only in-channel vegetation was used. All experiments consisted of vegetated and non-vegetated strips running parallel to the flow direction. Two vegetation arrangements were used: parallel and staggered. These arrangements, together with the dimensions for each arrangement, are as indicated in Figure 4-3 on page 33.

The range of experimental conditions used for each set of experiments is listed in Table 5-1. Details of the conditions for each experiment are tabulated in Appendix A. (Note that Appendix A also includes details for current experiments (Tests 1 to 8), which will be described in Chapter 6.

5.2 Velocity Profile

The typical velocity profile observed in most experiments is similar to that shown in Figure 5-1. (This is similar to the idealised profile depicted by Nuding, 1994.) Far from the interface, a constant velocity is reached. Within both the vegetation zone and the non-vegetated zone, there is region close to the interface over which the velocity changes. Lateral distances are measured as defined in Figure 5-1. (Note that for more complex arrangements, some regions may be repeated. In these cases, bfo and Bv will be measured as depicted in Figure 4-2 on page 33. Note that, while it is seems more natural to measure distances from the interface itself, many calculations are considerably simplified by defining a distance y from the start of the contributing width within the vegetation as depicted. In line with this, distance bfo is also replaced by bf as indicated.

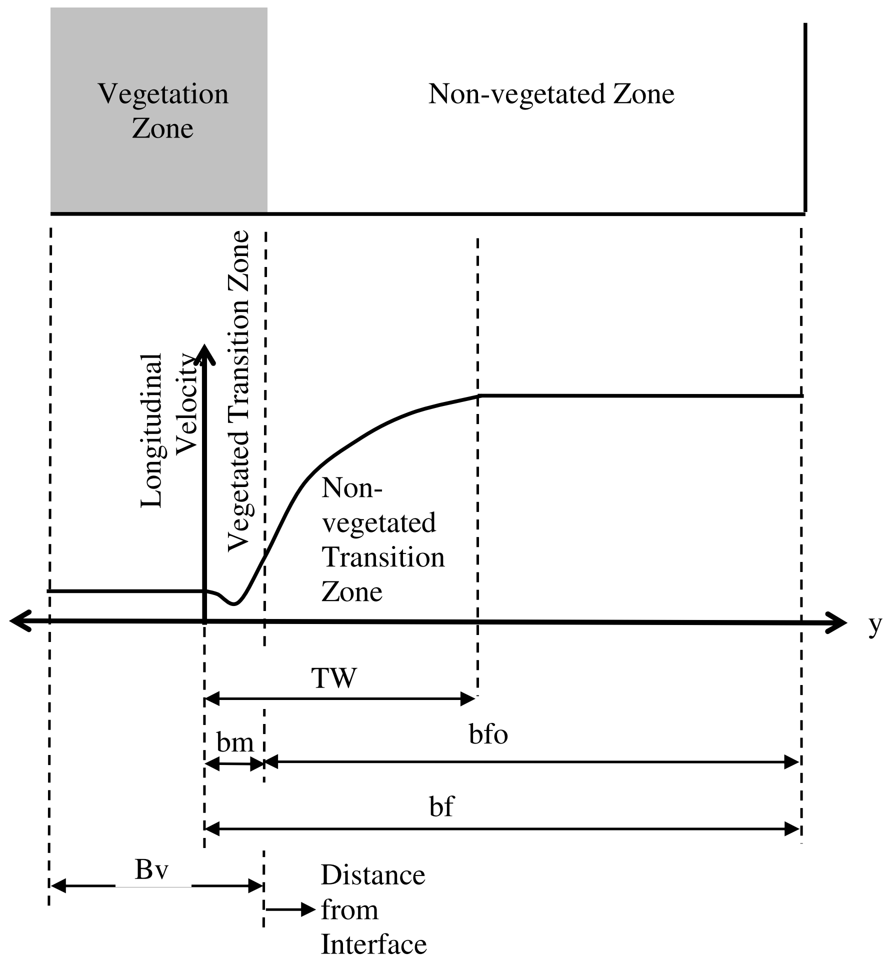

Figure 5-1: Idealised lateral velocity profile and definition of lateral dimensions

5.3 Effect of Width

The data originally plotted by James et al. (2001) in their Figure 8.20 are re-plotted here in Figure 5-2. All of these experiments achieved uniform flow in the same flume with the same vegetation at the same slope and approximately the same depth. In all of these experiments, the velocity profiles plotted level off far from the vegetation. (In other words, there is a region in which the velocity no longer depends on distance from the vegetation interface.) However, it is clear that in each case, the velocity profile (and in particular the maximum velocity reached) depends on the widths of the vegetation and non-vegetated zones. This trend is also depicted for a different depth by James et al. (2001) in their Figure 8.19. This effect was therefore identified as important for the prediction of lateral velocity distributions. The experiments of James et al. (2001) had relatively narrow non-vegetated zone widths (non-vegetated zone half width bfo <= 0.25m.). A series of experiments (which will be described in Chapter 6) was conducted to determine whether the same dependence on width would be found with wider non-vegetated zones.

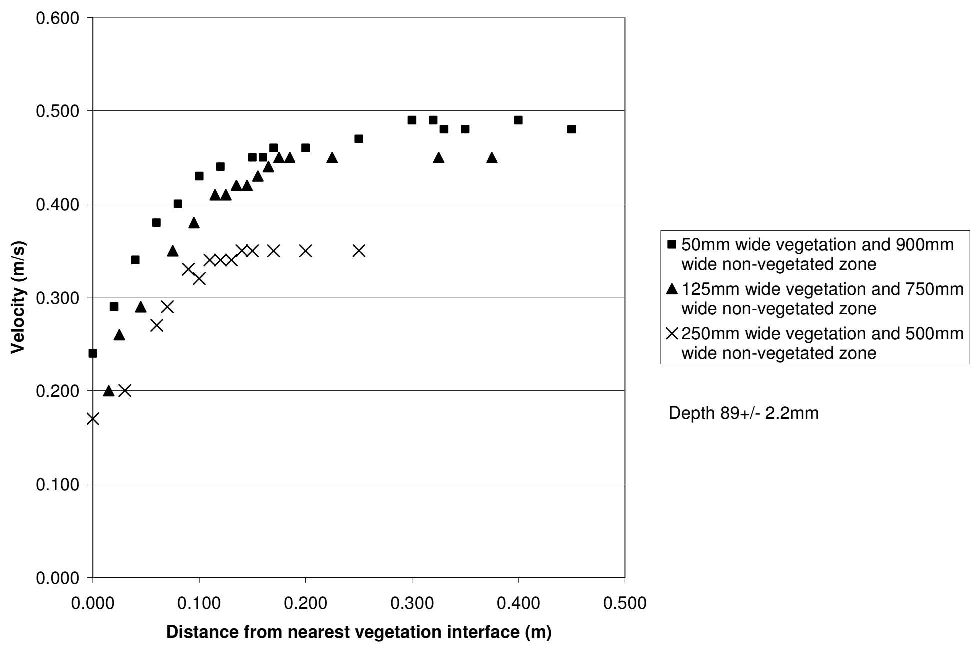

Figure 5-2: Effect of Widths of Vegetation and Non-vegetated Zones According to James et al. (2001)

6 Effect of Zone Width: Laboratory Experiments

6.1 Aims

As stated above, James et al. (2001) indicated that the velocity distribution is strongly dependent on either the width of the vegetation strip or the width of the non-vegetated zone. (Since both of these widths were varied together, it is not clear which width had the major effect.) However, this effect is not accounted for in the equations previously proposed. (In the method of Nuding (1991, 1994) the width of the non-vegetated zone affects the velocity distribution through its effect on the average velocity in this zone. However, the vegetation zone width has no effect provided that it is greater than the very narrow transition width bm.) The methods of Tsujimoto and Kitamura (1994) and Ikeda et al. (1991, 1994) do not consider any width effect.)

Certain other findings also suggest that width may have an important effect. Fukuoka and Fujita (1990) found that the shear stress at the vegetation interface is affected by the width of the vegetated zone, even when this zone is up to 50 times wider than the transition zone. Since velocities are determined by the momentum transfer caused by this shear, velocities are also expected to be affected by width. An effect of vegetation zone width on velocities reached in the non-vegetated zone is also predicted by the model of de Lemos and da Silva (2002). A need to explore the effect of zone widths by means of laboratory experiments was therefore identified. This experimental investigation therefore aims to explore and quantify the effect of the width of both vegetated and non-vegetated zones on lateral velocity profiles.

6.2 Procedure and Equipment

Experiments were performed in a 1.988m wide flume with an adjustable slope. The flume walls and floor are coated with a smooth, rubbery material, except for windows in the flume walls.

Vegetation was represented by wooden frames approximately 1m long, each holding a staggered array of 5mm diameter rusty steel rods with longitudinal and transverse spacings ax=25mm and ay=12.5mm as indicated in Figure 4-3 on page 33. In order to alter the non-vegetated or total width, a structure was made to constrict the flow width within the flume.

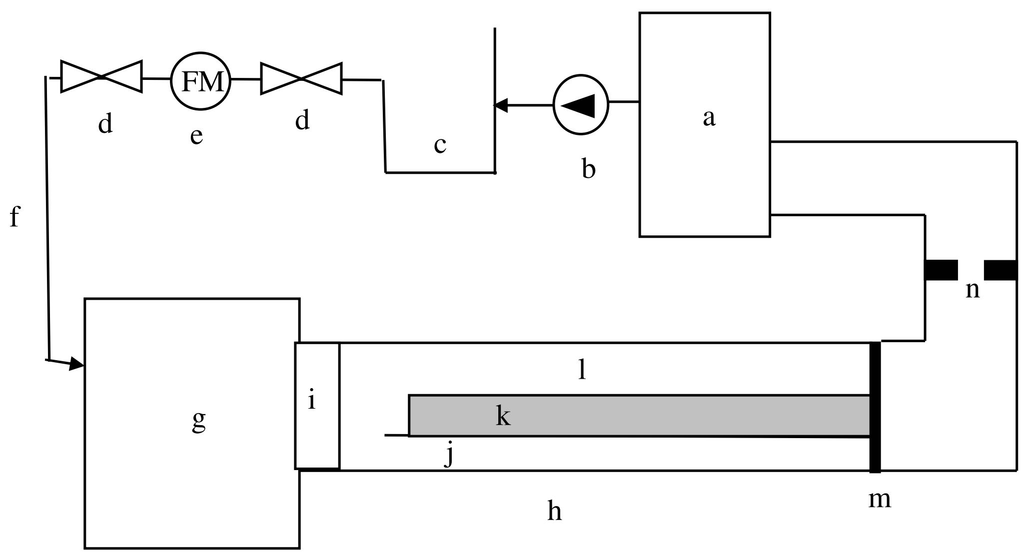

a	Pump Sump	h	Flume
b	Pump	i	Wave Damper (some experiments only)
c	Constant Head Tank	j	Width Constriction Structure (No flow)
d	Control Valve	k	Artificial Vegetation
e	Pipe Flowmeter	l	Non-vegetated Zone
f	Supply Pipe	m	Adjustable Tailgate
g	Flume Inlet Tank	n	V-notch Weir Flowmeter

Figure 6-1: Schematic diagram of recirculating water system

Water was supplied through the recirculating system illustrated diagrammatically in Figure 6-1. Flow was controlled via the valves in the supply pipeline. Flowrates were measured both by means of the pipe flowmeter and by means of the V-notch weir downstream of the flume. In some experiments, a miniature propeller was used to measure velocity. For other experiments, a two-dimensional Acoustic Doppler Velocity meter (ADV) was used.

For the earliest experiments, flow depths and water slopes were measured directly in the flume using a pointer gauge. Later measurements used stilling pots attached to the flume centreline to measure slope and depth, with a pointer gauge in the stilling pots. Water surface slope and flume bed slopes were taken from a single pair of level measurements taken over a distance of 8m immediately upstream of the measurement section, which was located 10m from the upstream end of the flume. In order to determine a zero or base level for water surface slope (i.e. horizontal water surface), water surface elevations were measured at these same points before and after each test with no flow in the flume. The actual slope was then calculated as the difference between the slope measured during the test and the average of these two horizontal water surface readings. In each experiment, a steady flow was established with a water surface slope approximately equal to the average flume bed slope of 0.000 44. (Some variation in water surface slope remained, as indicated in Table 6-1.)

Velocities were then measured at irregular intervals across the flume at approximately 0.4 to 0.5 times the depth above the bed. The velocity meters were positioned using an instrument bridge with longitudinal, vertical and transverse scales attached.

Experiments performed are as summarized in Table 6-1. Experiments C1 to C3 were performed with no vegetation in order to determine the velocities achieved with bed resistance only. Experiments 1 to 8 had a strip of vegetation along one side of the flume only. Further conditions for experiments 1 to 8 are tabulated in Appendix A.

Table 6-1: Conditions for Vegetation Zone Laboratory Experiments

Test	Vege-tation Zone Width	Non-vegetated Zone width	Depth	Water Surface Slope	Discharge (V-notch)	Velocity Meter
	(mm)	(mm)	(mm)		(m3/s)	
C1	0	1988	29.5	0.000 41	0.007 9	ADV
C2	0	1988	60.8	0.000 44	0.033 0	Propeller
C3	0	1988	61.2	0.000 43	0.033 4	Propeller
1	126	1862	29.6	0.000 42	0.008 7	ADV
2	126	1862	60.8	0.000 58	0.033 0	Propeller
3	126	1862	60.5	0.000 40	0.030 2	Propeller
4	126	1349	59.9	0.000 41	0.020 9	ADV
5	126	1598	60.6	0.000 57	0.029 5	ADV
6	126	1598	60.6	0.000 59	0.029 7	Propeller
7	126	1223	59.9	0.000 35	0.020 9	ADV
8	254	1223	60.3	0.000 36	0.019 9	ADV

6.3 Readings

The full readings for each experiment are presented in Appendix B. Velocity readings, as well as graphs showing these readings, are also included in Appendix C.

6.4 Results

As expected, all measured velocity profiles indicated a smooth progression from a low velocity within the vegetation to a higher velocity far from the vegetation as indicated in Figure 6-3 on page 57 and Figure 6-4 on page 58.

In certain cases, the velocity peaks a certain distance from the vegetation, rather than reaching a constant maximum value over most of the non-vegetated zone. (This was also observed from the data of Ikeda et al. (1991).) However, an examination of the longitudinal development of a typical velocity profile (Figure 6-2) illustrates that these peaks are due to longitudinal development of the lateral profiles following a constriction at the flume entrance. These peaks die out by a longitudinal distance of approximately 10m. Further experiments were conducted at this longitudinal position, in order to minimise the effect of longitudinal development on the measured velocity profiles.

In order to correct for the effect of slight differences in the water surface (or energy) slope, all velocities are plotted as the ratio $Velocity \Big/ \sqrt{\text{Water Surface Slope}}$, where water surface slope was taken over a distance of 8m immediately upstream of the measurement section.

The effect of the width of the vegetation zone is indicated in Figure 6-3. This shows measured velocity profiles for vegetation zones 5 stems (or 125mm) wide and 10 stems (or 250mm) wide for the same width of the non-vegetated zone. No difference is apparent between the velocity profiles produced using the two vegetation widths.

The effect of the width of the non-vegetated zone is examined in Figure 6-4. This shows measured velocity profiles for a vegetation zone 5 stems (or 125mm) wide, for various widths of the non-vegetated zone as indicated. While there may be some small difference between the velocity profiles produced using the three different non-vegetated zone widths, differences are not significant compared to the possible experimental error due to the estimation of water surface slope (as indicated by error bars). This is confirmed by the observation that there is no directional trend with changing non-vegetated zone width. The highest velocities were measured for the intermediate width; the lowest velocities were measured for the greatest width, and intermediate velocities were measured for the narrowest width.

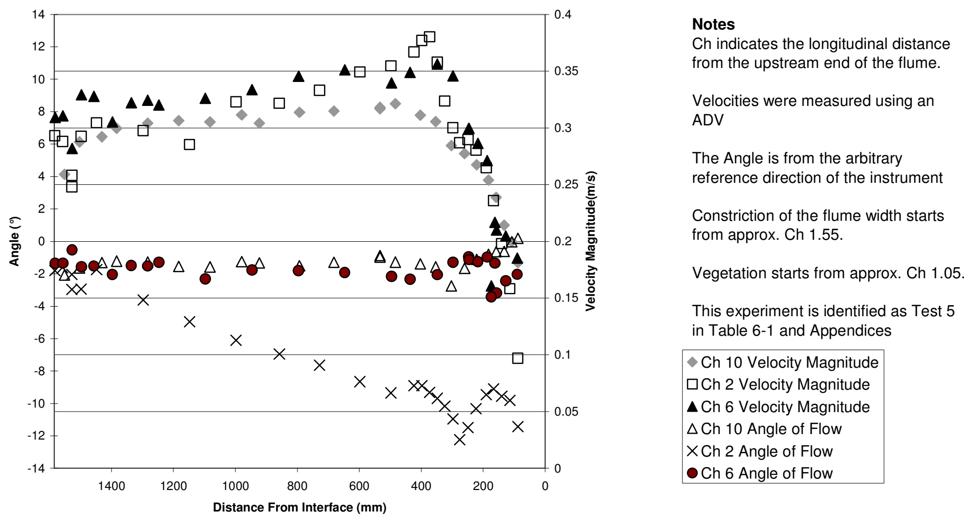

Figure 6-2: Longitudinal Development of Velocity Profile

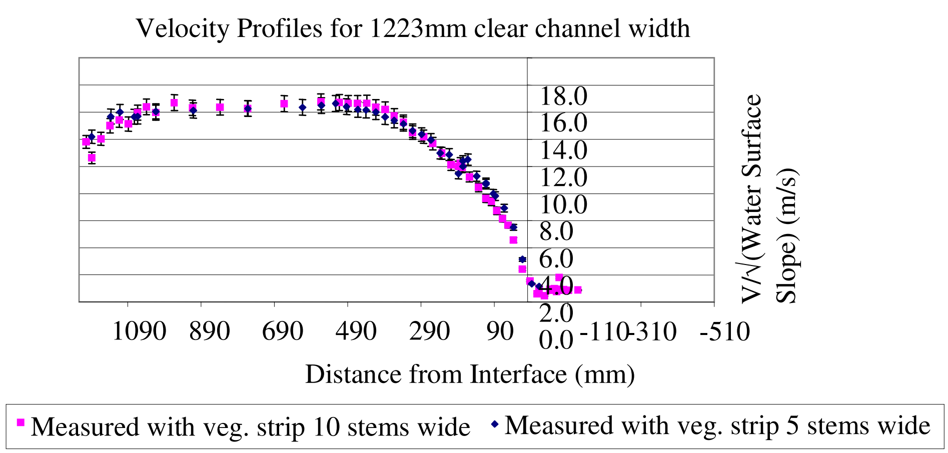

Figure 6-3: Velocities for Two Different Vegetation Strip Widths

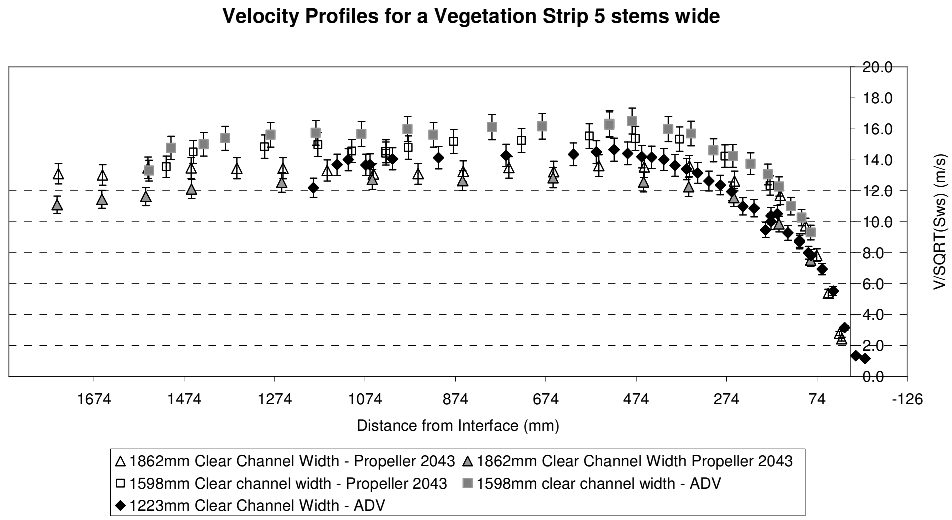

Figure 6-4: Measured Velocities for Different Clear Channel Widths & Vegetation Strip 5 stems wide

6.5 Discussion and Conclusions

Longitudinal development of the velocity profiles takes place over several metres, as indicated in Figure 6-2. Close to the flume entrance (at Chainage 2m), the velocity profile is highly irregular, and there are strong transverse velocities caused by the flow constriction, as indicated by the large angle of the flow close to the interface.

The major source of experimental error identified was in the measurement of water surface slope. The error in measurement of water surface slope was taken as the largest difference for any single test between slope measurements of the horizontal water slopes measured with no flow before and after the test. This maximum error was approximately $62x10^{-6}$ or 14%. This would cause an error in the magnitude of $V/\sqrt{S}$ of up to 7%. A further error would have been caused by the difference between the local slope at the section where measurements were taken and the average slope measured over a distance of 8m upstream. This difference is clearly visible for the two longitudinal water surface elevation profiles which were measured. (Longitudinal profiles of water surface elevation were measured only at the end of test 4 and at the end of test 7. Graphs of these two profiles are included in Appendix B together with the readings of these tests.) It is, however, expected that this difference between local and average slopes would be similar for all measurements, and it would therefore not invalidate the comparison of velocity profiles. Furthermore, since (as indicated in Figure 6-2) the velocity profile develops over much of the flume length, both the local and average slopes are expected to influence the velocity profile.

Within the range of widths tested, neither vegetation zone width nor non-vegetated zone width has a significant effect on the velocity profile (Figure 6-3 and Figure 6-4). Note that this is in contrast to the results presented by James et al. (2001) which showed that over a range of narrower non-vegetated zone widths ($0.084m \leq bfo \leq 0.450m$), the relative widths of the two zones do have a definite effect.

No evidence for any effect of vegetation zone width was found. (The exception suggested by Nuding (1991, 1994) is a single row of vegetation only. This is not relevant here, since the effect of vegetation strips rather than single rows of vegetation is being considered.) It is therefore concluded that for vegetation strips, the vegetation zone width has no effect on the velocity profile.

It would appear that non-vegetated zone width has an effect on the velocity profile only within the narrower range of widths tested by James et al. (2001), and not where the non-vegetated zone widths are wider. The analysis presented in section 8.4 suggests a definite criterion for the range of non-vegetated widths which affects the velocity profile. It is suggested in section 8.4 that the non vegetated zone (half) width (bfo) will affect the velocity profile only if it is less than 1.29 times the width over which the velocity change occurs in a similar wide non-vegetated zone.

7 Lateral Velocity Distribution Methods

7.1 Introduction

As explained previously, a lateral velocity profile results from the transfer of momentum between slower-flowing water in the vegetated zones and faster flowing water in the non-vegetated zones. Before considering the interaction, it is necessary to estimate separately the characteristic velocity produced by each zone in the absence of the other. In other words, as stated previously, a channel with no vegetation, and a certain depth and slope is assumed to exhibit a known flow velocity V_{inf}, corresponding to friction factor λ_b. Similarly, a fully vegetated channel is assumed, at the same depth and slope, to exhibit a known flow velocity $V_{VegZone}$, corresponding to a vegetation resistance which may be expressed in terms of various parameters.

Methods for estimation of this velocity ($V_{VegZone}$) exist, and will not be considered here. These include the method of Jordanova et al. (2006) for reeds, the method of Järvelä (2004) for woody vegetation and the method of Freeman et al. (2002) for trees and bushes. The last is the only one of these methods to explicitly consider the effect of combinations of different plants in the same area. All of these methods are resistance relations. In other words, they relate average velocity to depth, loss of flow energy (as energy slope S) and a resistance coefficient which depends on the vegetation characteristics. In all cases, measures of the vegetation density, drag coefficient and projected cross-sectional area (or diameter) are required.

Assuming that appropriate methods for the estimation of these two velocities ($V_{VegZone}$ and V_{inf}) have already been applied, this section will discuss existing methods for the estimation of the velocity profiles produced by the interaction of these known velocities. Velocity profiles are derived by assuming certain relationships for the transfer of momentum between these two zones of known characteristics.

.

7.2 Method of Pasche and Rouvé (1985)

Pasche and Rouvé (1985) suggested that, for the purpose of analysis of flow in the non-vegetated zone, the interface could be treated as a solid boundary. By this assumption, a logarithmic velocity profile away from the interface is expected, similar to that above a uniform channel bed, but in a horizontal rather than a vertical plane. As stated in section 3.4, this method was developed for floodplain vegetation in a compound channel section, as depicted in Figure 3-1. However, in this chapter, its application to in-channel vegetation will be tested.

With this approach, it is necessary to evaluate the friction factor of the interface, and their method for estimation of this friction factor was presented in section 4.4.1. They found that the friction factor is not dependent on characteristics of the non-vegetated zone flow. Instead, it depends on the stem diameter, lateral and longitudinal stem spacing, stem wake dimensions and also on a co-operating width bm within the vegetation zone. "It can be assumed that the whole flood plain section does not contribute to the flow resistance of the main channel flow, but only within a co-operating width bm." By assuming a cubic velocity distribution within the influencing vegetation zone, Pasche and Rouvé (1985) provided an equation to calculate the co-operating width from the momentum balance, which was also presented in section 4.4.1 on page 34.

As explained in section 4.4.1, the velocity at the vegetation interface (V_{int}) is required. A useful estimate of this is provided by the methods presented in section 7.4, which indicate:

$$V_{\text{int}} = \sqrt{V_{\text{inf}} \cdot V_{VegZone}} \qquad (16)$$

In addition to the equations presented in section 4.4.1 on page 34, the following additional equations are required to predict the velocity distribution:

$$u^*_{\text{int}} = V_{\text{int}} / C_T \tag{26}$$

$$V(Y) = \frac{1}{0.41} \cdot u^*_{\text{int}} \cdot \ln\left(1 + \frac{Y}{k_t}\right) + c_T \tag{27}$$

Where: u^*_{int} is the interface shear velocity

C_T is a dimensionless interface velocity, calculated using equations (10) to (14) on page 34.

V(Y) is the velocity at any distance Y from the interface.

This treatment could be a useful simplification, particularly for calculating the average depth and velocity within each zone. However, it can neither describe nor take account of the turbulent structure associated with the interface. Indeed, Naot et al. (1996) comment that "The shear layer formed in a wide vegetated domain … is no longer described by the … logarithmic profile."

7.3 Method of Nuding (1991, 1994)

Nuding's aim was to develop an equivalent roughness for 1-D flow calculations (as presented in section 4.4), rather than a description of the velocity profile. However, the inter-relation between velocity profile and resistance are presented. He considered both bank and in-channel vegetation. Nuding's equation is derived from boundary layer theory, "the lateral velocity variation V(y) is characterized as a function of shear flow of a free jet entering an area of slow flow …" from which an expression for eddy viscosity is derived. Nuding assumed that only the transition region (as specified by contributing width bm) contributes to eddy production. This formulation leads to a relation in which eddy viscosity is proportional to the rate of change of velocity with lateral distance.

Nuding's (1991, 1994) equation for the transverse velocity profile is:

$$V(y) = \frac{2.2u^*_v}{\log\left(\frac{V_{\text{inf}}}{V_{VegZone}}\right)} \cdot \sqrt{\frac{h_T}{R_V}} \cdot \sqrt{1 + \frac{y}{bm}} \tag{28}$$

Where: V(y) is the depth-averaged velocity at a lateral position y.
y is as defined in Figure 5-1 on page 50.
u_v^* is the apparent shear velocity on the vegetation interface.
V_{inf} is the velocity of a wide channel with the same bed, but without vegetation.
$V_{VegZone}$ is the average velocity within the vegetated zone.
h_T is the depth at the interface.
R_V is the hydraulic radius of the vegetation zone, excluding the interface.
bm is the transition zone width, evaluated according to the set of empirical conditions presented in section 4.4.5 on page 38.

Note that this velocity will tend to increase without limit as the distance from the vegetation interface increases. For a wide channel, this is clearly impossible. It will therefore be assumed that the velocity is limited to a maximum value of the velocity V_{inf} which would be produced with bed resistance only.

In order to predict the velocity profile, it is first necessary to calculate the average resistance or velocity of the non-vegetated zone and the interface shear velocity. The procedure for this is as follows:

1. Estimate a friction factor λ_b for the bed.

2. Calculate the interface friction factor λ_v according to equation (23):

$$\frac{1}{\sqrt{\lambda_v}} = \frac{0.518}{\log\left(\frac{V_{\inf}}{V_{VegZone}}\right)} \cdot \sqrt{\frac{h_T}{R_v}} \cdot \sqrt{\frac{bfo}{bm}} \qquad (23)$$

3. Calculate a composite friction factor (λ_{Comp}) according to the method of Pavlovski (1931):

$$\lambda_{comp} = \left(\lambda_v \cdot h_T + \lambda_b \cdot bfo\right) / \left(h_T + bfo\right) \qquad (7)$$

Where: h_T is the depth at the vegetation interface
bfo is the half-width of the non-vegetated zone.

4. Calculate the average velocity in the non-vegetated zone (Vave,nv) using the Darcy-Weisbach resistance equation:

$$V_{Ave,nv} = \sqrt{8 \cdot g \cdot R_{nv} \cdot S \big/ \lambda_{Comp}} \qquad (29)$$

Where: S is the energy slope

R_{nv} is the hydraulic radius of the non-vegetated zone.

Note that the average velocity (Vave,nv) (which is influenced by the vegetation) is used rather than the velocity with bed resistance only (V_{inf}), since the Darcy-Weisbach resistance equation is defined in terms of average velocity.

5. Nuding (1994) gives a relation which may be re-arranged as:

$$u_T^* = V_{ave,nv} \cdot \sqrt{\lambda_T / 8}, \qquad (30)$$

Where u_T^* is the apparent shear velocity on the vegetation interface. (This equation also follows from the definitions of friction factor and shear velocity.)

Equation (28) can then be applied to calculate the velocity at any lateral position.

Since Nuding's velocity distribution is derived from boundary layer theory, it may be assumed valid within the boundary layer, i.e. that layer within which the fluid is slowed down by the bank vegetation. The equation does not account for the effect of resistance of the bed on velocity, since this has been considered separately in the resistance formulation. Nuding (1994) recognised that his approach is general, and is therefore not exact for specific flume studies.

7.4 Method of Ikeda et al. (1991, 1994) and Tsujimoto & Kitamura (1994)

Ikeda et al. (1991) aimed to describe the flow velocities adjacent to pile dykes and their effect on the scour and deposition of sediment. Tsujimoto and Kitamura (1994) aimed to describe the dynamic nature of flow past vegetation and to predict lateral transport of bed load. Their derivation is based on the application of the momentum equation in three regions: within vegetation zone, in the non-vegetated zone and at a remote location where $V = V_{inf}$. A large width to depth ratio is assumed. Considering the turbulent structure of the interaction between the vegetated and non-vegetated zones, Tsujimoto and Kitamura (1994) suggested "horizontal shear flow with a constant eddy viscosity." The assumption of constant eddy viscosity leads to an exponential form of the lateral velocity distribution equation in each zone as shown in Figure 7-1. Note that the velocity is asymptotic to V_{inf} and $V_{VegZone}$.

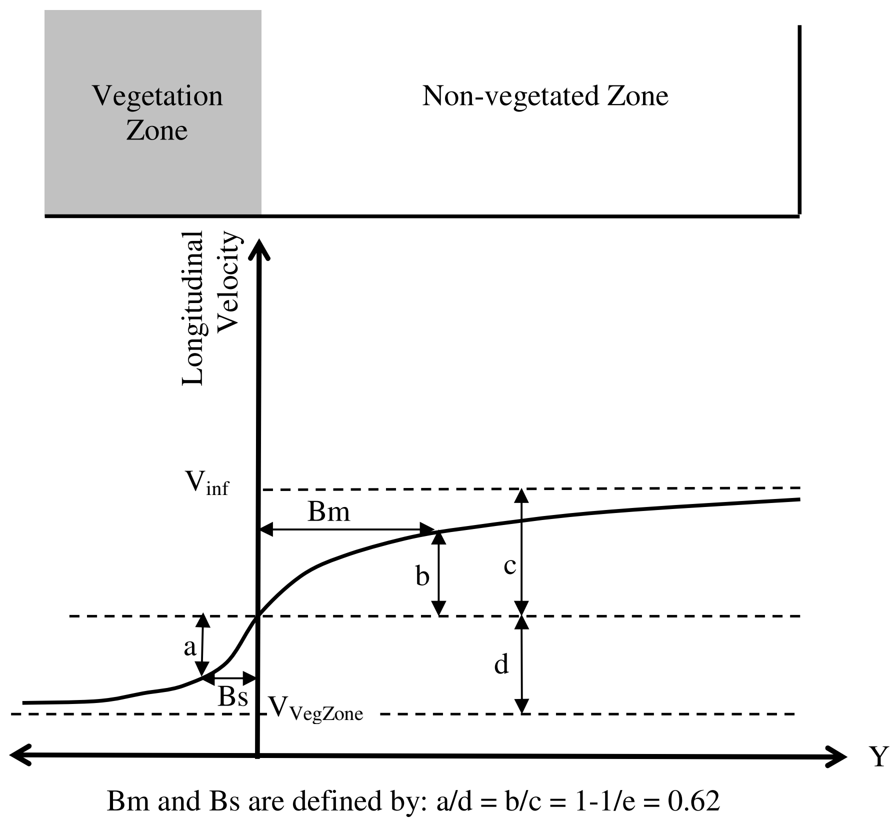

Figure 7-1: Definition sketch for the method of Ikeda et al. (1991, 1994) and Tsujimoto and Kitamura (1994)

These exponential distributions are scaled by transition widths Bm and Bs within the non-vegetated and vegetated zones respectively. These transition widths are analogous to, but different to Nuding's bm. They can be shown to be equal to the width over which (1-1/e) or 62% of the velocity change (from the interface to V_{inf} or $V_{VegZone}$ respectively) occurs. These widths are indicated in Figure 7-1.

Intuitively, it would be expected that the transition width is proportional to the depth, since this formulates a geometric scaling. It is also expected that the transition width should be reduced by increasing bed friction factor, since it is the bed friction which damps out the momentum transfer. Finally, it is expected that the width would be a function of the ratio of velocities within the vegetation and the clear channel. The equations derived display all of these expected properties.

Using the same symbols as for Nuding's (1991, 1994) equation, manipulation of the equations for both the method of Ikeda et al. (1991, 1994) and the method of Tsujimoto and Kitamura (1994) gives:

For the non-vegetated zone:

$$V(Y) = V_{\inf} - \left(V_{\inf} - \sqrt{V_{\inf} \cdot V_{VegZone}}\right) \cdot e^{-Y/Bm} . \qquad (31)$$

For the vegetation zone:

$$V(Y) = V_{VegZone} + \left(\sqrt{V_{\inf} \cdot V_{VegZone}} - V_{VegZone}\right) \cdot e^{Y/Bs} \qquad (32)$$

In these equations, Y is measured directly from the interface (as shown in Figure 7-1) and not in the same way as Nuding's y. Note that Y is negative within the vegetation zone and positive within the non-vegetated zone.

The Transition widths Bm and Bs may be calculated according to the following set of equations:

$$Bm = D \cdot (1 - J)(1 + J)^2 \cdot f(J) \Big/ \left[2\left(\lambda_b / 8 \right)^z \right] \qquad (33)$$

$$Bs = Bm \cdot J \qquad (34)$$

Where: D is the flow depth at the interface as before.

λ_b is the Darcy-Weisbach friction factor for the bed as before

$$J = \sqrt{\frac{V_{VegZone}}{V_{\inf}}} \qquad (35)$$

z is a constant equal to 0.75 according to Ikeda et al. (1991, 1994) and equal to 1 according to Tsujimoto and Kitamura (1994)

f is an empirical function of the velocity ratio J. According to Tsujimoto and Kitamura (1994), f represents a "mixing coefficient." Both sets of authors adopt a double exponential form for f, but the relations differ in their coefficients. According to Ikeda et al. (1991, 1994):

$$f = 0.035e^{-2.95e^{-3.8J^2}} . \qquad (36)$$

According to Tsujimoto and Kitamura (1994):

$$f = 0.03e^{-4e^{-6J^2}} \qquad (37)$$

Substituting y=0 into the velocity expression for either zone (Equation 31 or Equation 32) yields a useful and simple expression for the interface velocity (V_{int}), which was presented previously:

$$V_{int} = \sqrt{V_{inf} \cdot V_{VegZone}} \qquad (16)$$

The velocity expressions may be simply integrated to give expressions for the discharge in each zone. This integration is performed in Appendix D. The discharge in (half of) a rectangular non-vegetated zone of (half) width bfo and depth D is given by:

$$Q_c = V_{inf} \cdot D \cdot \left[bfo - Bm\left(e^{-bfo/Bm} - 1 \right)\left(\sqrt{\frac{V_{VegZone}}{V_{inf}}} - 1 \right) \right] \qquad (38)$$

Similarly, the discharge within (half of) a rectangular vegetated zone of (half) width Bv and depth D is given by:

$$Q_v = D \cdot Bv\left[V_{VegZone} - \frac{Bs}{Bv}\left(1 - e^{-Bv/Bs} \right)\left(\sqrt{V_{inf} \cdot V_{VegZone}} - V_{VegZone} \right) \right] \qquad (39)$$

7.5 Comparison of Velocity Distribution Methods with Laboratory Data

7.5.1 Selection from Available Laboratory Data

Out of the data available from the laboratory experiments discussed in Chapters 5and 6, five experimental runs (Tests 7, 8, 9, 24 and 27) were selected for comparison of the various methods. The conditions for these runs are summarised in Table 7-1 and detailed in Appendix A. These experiments were selected to give a variety of experimental conditions as used by different authors. The selected experiments included both staggered and parallel vegetation patterns with vegetation on either one or both sides of the channel. Dimensions are as indicated in Figure 4-2 on page 33 and Figure 4-3 on page 33.

7.5.2 Predictions produced using various Methods

The various velocity distribution methods were applied to the conditions of the selected laboratory experiments to derive predicted velocity profiles. These were compared to the measured profiles. The method of Pasche and Rouvé (1985) yielded completely un-realistic predictions, so this method was not considered further. (Note that this method also yielded a completely un-realistic friction factor for the interface, as discussed in section 4.4.6. As noted previously, Helmiö (2004) already noted that this method is not applicable for simple channels with in-channel vegetation. (See Table 3-1.) All other predictions were plotted, together with the measured data.

The method of Nuding (1991, 1994) is based on experiments using either the parallel arrangement (Figure 4-2 on page 33) or wire mesh. It was therefore initially unclear whether, for a staggered arrangement, the transverse spacing ay should be taken as indicated in Figure 4-2, or as twice this distance. However, the results obtained were far more realistic when ay is taken as indicated in Figure 4-2, and this measurement was therefore used.

Table 7-1: Experimental Data Used to Compare Velocity Distribution Methods

Test No.	Reference	Test	Vegetation Pattern	Vegetation Location	Bv	bfo	S	ax	ay	dp	Depth	V_{inf}	$V_{VegZone}$
					(m)	(m)		(m)	(m)	(m)	(m)	(m/s)	(m/s)
7	Current Experiments	13-Feb-06	Staggered	One Side	0.126	1.223	0.000 35	0.025	0.012 5	0.005	0.059 9	0.256	0.029
8	Current Experiments	15-Feb-06	Staggered	One Side	0.254	1.223	0.000 36	0.025	0.012 5	0.005	0.060 3	0.260	0.029
9	James et al (2001)	250mm strips Depth 68.5mm	Staggered	Both Sides	0.250	0.250	0.001 07	0.025	0.012 5	0.005	0.068 5	0.522	0.039
24	Ikeda et al. (1991)	Run 1	Staggered	One Side	0.270	0.690	0.001 61	0.050	0.05	0.005	0.060 0	0.395	0.113
27	Kan and Nakai (1993) in Tsujimoto & Shimizu (1994)	Run A-1	Parallel	Both Sides	0.200	0.300	0.002 00	0.020	0.020	0.0028	0.041 0	0.481	0.070

$V_{VegZone}$ is the velocity predicted or measured for a fully vegetated channel.
V_{inf} is the velocity predicted or measured for the bed in the absence of vegetation.
S is the water surface (or energy) slope.
Refer to Figure 4-2 on page 33 and Figure 4-3 on page 33 for all other definitions.

For test 9, one other comparison has been made. The method of Ikeda et al. (1991, 1994) and Tsujimoto and Kitamura (1994) suggests an exponential velocity profile which includes an empirical mixing coefficient. It was thought that the exponential form may be correct, even though the empirical parameters suggested by these authors may not apply. In order to test the applicability of the exponential form, the best fit exponential equation to the velocity readings of test 9 is also presented in Figure 7-3 and Table 7-2.

Plots of distance from vegetation interface vs. predicted and measured velocity magnitude are included as Figure 7-2 to Figure 7-5. (A plot of test 8 is not shown, since both results and predictions are almost identical to those for test 7). Root mean square percentage errors in velocity prediction are given in Table 7-2. These were calculated by first calculating, for each velocity measurement, the error as a percentage of the measured velocity. A root mean square value of these percentages was then calculated. Note that the graphs include predictions using the original equation of Nuding (1991, 1994) which increases without limit. However, as mentioned previously, it was decided to limit the predicted velocity to a maximum of the velocity with bed resistance only (V_{inf}). The errors indicated in Table 7-2 are therefore calculated using this limit.

7.6 Selection of the Method of Nuding (1991, 1994)

A consistent trend in the results is noticeable: Except for the method of Nuding (1991, 1994), all methods predict that velocity will change over a certain distance to reach approximately the velocity which would be present without vegetation. However, the method of Tsujimoto and Kitamura (1994) consistently predicts that velocity will change more steeply over a shorter distance than is actually the case. The method of Ikeda et al. (1991, 1994) predicts that velocity will change more slowly, over a longer distance than is actually the case. The method of Nuding (1991, 1994) provides the best estimate of the distance over which velocity changes. The shape of the velocity profiles suggests that the rate of change of velocity with distance changes to zero suddenly as the final velocity V_{inf} is reached. Only the method of Nuding (1991, 1994) with V limited to V_{inf} predicts this sudden change.

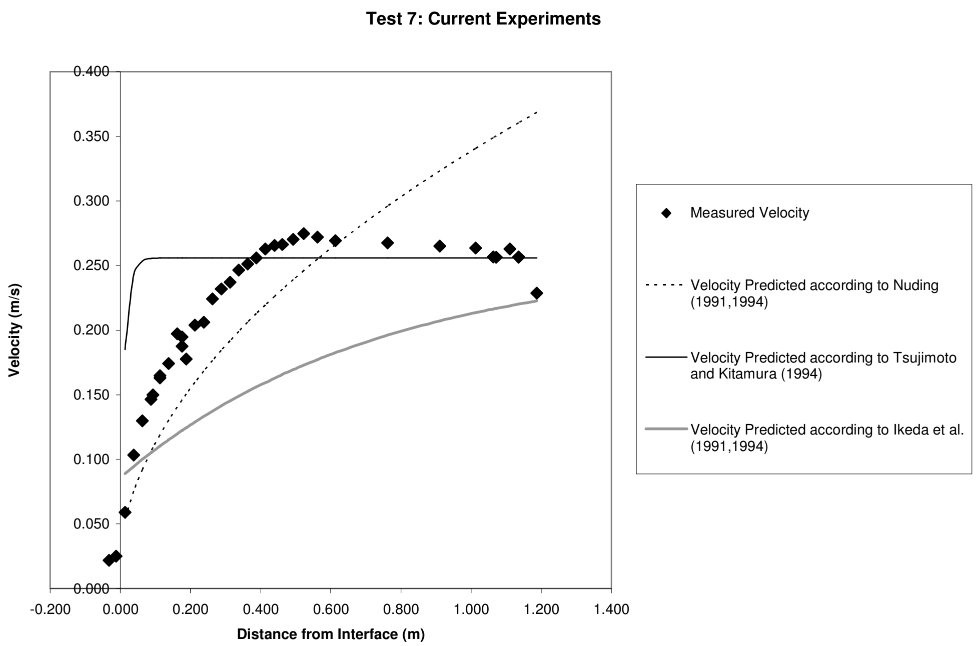

Figure 7-2: Predictions compared to Results of Current Experiments Test 7.

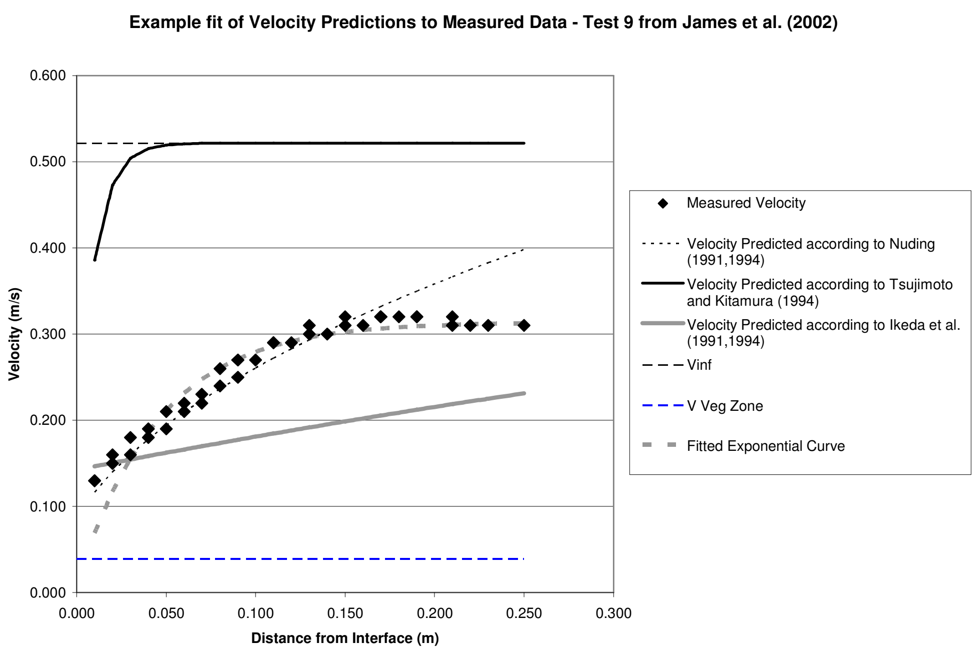

Figure 7-3: Predictions compared to Results of Test 9 from James et al. (2001)

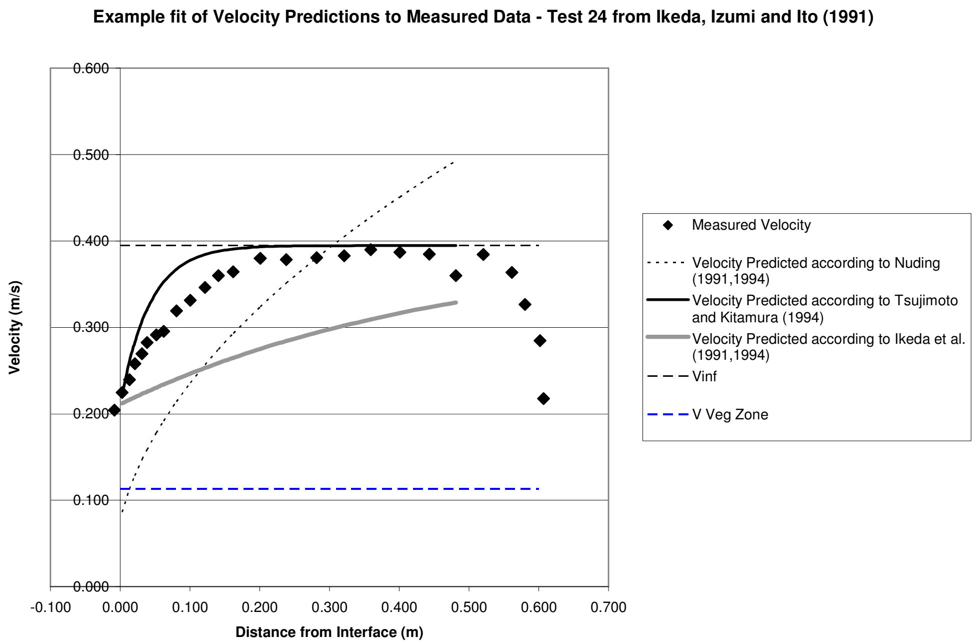

Figure 7-4: Predictions compared to Results of Test 24 from Ikeda, et al. (1991)

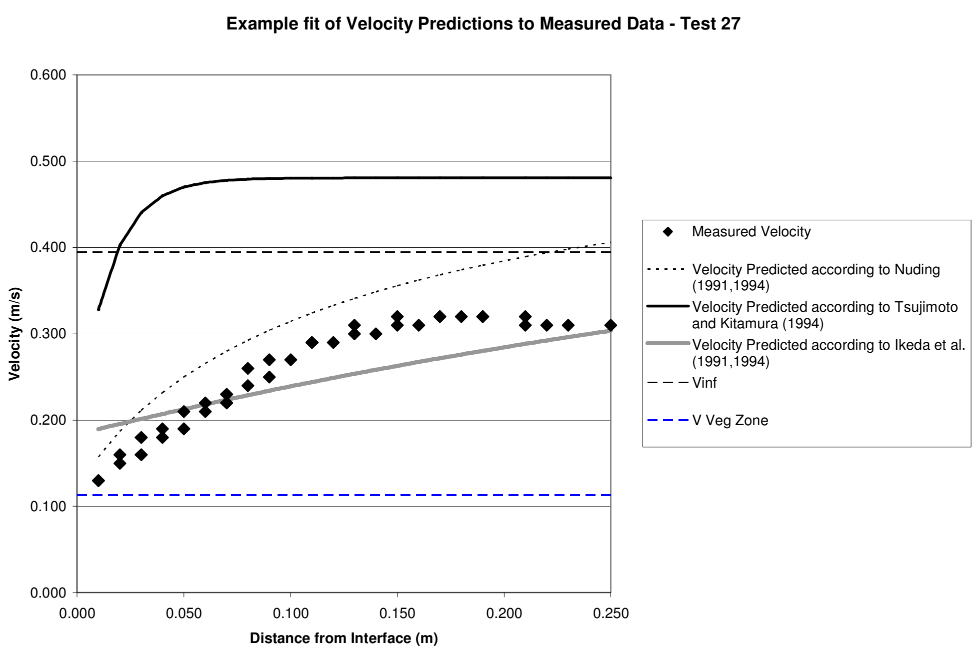

Figure 7-5: Predictions compared to Results of Test 27 from Kan and Nakai (1993) in Tsujimoto & Shimizu (1994)

Table 7-2: Root Mean Square Percentage Error in Velocity Prediction for Various Methods

Test	Method					
	Pasche and Rouvé (1985)	Nuding (1991, 1994) limited to V_{inf}	Nuding Modified for Bed Shear as specified in section 8.2.5	Tsujimoto and Kitamura (1994)	Ikeda et al. (1991, 1994)	Fitted Exponential Curve
7	1215%	18%	26%	53%	32%	
8	1123%	15%	24%	44%	29%	
9	1166%	9%	9%	117%	29%	13%
24	1993%	31%	31%	10%	21%	
27	3371%	14%	69%	154%	39%	

In conclusion, the method of Nuding (1991, 1994) performs best. For test 9, the root mean square percentage error in velocity is greater even for the fitted exponential distribution than for the prediction of Nuding (1991, 1994). The method of Nuding (1991, 1994) also performs particularly well in the experiment with the narrowest non-vegetated zone (test 9), indicating that it should be applicable for narrow non-vegetated zones despite the dependence of the velocity profile on the width for this case. The method of Nuding (1991, 1994) is also preferred because eddy viscosity is formulated as proportional to $(\partial V/\partial y)$, which is as was suggested in section 3.2. (See section 11.2.4 on page 130.)

This method was therefore selected as the basis for the further developments to be described in chapter 8.

8 Modifications to the Method of Nuding (1991, 1994)

8.1 Introduction

While the method of Nuding (1991, 1994) was shown to perform adequately against the data selected in Chapter 7, this method has shortcomings. This chapter will therefore propose improvements, using the velocity distribution equation of Nuding (1991, 1994) as a basis. Shortcomings are addressed as indicated below:

- The hydraulic resistance of the channel bed is expected to influence the lateral distribution of velocity. However, velocity profiles predicted according to the method of Nuding (1991, 1994) are independent of the bed resistance, except in so far as this affects the velocity with bed resistance only (V_{inf}) and the shear on the vegetation interface. In an attempt to directly incorporate the effect of bed shear, the basic velocity distribution equations are modified in section 8.2. The effect depends on the relation between the magnitude of depth-averaged velocity and the apparent shear on the vegetation interface. Three different velocity profiles are derived, based on different assumed relations between velocity and the apparent shear on the vegetation interface. Comparison with laboratory tests indicates problems with all three methods, and the original relation is therefore preferred.

- Velocity, and in particular the maximum velocity, has been shown to be lower in narrow channels. Two possible methods for taking this reduction into account are investigated. The superposition of velocity or momentum defects is described in section 8.3. An empirical relation between non-vegetated zone width and velocity is derived in section 8.4. The empirical relation is shown to perform well against independent laboratory data, whereas the superposition methods usually cannot predict the observed reduction in maximum velocity. The empirical relation is therefore selected.

- According to the method of Nuding (1991, 1994), the estimation of the interface shear velocity (u_v^*) involves a complicated procedure which incorporates the use of a composite roughness formula. Several approximations and assumptions are used, including the validity of the composite roughness formula, the validity of the equation suggested for calculation of the interface friction factor and the assumption of a constant friction factor for the bed. A more direct method of calculation is therefore suggested in section 8.5. A force balance over the non-vegetated zone can be used together with the velocity distribution equation to calculate the interface friction factor directly. Because this force balance incorporates the width, the effect of channel width on interface shear stress will be taken into account.

8.2 Incorporation of Bed Shear

8.2.1 Introduction and Shear Equation

The lateral velocity distribution equation of Nuding (1991, 1994) was presented as Equation (28):

$$V(y) = \frac{2.2u_v^*}{\log\left(\frac{V_{\inf}}{V_{VegZone}}\right)} \cdot \sqrt{\frac{h_T}{R_V}} \cdot \sqrt{1+\frac{y}{bm}} \qquad (28)$$

This equation does not account for the effect of resistance of the bed of the non-vegetated zone. In Nuding's analysis, this is considered separately for the total non-vegetated zone flow, only after integration of the velocity equation. It was therefore thought that a more accurate velocity profile could be derived by incorporating the effect of bed shear directly into the velocity equation. In order to do this, it must be assumed that there are two independent shear stresses acting on the fluid: a shear caused by the vegetation along a vertical plane parallel to the interface (τ_v), and a shear at the clear channel bed (τ_b). I consider the simplified case of a constant depth (D) across the section.

The force balance for uniform flow is shown schematically in Figure 8-1.

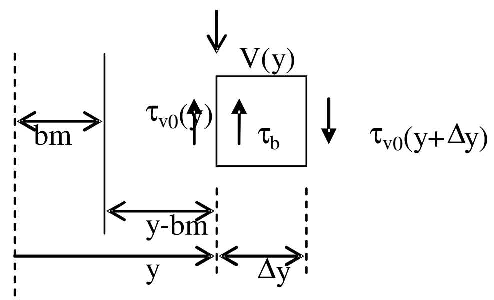

Figure 8-1: Balance of forces on an element extending through the flow depth (plan view)

$$[\tau_{vo}(y)-\tau_{vo}(y+\Delta y)]\cdot D\cdot l+\tau_b(y)\cdot\Delta y\cdot l=Weight \qquad (40)$$

Where : l is the length of channel being considered and

Weight is the weight of water within the control volume.

$$\therefore -\frac{d\tau_{vo}}{dy}\cdot\Delta y\cdot D\cdot l+\tau_b(y)\cdot\Delta y\cdot l=\gamma S\cdot\Delta y\cdot D\cdot l \qquad (41)$$

Where: γ is the weight of water per unit volume.

$$\therefore \frac{\tau_b(y)}{D}-\frac{d\tau_{v0}}{dy}=\gamma S \qquad (42)$$

An alternative derivation of this equation uses a control volume from the interface as shown in Figure 8-2, leading to:

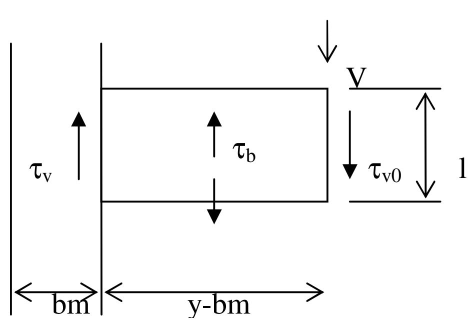

Figure 8-2: Balance of forces on an element extending from the vegetation boundary (plan view)

$$\left(\tau_v - \tau_{v0}\right) \cdot D \cdot \Delta x + \int_{bm}^{y} \tau_b \; dy \cdot l = Weight \times x$$

$$= \gamma \cdot S \cdot D \cdot l \cdot \left(y - bm\right) \qquad (43)$$

$$\tau_v - \tau_{v0} + \frac{1}{D}\int_{bm}^{y} \tau_b \; dy = \gamma \cdot S \cdot \left(y - bm\right)$$

This expression may be differentiated with respect to y:

$$\frac{\tau_b}{D} - \frac{d\tau_{v0}}{dy} = \gamma \cdot S \qquad (42)$$

Thus, equation (42) is again derived. Equation (42) incorporates both bed shear and the apparent shear on the vegetation interface. If this equation can be expressed in terms of (and solved for) velocity, the solution will yield a velocity profile in which both of these effects have been taken into account.

In order to solve this equation, relations for the magnitudes of the two shear stresses in terms of velocity are required. An expression for bed shear stress in terms of velocity is derived in section 8.2.2.There are various possible relations for the lateral vegetation shear (τ_v), depending on the assumptions made. I will suggest three possible methods, one in each of sections 8.2.3, 8.2.4 and 8.2.5.

8.2.2 Expression for Bed Shear Stress

Shear forces resisting flow (both skin friction and drag) are normally proportional to the square of the flow velocity. In this analysis, it is assumed that the friction at the bed (τ_b) is proportional to the square of the depth-averaged flow velocity. This assumption is implicit in resistance equations, such as the Darcy-Weisbach equation, which may be presented as:

$$\tau_b = \frac{\rho \cdot \lambda_b}{8} V^2 \tag{44}$$

We further note that for the case of a wide channel with bed shear only, the bed shear must be balanced by the downstream weight component, and the velocity is V_{inf} as defined previously. Thus:

$$\tau_b = \gamma \cdot D \cdot S = \frac{\rho \cdot f}{8} V_{\inf}^2 \tag{45}$$

Combining these two equations, we see that:

$$\tau_b = \gamma \cdot D \cdot S \frac{V^2}{V_{\inf}^2} \tag{46}$$

8.2.3 Shear on the Vegetation Interface using Nuding's (1991, 1994) Eddy Viscosity

From the definition of the horizontal eddy viscosity:

$$\tau_v = \rho \cdot \varepsilon_T \cdot \frac{dV}{dy} \tag{47}$$

Nuding (1994) gives an equation for horizontal eddy viscosity (ε_T), which is presented in section 11.2.4 on page 130. According to Nuding (1994), the factor $\varepsilon_3 = \varepsilon_T / (dV/dy)$ is a constant. Noting that for this situation dV/dy is positive, equation (47) becomes:

$$\tau_v = \rho \in_3 \left(\frac{dV}{dy} \right)^2 \tag{48}$$

Substituting Equations (46) and (48) into Equation (42) above:

$$\gamma \cdot S \frac{V^2}{V_{\inf}^2} - \frac{d}{dy}\left(\rho \cdot \varepsilon_3 \left(\frac{dV}{dy} \right)^2 \right) = \gamma S \tag{49}$$

$$\therefore \gamma \cdot S \frac{V^2}{V_{\inf}^2} - \rho \cdot \varepsilon_3 \cdot 2 \frac{dV}{dy} \frac{d^2 V}{dy^2} = \gamma S$$

$$\therefore \frac{V^2}{V_{\inf}^2} - \frac{2\varepsilon_3}{g \cdot S} \frac{dV}{dy} \frac{d^2 V}{dy^2} = 1 \tag{50}$$

(51)

Where: S is the energy slope.

Since this differential equation is implicit in depth average velocity (V), a numerical solution is suggested. The simplest approach is an explicit backward difference method. This approach is used without trying to ascertain the conditions under which the solution will converge. The notation used is: V_n is the velocity at distance y. V_{n-1} is the velocity at distance y-Δy etc.

$$\frac{V_n^2}{V_{\inf}^2} - \frac{2\varepsilon_3}{g \cdot S} \cdot \frac{V_n - V_{n-1}}{\Delta y} \cdot \frac{\dfrac{V_n - V_{n-1}}{\Delta y} - \dfrac{V_{n-1} - V_{n-2}}{\Delta y}}{\Delta y} = 1 \tag{52}$$

$$\therefore \frac{V_n^2}{V_{\inf}^2} - \frac{2\varepsilon_3}{g \cdot S} \cdot \frac{V_n - V_{n-1}}{\Delta y} \cdot \frac{V_n - 2V_{n-1} + V_{n-2}}{(\Delta y)^2} = 1 \tag{53}$$

$$\text{Let m} = \frac{2\varepsilon_3}{g \cdot S \cdot (\Delta y)^3} \tag{54}$$

$$\therefore \frac{V_n^2}{V_{\inf}^2} - m \cdot \left[V_n^2 - 2V_nV_{n-1} + V_nV_{n-2} - V_nV_{n-1} + 2V_{n-1}^2 - V_{n-1}V_{n-2}\right] = 1 \tag{55}$$

$$\therefore \frac{V_n^2}{V_{\inf}^2} - m \cdot \left[V_n^2 - 3V_nV_{n-1} + V_nV_{n-2} + 2V_{n-1}^2 - V_{n-1}V_{n-2}\right] = 1 \tag{56}$$

$$\therefore \left[\frac{1}{V_{\inf}^2} - m\right] V_n^2 + m \cdot \left[3V_{n-1} - V_{n-2}\right] \cdot V_n + \left[m \cdot V_{n-1} \cdot V_{n-2} - 2m \cdot V_{n-1}^2 - 1\right] = 0 \tag{57}$$

$$\boxed{\therefore \left[1 - \frac{1}{m \cdot V_{\inf}^2}\right] V_n^2 + \left[V_{n-2} - 3V_{n-1}\right] \cdot V_n + \left[\frac{1}{m} - V_{n-1} \cdot V_{n-2} + 2V_{n-1}^2\right] = 0} \tag{58}$$

This is a quadratic expression for V_n in terms of previous values, which can be solved using the usual quadratic formula:

$$x = \frac{-b \pm \sqrt{b^2 - 4a \cdot c}}{2a}. \tag{59}$$

8.2.4 Shear on the Vegetation Interface assuming that Lateral Shear Stress is inversely proportional to Distance

Nuding (1994) states that laboratory tests have suggested that shear stress due to vegetation is inversely proportional to transverse distance (y), leading to:

$$\tau_{v0}(y) = \tau_v \cdot bm/y \tag{60}$$

Where: bm is a transition width within the vegetation, as defined in section 4.4.5 on page 38 and
τ_{v0} is the transverse shear stress at any position y.

If this distribution is assumed to apply, then a different analysis may be used. Substituting equations (46) and (60) into equation (42) gives:

$$\gamma \cdot S \frac{V^2}{V_{\inf}^2} - \frac{d}{dy}\left(\tau_{v0} .bm \big/ y\right) = \gamma \cdot S \tag{61}$$

$$\therefore \gamma \cdot S \frac{V^2}{V_{\inf}^2} + \frac{\tau_v .bm}{y^2} = \gamma \cdot S \tag{62}$$

$$\therefore V^2 = V_{\inf}^2 \left(1 - \frac{\tau_v .bm}{y^2 \cdot \gamma \cdot S}\right) \tag{63}$$

$$\boxed{\therefore V = V_{\inf} \sqrt{1 - \frac{\tau_v .bm}{y^2 \cdot \gamma \cdot S}}} \tag{64}$$

Where: γ is again the weight of water per unit volume.

8.2.5 Shear on the Vegetation Interface assuming that τ_v (at the interface) α $(V-V_{VegZone})^2$ (at any distance away)

It was stated above that shear stress is generally proportional to the square of velocity. It is therefore assumed here that the vegetation shear stress (τ_v) is proportional to the square of the depth averaged velocity at any arbitrary distance (y-bm) from the interface. I will define constant of proportionality as G. This gives:

$$\tau_v(V) = G \cdot (V - V_{VegZone})^2 \tag{65}$$

Consider first the hypothetical case where the bed has no resistance and vegetation resistance only is acting on the flow. Assume a velocity at distance y-bm equal to the velocity V_{nb}, calculated according to Nuding's equation. Then:

$$\tau_v(V_{nb}) = G \cdot (V_{nb} - V_{VegZone})^2 = \gamma \cdot bf \cdot S \tag{66}$$

Where : bf is half the clear channel width

$$\therefore G = \frac{\gamma \cdot bf \cdot S}{(V_{nb} - V_{VegZone})^2} \tag{67}$$

$$\therefore \tau_V(V) = G \cdot (V - V_{VegZone})^2 = \frac{\gamma \cdot bf \cdot S}{(V_{nb} - V_{VegZone})^2} \cdot (V - V_{VegZone})^2 \tag{68}$$

A force balance over the entire non-vegetated zone gives:

$$\tau_b \cdot bf + \tau_v \cdot D = \gamma \cdot D \cdot S \cdot bf \tag{69}$$

$$\therefore \frac{\tau_b}{D} + \frac{\tau_v}{bf} = \gamma \cdot S \tag{70}$$

Substituting equations (46) and (68) into equation (70):

$$\therefore \frac{\gamma \cdot S}{V_{\inf}^2} \cdot V^2 + \frac{\gamma \cdot S}{(V_{nb} - V_{VegZone})^2} \cdot (V - V_{VegZone})^2 = \gamma \cdot S \tag{71}$$

$$\therefore \frac{V^2}{V_{\inf}^2} + \frac{V^2 - 2V \cdot V_{VegZone} + V_{VegZone}^2}{(V_{nb} - V_{VegZone})^2} = 1 \tag{72}$$

$$\therefore V^2 \left(\frac{1}{V_{\inf}^2} + \frac{1}{(V_{nb} - V_{VegZone})^2} \right) + V \left(\frac{2}{1 - \frac{V_{nb}}{V_{VegZone}}} \right) - 1 = 0 \tag{73}$$

By the quadratic formula:

$$V = \frac{\dfrac{2}{\dfrac{V_{nb}}{V_{VegZone}}-1} \pm \sqrt{\left(\dfrac{2}{\dfrac{V_{nb}}{V_{VegZone}}-1}\right)^2 + 4\left(\dfrac{1}{V_{\inf}^2} + \dfrac{1}{(V_{nb}-V_{VegZone})^2}\right)}}{2\left(\dfrac{1}{V_{\inf}^2} + \dfrac{1}{(V_{nb}-V_{VegZone})^2}\right)} \tag{74}$$

$$\therefore V = \frac{\dfrac{1}{\dfrac{V_{nb}}{V_{VegZone}}-1} \pm \sqrt{\left(\dfrac{1}{\dfrac{V_{nb}}{V_{VegZone}}-1}\right)^2 + \dfrac{1}{V_{\inf}^2} + \dfrac{1}{(V_{nb}-V_{VegZone})^2}}}{\dfrac{1}{V_{\inf}^2} + \dfrac{1}{(V_{nb}-V_{VegZone})^2}} \tag{75}$$

Where V_{nb} is the velocity calculated according to Nuding's (1991, 1994) original velocity equation (28) on page 62 without considering the effect of bed shear.

8.2.6 Comparison with Experimental Measurements

In order to see whether any of the above methods are appropriate, I have compared the velocities calculated by the methods described above with the measured velocity profile for test 9 (by Nagdi and Sharp (2000) in James et al., 2001). The experiment used a flow depth of 69.5mm in a channel with 250mm wide artificial vegetation strips on both sides and a 500mm total clear channel width. (See Appendix A.) The velocity with bed resistance only ($V_{\inf}$) was calculated using the value of Manning's n calculated for an empty flume. Interface shear stress is derived using a force balance and measured bed shear stress data, as described in section 4.4.6. This value is used in all calculations. For those methods which rely on previously calculated velocities at previous lateral positions, the original equation of Nuding (1991, 1994) is used to estimate the first two velocities closest to the interface. Results are plotted in Figure 8-3.

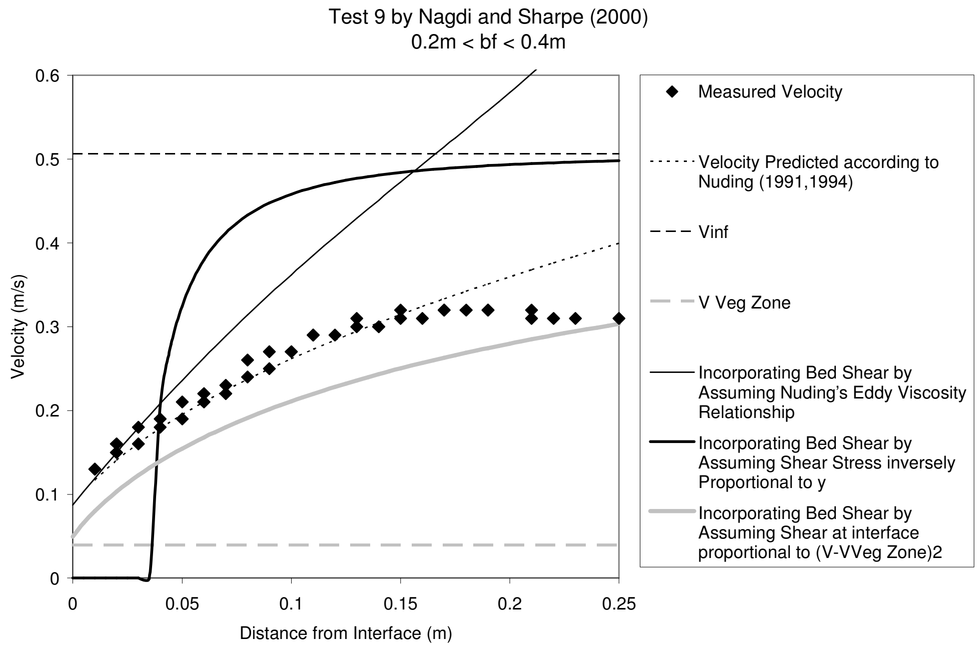

Figure 8-3: Comparison of Velocities Predicted by Incorporation of Bed Shear in Nuding's (1991, 1994) Equation with Test 9 from James et al. (2001)

The plot of predicted values calculated using Nuding's (1991, 1994) eddy viscosity relationship shows velocity increasing unrealistically to greater than V_{inf}. This method therefore seems incorrect.

Velocities calculated assuming that transverse shear stress is inversely proportional to lateral distance are also plotted. Close to the interface, velocities calculated in this way drop off very sharply, becoming imaginary close to the interface. This may, however, depend on the selection of an appropriate value of transition width bm. Further from the interface, they increase too quickly, even though they are still limited to Vinf.

The velocity profile produced using the assumption that transverse shear stress (τ_v) is proportional to the square of the velocity difference $(V - V_{VegZone})^2$, which was described in section 8.2.5 produces reasonably realistic results, and is clearly the best assumption. This method was therefore selected for comparison with those experiments to which the original equations were compared in section 7.5. Average percentage errors in velocity for the original and modified equations are presented in Table 7-2 on page 73. Incorporation of bed shear by this method makes no difference to the results of tests 9 and 24. For tests 7, 8 and 27, the prediction errors are greater when incorporating bed shear using this method than the prediction errors using the original equation of Nuding (1991, 1994) limited to V_{inf}. Furthermore, as has already been noted, the shape of several measured velocity profiles suggests that the rate of change of velocity with distance changes to zero suddenly as the final velocity V_{inf} is reached. Only the original method of Nuding (1991, 1994) predicts this sudden change. Incorporation of bed shear results in a more gradual, asymptotic change. The original equation is therefore preferred.

8.3 Superposition

8.3.1 Limit of Velocity with Bed Only & Superposition Purpose

As stated previously, the non-vegetated zone velocity predicted by Nuding (1991, 1994) continues to increase indefinitely with distance from the interface. For wider non-vegetated zones there will therefore also be a region in which the velocity predicted by the equation of Nuding (1991, 1994) is above V_{inf}. In this zone, velocity will apparently not be retarded by the vegetation, and the velocity may be taken as equal to the velocity V_{inf} which would be produced by bed resistance only.

In narrow non-vegetated zones, the lateral velocity distribution is produced by the interaction of the two interfaces on opposite sides of the non-vegetated zone. Where there is vegetation on both sides of the non-vegetated zone, there will be two interacting vegetation interfaces. Where there is vegetation on one side only, there may be a wall or other interface on the other side which will interact with the vegetation interface to produce a lateral velocity distribution. Some method is needed to take these interactions into account. The methods to be described here are a set of related simple methods to account for these interactions.

8.3.2 Superposition of Positive Velocity Defects

Where the velocity predicted by the equation of Nuding (1991, 1994) is less than the velocity produced with bed resistance only (V_{inf}), a velocity defect may be defined as the difference between the predicted or measured velocity and V_{inf}. In other words, the defect is the amount by which the velocity which would have been present with bed resistance only is reduced by the presence of the vegetation. (See Figure 8-4.) Where the predicted velocity would be greater than V_{inf}, there is no reduction, and the velocity defect may be taken as zero.

According to Desai and Chicktay (2005), it was suggested by Petryk (1969) that the velocity defects produced by different flow obstacles at any defined position may be added to derive a total velocity defect at that position which would be produced by a combination of obstacles. In a similar way, it is suggested here that the velocity defects produced by the interfaces on each side of a non-vegetated zone may be added to derive a total velocity defect at any lateral position. Following the method of Petryk (1969), the final velocity can then be predicted by subtracting the total velocity defect from the undisturbed velocity V_{inf}.

This method was tested specifically for the case of a narrow non-vegetated zone with vegetation on both sides. The procedure adopted is illustrated in Figure 8-4. For any lateral position, a different distance to each vegetation interface is defined. The velocity distribution equation of Nuding (1991, 1994) (Equation on page 62) was applied separately to each vegetation interface to derive a basic predicted velocity (V_{nb}). A velocity defect was then calculated as:

$$\text{Velocity Defect} = \begin{cases} V_{inf}-V_{nb} & \text{if } V_{nb}<V_{inf} \\ 0 & \text{if } V_{nb}>= V_{inf} \end{cases} \qquad (76)$$

The final velocity at each lateral position was then calculated as:

$$V = V_{inf} - (\text{Velocity Defect for Side 1} + \text{Velocity Defect for Side 2}) \quad (77)$$

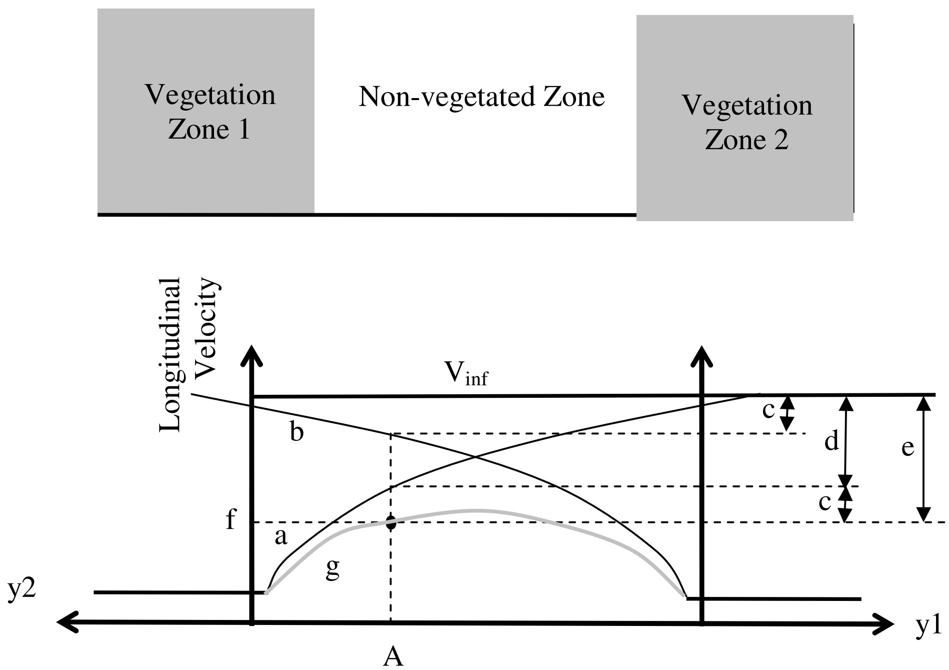

a: Predicted velocity profile for side 1 interface (V_{nb})
b: Predicted velocity profile for side 2 interface (V_{nb})
c: Velocity defect at position A for side 2 interface ($V_{inf} – V_{nb}$)
d: Velocity defect at position A for side 1 interface ($V_{inf} – V_{nb}$)
e: Total velocity defect at position A (e = c+d)
f: Velocity predicted by superposition of velocity defects ($V_{inf} – e$)
g: Velocity profile predicted by superposition of velocity defects (repeat procedure performed at A for all lateral positions)

Figure 8-4: Schematic Diagram for Superposition of Velocity Defects

This procedure was applied to the tests 9 to 17 (see Appendix A) performed by Nagdi and Sharpe (2000) in James et al. (2001). Results are presented in section 8.3.5.

8.3.3 Superposition of Measured Velocity Defects

When the velocity predictions by superposition of velocity defects are inaccurate, it is unclear whether the prediction errors are due to the superposition method, or due to inaccuracy in the original predictions which have been superimposed. It was therefore decided to test the method of superposition based on measured velocity distributions, rather than on predictions. The basic velocity defect used for superposition was that measured in Test 8. This test used the same type of vegetation used by Nagdi and Sharpe (2000) in James et al. (2001). It is shown in Chapter 6 that the channel used in test 8 was sufficiently wide that no significant change of velocity with non-vegetated zone width is expected. Velocity defects measured in test 8 were therefore taken as representative of the velocity profile to be expected in the absence of interaction with a wall or interface on the other side of the non-vegetated zone. These velocity defects were interpolated linearly with respect to lateral distance. They were then scaled for the effect of different (water surface) slopes by multiplying by the square root of the ratio of the slope used for test 8 (0.000 36) to the slope of used by Nagdi and Sharpe (2000) in James et al. (2001) (0.00107). These velocity defects were then superimposed as described above, and compared to the measured data for Tests 9, 10 and 11 of Nagdi and Sharpe (2000) in James et al. (2001). Results are presented in section 8.3.5.

8.3.4 Superposition of Momentum Defects

"Yano (1966) suggested a method for obtaining multi-cylinder wake behaviour through superposition of momentum defect fluxes, i.e.:

$$u_{total}^2 = u_1^2 + u_2^2 + ... \qquad (78)$$

where u = the velocity defect," Desai and Chicktay (2005). It was thought that this superposition method may be applied for superposition of the effect of two vegetation interfaces in the same way as the superposition of velocity defects. This method was applied by again using the velocity distribution equation of Nuding (1991, 1994) (Equation 28 on page 62) to derive a velocity defect for the vegetation interface on each side of the non-vegetated zone. However, instead of superimposing the velocity defects, the square of these defects was superimposed, as suggested by the equation above. These predictions were again compared to the results by Nagdi and Sharpe (2000) in James et al. (2001).

8.3.5 Results and Discussion

As stated above, superposition methods were applied to predict velocities for the tests 9 to 17, performed by Nagdi and Sharpe (2000) in James et al. (2001). The experiments were conducted with vegetation represented by staggered arrays of 5mm diameter steel rods with spacings ax = 12.5mm and ay = 25mm as defined in Figure 4-3. Experiments were conducted in a 1m wide flume at a constant slope of 0.00107. The range of depths is 32 to 91.2mm. Further details of each test are given in Appendix A. Based on these results, some comments will be made regarding the applicability of these superposition methods.

Superposition of the velocity readings of the wide channel test was applied to only three tests. In all cases, this method performed worse than the superposition of the predictions of Nuding (1991, 1994). It was therefore clear that the accuracy of the superposition method could not be improved by using available experimental data. Superposition of the wide channel results was therefore not considered for the other tests.

For most tests (i.e. tests 10 to 13, 15 and 17), the width of the non-vegetated zone is sufficient for the predicted velocity from each side to reach the maximum value of V_{inf} in the middle of the non-vegetated zone. This situation is depicted in Figure 8-7. In this case, the velocity predicted by the original equation of Nuding (1991, 1994) reaches V_{inf}, and is therefore limited to V_{inf}. There is no difference between the predictions using the superposition of either velocity or momentum defects and those using the original equation limited to V_{inf}. This is because, in the region influenced by any one interface, there is no velocity defect for the other interface to be added. The final result is therefore the original velocity distribution. However, the test results do indicate a dependence of velocity on

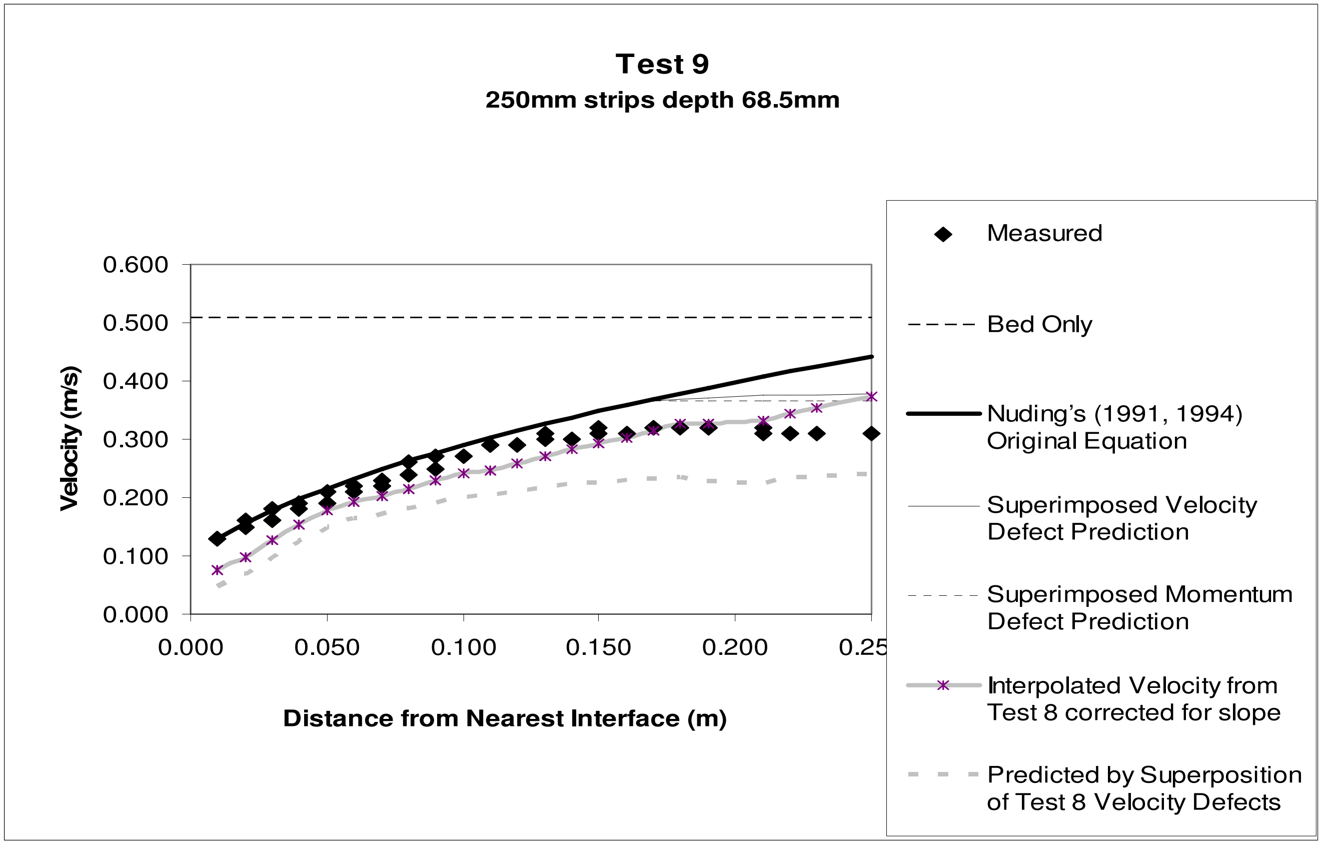

Figure 8-5: Results for Superposition Methods: Test 9 by Nagdi and Sharpe (2000) in James et al. (2001)

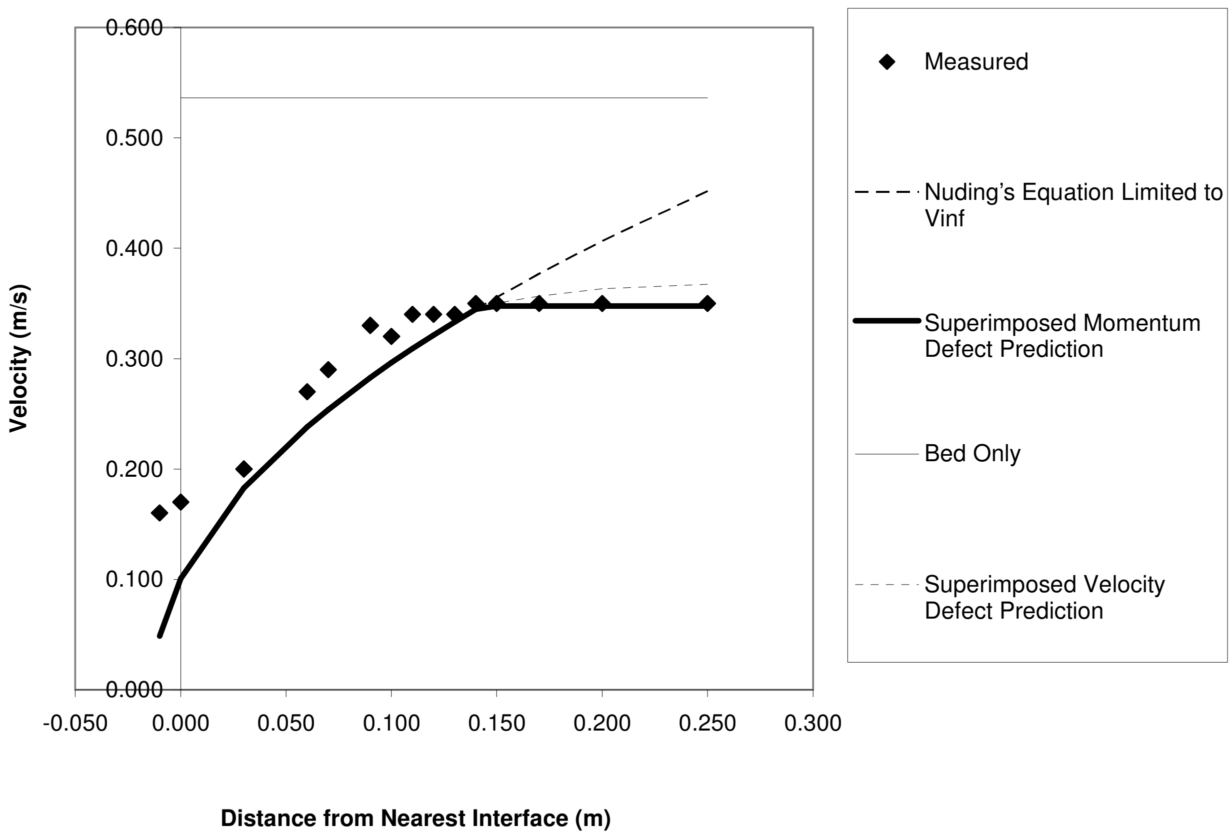

Figure 8-6: Results for Superposition Methods: Test 14 by Nagdi and Sharpe (2000) in James et al. (2001)

Table 8-1: Errors in Velocity Prediction for Superposition Methods

		Test	9	10	11	12	13	14	15	16	17
		bf / TW Wide	0.6	1.1	1.0	1.7	1.1	0.6	1.1	0.9	1.0
Average Absolute Error in Velocity Prediction	(m/s)	Nuding's Equation for one side limited to V_{inf}	0.035	0.054	0.082	0.020	0.040	0.039	0.098	0.072	0.036
		Superposition of Velocity Defects Predicted by Nuding's Equation	0.028	0.054	0.093	0.020	0.040	0.029	0.098	0.072	0.036
		Superposition of Slope Adjusted Velocity Defects Measured in Wide Channel Test	0.076	0.115	0.241						
		Superposition of Momentum Defects Predicted by Nuding's Equation	0.06	0.054	0.082	0.020	0.040	0.027	0.098	0.072	0.036
Maximum Absolute Error in Velocity Prediction	(m/s)	Nuding's Equation for one side limited to V_{inf}	0.132	0.177	0.143	0.040	0.095	0.111	0.143	0.094	0.075
		Superposition of Velocity Defects Predicted by Nuding's Equation	0.067	0.177	0.158	0.040	0.095	0.111	0.143	0.094	0.075
		Superposition of Slope Adjusted Velocity Defects Measured in Wide Channel Test	0.095	0.182	0.332						
		Superposition of Momentum Defects Predicted by Nuding's Equation	0.056	0.177	0.143	0.040	0.095	0.111	0.143	0.094	0.075
Root Mean Square of (Prediction Error as % of Measured Velocity)	(%)	Nuding's Equation for one side limited to V_{inf}	16%	25%	27%	9%	24%	24%	31%	21%	23%
		Superposition of Velocity Defects Predicted by Nuding's Equation	12%	25%	27%	9%	24%	22%	31%	21%	23%
		Superposition of Slope Adjusted Velocity Defects Measured in Wide Channel Test	33%	46%	58%						
		Superposition of Momentum Defects Predicted by Nuding's Equation	11%	25%	27%	9%	24%	22%	31%	21%	23%

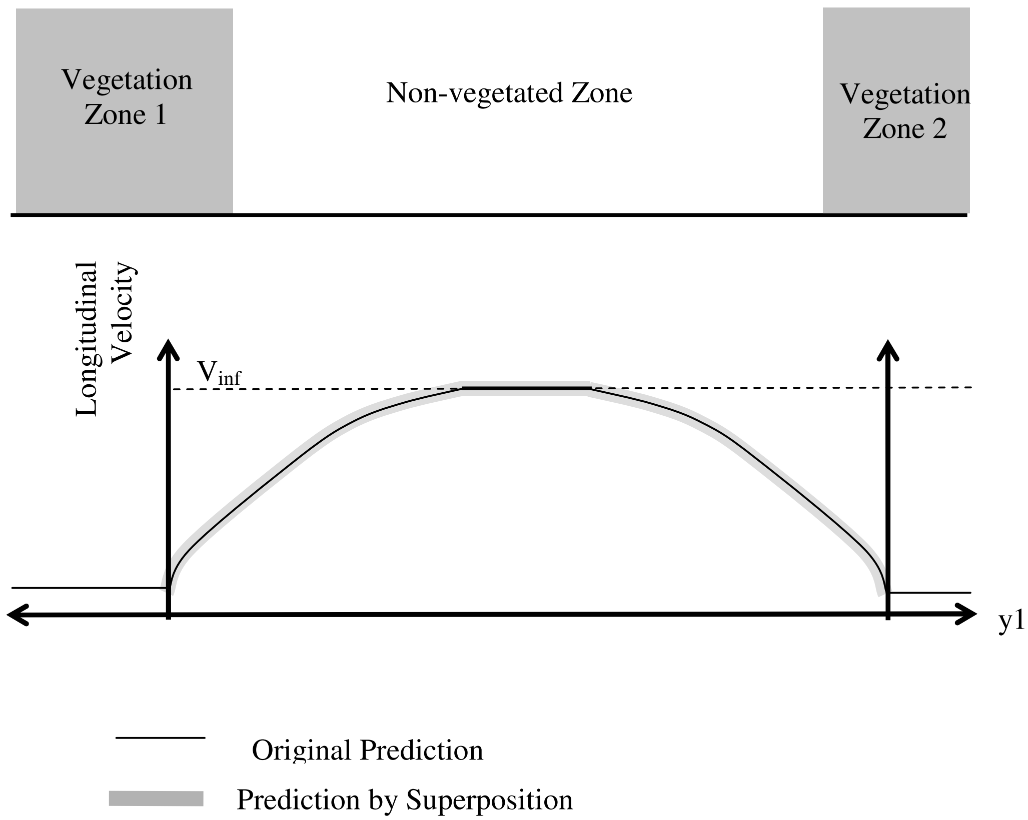

Figure 8-7: Schematic Diagram of Superposition in a Wider Channel

non-vegetated zone width. The analysis in section 8.4 indicates that the non-vegetated zone width in all but one of these tests is sufficiently narrow for the velocity profile (and the maximum velocity) to be affected by the width. This influence cannot be predicted by any superposition method.

Superposition therefore affects only tests 9 and 14. (In test 16, there is theoretically a slight effect, since bf / TW Wide = 0.9<1, but the effect is negligible.) The results of these two tests are plotted in Figure 8-5 and Figure 8-6 respectively, together with the velocities predicted by the various superposition methods. The accuracy of the predictions is analysed in Table 8-1. While superposition does predict some reduction in velocity for tests 9 and 14, the maximum velocity in test 9 remains too high. For test 14, the velocity defect superposition is fairly accurate, although the maximum velocity is slightly over-predicted. For test 14, the momentum defect superposition provides a good estimate of the maximum velocity.

A final comment is that superposition methods can predict that the lateral velocity profile will flatten out at a velocity below that produced by the bed only. The predictions for test 9 (illustrated in Figure 8-5) are a clear example of this effect. Flattening of the velocity profile has been observed in several tests.

8.4 Reduction of Maximum Velocity in Narrow Channels

8.4.1 Introduction

If a non-vegetated zone is wide enough, it is expected that (far enough from the vegetation), the effect of the vegetation would die out, and the velocity would be that produced by the bed only. The current experiments (described in Chapter 6) were designed to illustrate that this is indeed the case.

In a narrower non-vegetated zone, the vegetation will be expected to influence velocities all the way across the zone, and the velocity produced by bed resistance only will not be reached. This effect was described in section 5.3, and was illustrated with respect to the results of James et al. (2001) in Figure 5-2 on page 51. As mentioned above, this effect cannot be accounted for by the superposition methods. A more empirical formulation for maximum velocity in terms of non-vegetated zone width is therefore suggested here, based on the results in James et al. (2001).

Tests 9, 11, 14, 15, 16, 18, 19, 20, 39, 43, 44, 45, 48, 51, 53, 56, 63, 64, 65, 68, 73 (See Appendix A) were selected for the development of this empirical relation. All of these are tests of James et al. (2001), the conditions of which were described in Table 5-1 on page 48. Detailed conditions for each test are listed in Appendix A. These tests were selected to cover a wide range of non-vegetated zone widths. (bfo varied from 0.087 to

0.450 m.). They were also selected to include experiments performed by both Makoa (2001) (Four tests) and Nagdi and Sharpe (2000) (Five tests).

8.4.2 Non-dimensional Parameters

The aim was to relate maximum velocity to non-vegetated zone width. In order to allow the relations developed to be generalised, it was desired to express both these quantities in dimensionless form. As mentioned previously, the velocity profile is produced to form a transition between the two extremes of velocity with bed resistance only (V_{inf}) and the velocity in a fully vegetated channel ($V_{VegZone}$). The obvious non-dimensional form for velocity is therefore in terms of these two extremes. Thus, the dimensionless velocity V_{DL} is expressed as:

$$V_{DL} = (V-V_{VegZone})/ (V_{inf}-V_{VegZone}) \qquad (79)$$

When V refers to the maximum velocity (V_{max}), V_{DL} will refer to the dimensionless maximum velocity ($V_{DL\ max}$).

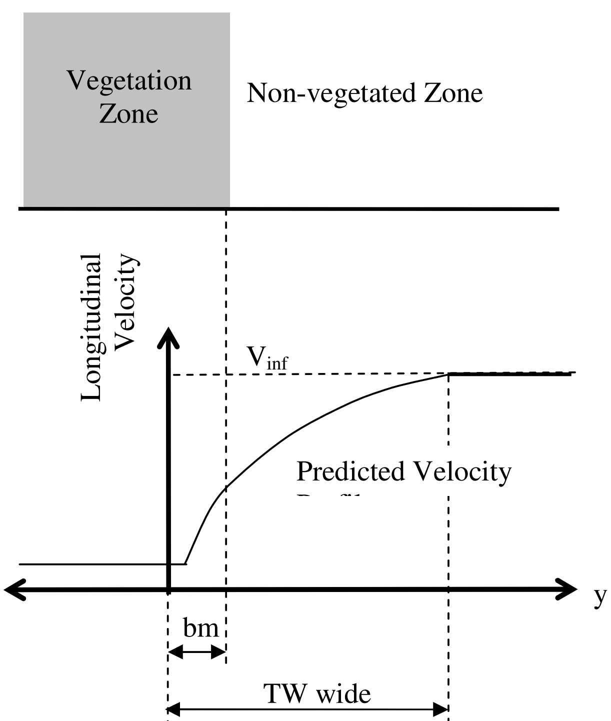

Figure 8-8: Definition Sketch for Transition Width

Note that this dimensionless velocity will be equal to 0 for a velocity of $V_{VegZone}$ and equal to 1 for a velocity of V_{inf}. Several possible non-dimensional ratios for the non-vegetated zone width were considered. These included the ratio of non-vegetated zone width to depth, vegetation spacing and Nuding's (1991, 1994) transition width parameter bm. The final choice seemed more intuitively appropriate, and will be described below.

Consider the velocity distribution equation of Nuding (1991, 1994) (Equation 28 on page 62). For a wide non-vegetated zone, there will be a certain transition width (TW Wide) over which the velocity reaches V_{inf}, as illustrated in Figure 8-8. (Note that as indicated in the figure, the transition width is measured from the origin of the velocity distribution equation a distance bm within the interface.) Because TW Wide is the width over which the velocity profile is scaled, it is seen as a particularly appropriate length dimension with which to non-dimensionalise the non-vegetated zone width. The non-dimensional width is therefore taken as the ratio of the non-vegetated zone width to TW Wide. An expression for TW Wide was needed, and this will now be derived:

8.4.3 Derivation of an Expression for TW Wide

Consider the shear stress with bed resistance only:

$$\tau_{b\,\inf} = \rho \cdot g \cdot D \cdot S \tag{80}$$

Where: $\tau_{b\,\inf}$ is the bed shear stress with bed resistance only.

Darcy-Weisbach resistance equation:

$$V_{\inf} = \sqrt{\frac{8}{\lambda_b}} \cdot \sqrt{g \cdot D \cdot S} \tag{81}$$

$$\therefore \tau_{b\,\inf} = \frac{\rho \cdot \lambda_b}{8} \cdot V_{\inf}^2 \tag{82}$$

Consider a force balance on the transition width only:

$$\frac{F_v}{\rho \cdot l} + \frac{F_b}{\rho \cdot l} = g \cdot D \cdot S \cdot (TW\ wide - bm) \tag{83}$$

Where: F_v is the apparent shear force on the vegetation interface.

F_b is the bed shear force.

L is the length of the channel.

$$\frac{F_v}{\rho \cdot l} = D \cdot \tau_b / \rho = D \cdot u_v^{*2} \tag{84}$$

$$\frac{F_b}{\rho \cdot l} = \frac{1}{\rho} \int_{bm}^{TW\ wide} \tau_b\ dy \tag{85}$$

Subs (82):

$$\frac{F_b}{\rho \cdot l} = \frac{\lambda_b}{8} \int_{bm}^{TW\ wide} V^2\ dy \tag{86}$$

Nuding's (1991, 1994) velocity distribution equation:

$$V = \frac{K \cdot u_v^*}{\log\left(\dfrac{V_{\inf}}{V_{VegZone}}\right)} \cdot \sqrt{\frac{h_T}{R_v}} \cdot \sqrt{\frac{y}{bm}} \tag{28}$$

Subs (86):

$$\begin{aligned} \frac{F_b}{\rho \cdot l} &= \frac{\lambda_b}{8} \frac{h_T}{R_v} \frac{K^2 \cdot u_v^{*2}}{bm \cdot \left[\log\left(\dfrac{V_{\inf}}{V_{VegZone}}\right)\right]^2} \cdot \int_{bm}^{TW\ wide} y\ dy \\ &= \frac{\lambda_b \cdot h_T \cdot K^2 \cdot u_v^{*2}}{8 \cdot bm \cdot R_v \cdot \left[\log\left(\dfrac{V_{\inf}}{V_{VegZone}}\right)\right]^2} \cdot \left[\frac{y^2}{2}\right]_{bm}^{TW\ wide} \end{aligned} \tag{87}$$

$$\frac{F_b}{\rho \cdot l} = \frac{\lambda_b \cdot h_T \cdot K^2 \cdot u_v^{*2} \cdot \left(TW\ wide^2 - bm^2\right)}{8 \cdot bm \cdot R_v \cdot \left[\log\left(\dfrac{V_{\inf}}{V_{VegZone}}\right)\right]^2} \tag{88}$$

Subs (82) and (86) into (83):

$$D \cdot u_v^{*2} + \frac{\lambda_b \cdot K^2 \cdot h_T \cdot u_v^{*2} \cdot \left(TW\ wide^2 - bm^2\right)}{16 \cdot bm \cdot R_v \cdot \left[\log\left(\frac{V_{\inf}}{V_{VegZone}}\right)\right]^2} = g \cdot D \cdot S \cdot \left(TW\ wide - bm\right) \tag{89}$$

$$\therefore u_v^{*2} = \frac{g \cdot D \cdot S \cdot \left(TW\ wide - bm\right)}{D + \frac{\lambda_b \cdot K^2 \cdot h_T \cdot TW\ wide^2 - bm^2}{16 \cdot bm \cdot R_v \cdot \left[\log\left(\frac{V_{\inf}}{V_{VegZone}}\right)\right]^2}} \tag{90}$$

$$\therefore u_v^{*2} = \frac{g \cdot D \cdot S \cdot \left(TW\ wide - bm\right)}{\frac{g \cdot D \cdot S}{g \cdot S} + \frac{\lambda_b}{8} \cdot \frac{K^2 \cdot h_T \cdot TW\ wide^2 - bm^2}{2 \cdot bm \cdot R_v \cdot \left[\log\left(\frac{V_{\inf}}{V_{VegZone}}\right)\right]^2}} \tag{91}$$

From (81): $g \cdot D \cdot S = \frac{\lambda_b}{8} \cdot V_{\inf}^2$ (92)

$$\therefore u_v^{*2} = \frac{\frac{\lambda_b}{8} \cdot V_{\inf}^2 \cdot \left(TW\ wide - bm\right)}{\frac{\lambda_b \cdot V_{\inf}^2}{8 \cdot g \cdot S} + \frac{\lambda_b}{8} \cdot \frac{K^2 \cdot h_T \cdot \left(TW\ wide^2 - bm^2\right)}{2 \cdot bm \cdot R_v \cdot \left[\log\left(\frac{V_{\inf}}{V_{VegZone}}\right)\right]^2}} \tag{93}$$

$$\boxed{\therefore u_v^{*} = \sqrt{\frac{\left(TW\ wide - bm\right)}{\frac{1}{g \cdot S} + \frac{K^2 \cdot h_T \cdot \left(TW\ wide^2 - bm^2\right)}{2 \cdot bm \cdot R_v \cdot V_{\inf}^2 \cdot \left[\log\left(\frac{V_{\inf}}{V_{VegZone}}\right)\right]^2}}}} \tag{94}$$

From Equation (28):

$$V^2 = \frac{K^2 \cdot h_T \cdot u_v^{*2} \cdot y}{bm \cdot R_v \cdot \left[\log\left(\frac{V_{\inf}}{V_{VegZone}}\right)\right]^2} \tag{95}$$

At y = TW wide, V = V_{inf}

$$\therefore V_{\inf}^2 = \frac{K^2 \cdot h_T \cdot u_v^{*2} \cdot TW\ wide}{bm \cdot R_v \cdot \left[\log\left(\frac{V_{\inf}}{V_{VegZone}}\right)\right]^2} \tag{96}$$

Subs (94):

$$\therefore V_{\inf}^2 = \frac{K^2 \cdot h_T \cdot TW\ wide}{bm \cdot R_v \cdot \left[\log\left(\frac{V_{\inf}}{V_{VegZone}}\right)\right]^2} \times \frac{TW\ wide - bm}{\frac{1}{g \cdot S} + \frac{K^2 \cdot h_T \cdot \left(TW\ wide^2 - bm^2\right)}{2 \cdot bm \cdot R_v \cdot V_{\inf}^2 \cdot \left[\log\left(\frac{V_{\inf}}{V_{VegZone}}\right)\right]^2}} \tag{97}$$

$$\therefore V_{\inf}^2 = \frac{TW\ wide \cdot \left(TW\ wide - bm\right)}{\frac{bm \cdot R_v \cdot \left[\log\left(\frac{V_{\inf}}{V_{VegZone}}\right)\right]^2}{K^2 \cdot h_T \cdot g \cdot S} + \frac{\left(TW\ wide^2 - bm^2\right)}{2 \cdot V_{\inf}^2}} \tag{98}$$

$$\therefore V_{\inf}^2 \left[\frac{bm \cdot R_v \cdot \left[\log\left(\frac{V_{\inf}}{V_{VegZone}}\right)\right]^2}{K^2 \cdot h_T \cdot g \cdot S}\right] + \frac{TW\ wide^2}{2} - \frac{bm^2}{2} = TW\ wide^2 - TW\ wide \cdot bm \tag{99}$$

$$\therefore \frac{1}{2} TW\ wide^2 - bm \cdot TW\ wide + \frac{1}{2} bm^2 - \frac{bm \cdot R_v \cdot V_{\inf}^2 \cdot \left[\log\left(\frac{V_{\inf}}{V_{VegZone}}\right)\right]^2}{K^2 \cdot h_T \cdot g \cdot S} = 0 \tag{100}$$

$$\therefore TW\ wide^2 - 2 \cdot bm \cdot TW\ wide + \left[bm^2 - \frac{2 \cdot bm \cdot R_v \cdot V_{\inf}^2 \cdot \left[\log\left(\frac{V_{\inf}}{V_{VegZone}}\right)\right]^2}{K^2 \cdot h_T \cdot g \cdot S}\right] = 0 \tag{101}$$

Quadratic Formula:

$$TW\ wide = \frac{2 \cdot bm \pm \sqrt{4 \cdot bm^2 - 4 \cdot bm^2 + \dfrac{4 \cdot 2 \cdot V_{\inf}^2 \cdot bm \cdot R_v \cdot \left[\log\left(\dfrac{V_{\inf}}{V_{VegZone}}\right)\right]^2}{K^2 \cdot h_T \cdot g \cdot S}}}{2} \quad (102)$$

Note that the one root will fall inside the vegetation. Take the one outside:

$$\boxed{TW\ wide = bm + \sqrt{\frac{2 \cdot bm \cdot R_v}{h_T \cdot g \cdot S}} \cdot \frac{V_{\inf}}{K} \cdot \log\left(\frac{V_{\inf}}{V_{VegZone}}\right)} \quad (103)$$

Where: K is a constant equal to 2.2, as suggested by Nuding (1994).
S is the energy slope
bm (Nuding's transition width) is calculated as described on page 38.

The relevant dimensionless parameter is then the non-vegetated zone (half) width plus contributing width (bfo+bm=bf) divided by the wide channel transition width (bf / TW Wide).

8.4.4 Check

This equation may be checked as follows:

From Equation (103):

$$(TW\ wide - bm)^2 = \frac{V_{\inf}^2}{K^2} \cdot \frac{2 \cdot bm \cdot R_v}{h_T \cdot g \cdot S} \cdot \left[\log\left(\frac{V_{\inf}}{V_{VegZone}}\right)\right]^2 \quad (104)$$

$$\therefore \frac{bm \cdot R_v}{K^2 \cdot h_T \cdot g \cdot S} \cdot \left[\log\left(\frac{V_{\inf}}{V_{VegZone}}\right)\right]^2 = \frac{(TW\ wide - bm)^2}{2 \cdot V_{\inf}^2} \quad (105)$$

In Equation (98):

$$\text{Right Hand Side} = \frac{TW\ wide \cdot (TW\ wide - bm)}{\frac{(TW\ wide - bm)^2}{2 \cdot V_{inf}^2} + \frac{TW\ wide^2 - bm^2}{2 \cdot V_{inf}^2}}$$

$$= \frac{2 \cdot TW\ wide \cdot V_{inf}^2}{(TW\ wide - bm) + (TW\ wide + bm)} \quad (106)$$

$$= \frac{2 \cdot TW\ wide \cdot V_{inf}^2}{2 \cdot TW\ wide}$$

$$= V_{inf}^2$$

$$= \text{Left Hand Side}$$

8.4.5 Development

The aim of this development was to relate the maximum velocity occurring in a non-vegetated zone to its width. A relationship therefore had to be found between the dimensionless parameters V_{DL} at the maximum velocity and bf / TW Wide. For a wide channel, the influence of the vegetation will not extend across the channel, and the maximum velocity reached will be equal to V_{inf}. We thus have a limit that V_{DL} will reach a maximum value of 1 for some unknown value of bf / TW Wide.

A relation had to be fitted to the maximum measured velocity for each experiment, expressed in dimensionless terms. A straight line with a slope of 0.674 and a $V_{DL\ max}$-intercept of 0.132 proved to provide a good fit ($r^2 = 0.82$) to the maximum measured velocities. The data and fitted line are shown in Figure 8-9. A line of the fitted slope reaches the maximum value of ($V_{DL\ max} = 1$) at (bf / TW Wide = 1.29). In other words, the non-vegetated zone width will reduce the maximum velocity reached if and only if it is less than 1.29 times the wide channel transition width. For wider channels, V_{DL} becomes constant. The full equation thus becomes:

$$V_{DL}\,max = \begin{cases} 0.674\ bf / TW\ Wide + 0.132 & : bf / TW\ Wide \le 1.29 \\ 1 & : bf / TW\ Wide \ge 1.29. \end{cases} \quad (107)$$

This will be used together with the definition of dimensionless velocity in Equation (79) on page 94.

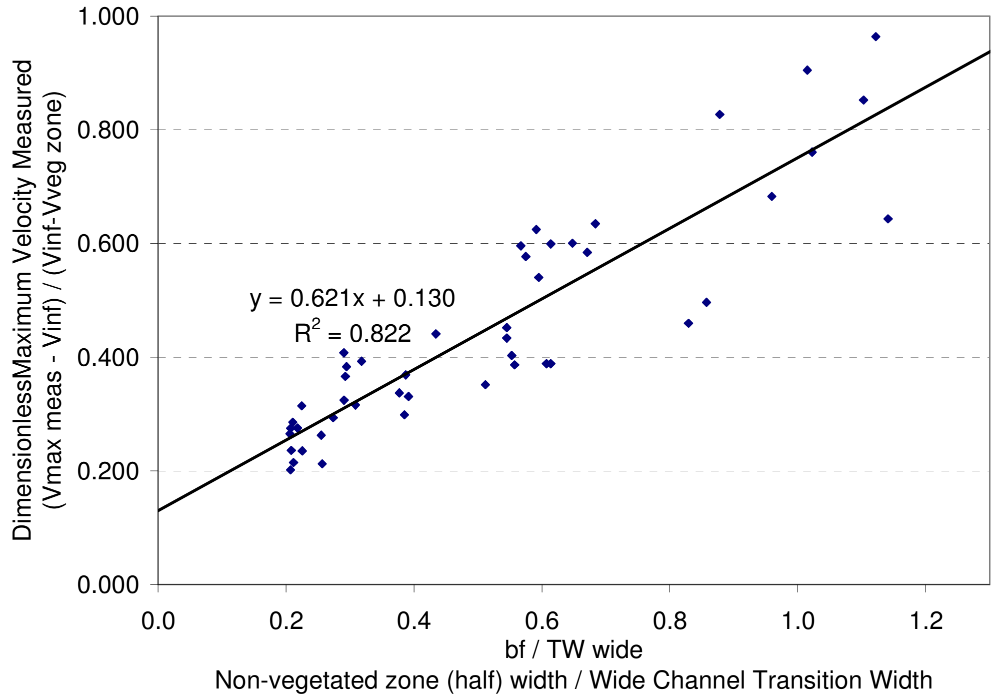

Figure 8-9: Fit of Equation for Maximum Velocity in Narrow Non-vegetated Zones

Finally, the predicted maximum velocity may be used to modify the entire velocity profile. The profile is driven by the velocity differences existing between the vegetation and non-vegetated zones. The velocity difference actually occurring is that between the maximum velocity (V_{max}) and $V_{VegZone}$. Consider again Nuding's velocity distribution equation (28) on page 62. Since the momentum transfer is now driven by V_{max} rather than V_{inf}, the distribution produced will reflect this. It is therefore proposed that in this equation V_{inf} should be replaced by V_{max}. Again, velocity must be limited to its own maximum value, leading to:

$$V(y) = \text{The smaller of : } \begin{cases} 2.2 \cdot u_v^* / \log\left(V_{max} / V_{VegZone}\right) \times \sqrt{h_T / R_v} \times \sqrt{y/bm} \\ V_{max} \end{cases} \quad (108)$$

Where: h_T is the depth at the vegetation interface

R_v is the hydraulic radius of the vegetation zone.

8.4.6 Results

Additional experimental data from a further 27 narrow channel tests and 49 wide channel tests not used in the development of equation (107) were used to test the equation. These included all tests listed in Table 5-1 on page 48 and all of the current tests (except those with no vegetation) listed in Table 6-1 on page 55. Full details of each test are given in Appendix A. The fit of equation (107) to all the tests analysed is indicated in Figure 8-10 and Figure 8-11. In Figure 8-10 , data are classified according to whether they were measured in narrow channels (with bf / TW Wide < 1.29) or wide channels (with bf / TW Wide > 1.29). For narrow channels, those experiments used to fit equation (107) are also separated from those which were not used.

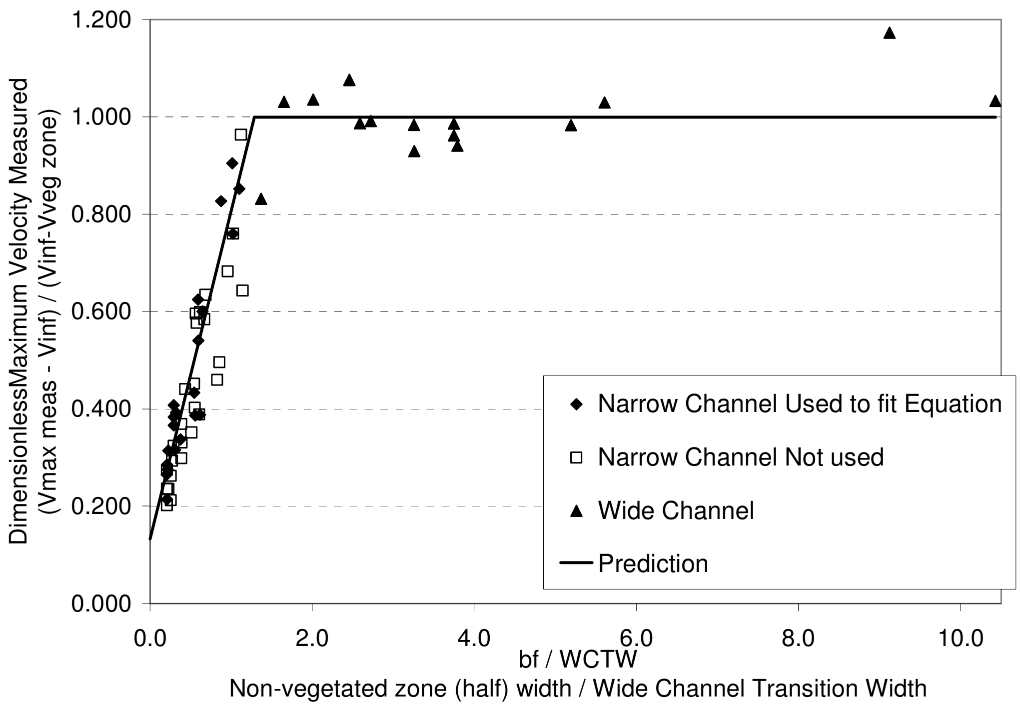

Figure 8-10: Prediction for Maximum velocity compared to maximum measured velocity in terms of non-vegetated zone width

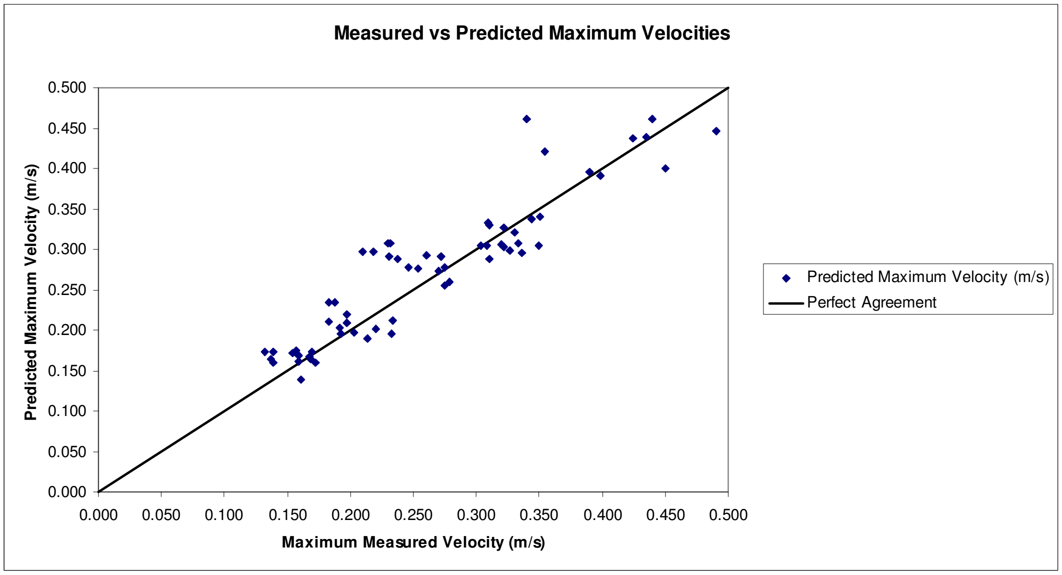

Figure 8-11: Graph of Predicted vs. Measured Maximum Velocity

8.4.7 Discussion

The equation proposed provides a reasonable estimate of the maximum velocity attained in both wide and narrow non-vegetated zones. (Average errors are 0.03m/s for the narrow channel experiments not used to fit the equation and also 0.03m/s for the wide channel experiments. The root mean square error (as a percentage of measured maximum velocity) for these sets of experiments were 13% and 19% respectively, giving an overall root mean square percentage error for all 49 experiments of 15%. It is not possible to isolate the errors caused by different factors. However, a large part of this error may be due to experimental error. In particular, as was discussed in section 6.5, errors in the measurement of slope are particularly significant. In view of these errors, it may not be possible to derive a more accurate method for the estimation of maximum velocity. The method described here is therefore proposed for further use.

The maximum velocity reached in the channel is itself an important consideration in ecological studies, and is frequently the first parameter to be estimated. However, it can also be used to estimate the entire transverse velocity profile using equation (108) on page 101. In this equation, the interface shear velocity (u_v*) will also change as the non-vegetated zone width changes. A method to determine the magnitude of interface shear will therefore be considered next.

8.5 Force Balance to Derive Interface Shear

8.5.1 Approach

Equations (24) on page 39 and (30) on page 64 were suggested by Nuding (1991, 1994) for estimation of the shear on the vegetation interface:

$$\frac{1}{\sqrt{\lambda_T}} = \frac{0.518}{\log\left(\frac{V_{\inf}}{V_{VegZone}}\right)} \cdot \sqrt{\frac{h_T}{R_v}} \cdot \sqrt{\frac{bfo}{bm}} \tag{24}$$

$$u_T^* = V_{ave,nv} \cdot \sqrt{\lambda_T / 8} \tag{30}$$

The estimation of the average velocity in the non-vegetated zone ($V_{ave,nv}$) involves a complicated procedure which incorporates the use of a composite roughness formula. Several approximations and assumptions are used, including the validity of the composite roughness formula, the validity of the equation suggested for calculation of the interface friction factor and the assumption of a constant friction factor for the bed. A more direct method of calculation is therefore desired. A force balance over the non-vegetated zone (or the portion within the wide channel transition width) can be used together with the velocity distribution equation to calculate the interface friction factor directly.

The assumption used is that bed shear stress is proportional to the square of depth average velocity. (This may also be formulated as a constant friction factor for the bed.) This assumption was already justified in section 8.1. It will not be completely accurate here, because the bed shear stress will depend on the shape of the vertical velocity profile, and not only on the depth-average value. Furthermore, it is known (for example, Sand-Jensen and Pedersen, 1999, Xiaohui and Li, 2002) that the vertical velocity profile changes from a more uniform profile close to the vegetation to approximate a logarithmic profile distant from the vegetation. Nevertheless, this assumption is expected to be sufficiently accurate to derive a reasonable estimate of the apparent shear stress on the interface.

The equations of this method will be derived and presented in sections 8.5.2, 8.5.3 and 8.5.5. In summary, the method is as follows:

1. A resistance equation is manipulated to derive the following expression for bed shear stress in terms of local depth average velocity (V) and V_{inf}:

   $$\tau_b = \gamma \cdot D \cdot S \cdot \left(V/V_{\inf}\right)^2 \qquad (46)$$

   Where: D is the flow depth
   γ is the weight of water per unit volume.

2. Combine this relation (equation 46) with the velocity distribution (equation 108 on page 101) to derive expressions for bed shear stress as a function of lateral position (y).

3. Integrate these expressions with respect to lateral position to derive an expression for total bed shear force per unit length.

4. The apparent shear force on the interface per unit length is calculated by subtracting the bed shear force from the down slope component of the water weight.

5. The apparent shear stress on the interface (τ_v) is simply the shear force per unit length divided by the depth.

6. Shear velocity may then be calculated from its own definition.

Using this method, equation (94) for shear velocity in a wide non-vegetated zone was derived in section 8.4.3, and is repeated below. A similar equation for narrow non-vegetated zones will be derived in section 8.5.3. (Wide and narrow non-vegetated zones are categorised according to whether the zone (half) width is greater or less than 1.29 times the wide channel transition width, as shown in section 8.4.5 on page 100.)

8.5.2 Wide Channel Interface Shear Equation

Equation (94) for the interface shear velocity in wide channels was presented in section 8.4.3. This equation is repeated below:

$$\therefore u_v^* = \sqrt{\frac{(TW\ wide - bm)}{\frac{1}{g \cdot S} + \frac{K^2 \cdot h_T \cdot (TW\ wide^2 - bm^2)}{2 \cdot bm \cdot R_v \cdot V_{\inf}^2 \cdot \left[\log\left(\frac{V_{\inf}}{V_{VegZone}}\right)\right]^2}}} \tag{94}$$

8.5.3 Narrow Channel Interface Shear

For a narrow channel, the interface shear velocity (u_v*) is expressed in terms of a transition width for the narrow channel (TW Narrow), analogous but different to TW Wide as follows:

From Equation (108):

$$V = \begin{cases} \frac{K \cdot u_v^*}{\log\left(\frac{V_{\max}}{V_{VegZone}}\right)} \sqrt{\frac{h_T}{R_v}} \cdot \sqrt{\frac{y}{bm}} & : y \le TW\ Narrow \\ V_{\max} & : y \ge TW\ Narrow \end{cases} \tag{109}$$

$$\text{Let } a = \frac{K}{\log\left(\frac{V_{\max}}{V_{VegZone}}\right)} \sqrt{\frac{h_T}{R_v \cdot bm}} \tag{110}$$

$$\text{Then } V = \begin{cases} \sqrt{a \cdot y} \cdot u_v^* & : y \le TW\ Narrow \\ V_{\max} & : y \ge TW\ Narrow \end{cases} \tag{111}$$

At y = TW Narrow, V = $V_{\max}$

$$\therefore \sqrt{a \cdot TW\ Narrow} \cdot u_v^* = V_{\max} \tag{112}$$

$$\therefore V = \begin{cases} \sqrt{a} \cdot \sqrt{y} \cdot u_v^* & : y \le TW\ Narrow \\ \sqrt{a} \cdot \sqrt{TW\ Narrow} \cdot u_v^* & : y \ge TW\ Narrow \end{cases} \tag{113}$$

From Equation (44):

$$\tau_b = \frac{\rho \cdot \lambda_b}{8} \cdot V^2 \tag{44}$$

Consider the force applied at the bed:

$$\frac{F_b}{l} = \int_{bm}^{bf} \tau_b \quad dy \tag{114}$$

$$\therefore \frac{F_b}{l} \cdot \frac{8}{\rho \cdot \lambda_b} = \int_{bm}^{bf} V^2 \quad dy$$
$$= \int_{bm}^{TW\ Narrow} u_v^{*2} \cdot a \cdot y\ dy + \int_{TW\ Narow}^{bf} u_v^{*2} \cdot a \cdot TW\ Narrow\ dy$$
$$= u_v^{*2} \cdot a \cdot \left[y^2/2\right]_{bm}^{TW\ Narrow} + u_v^{*2} \cdot a \cdot TW\ Narrow \cdot \left[y\right]_{TW\ Narrow}^{bf} \tag{115}$$
$$= a \cdot u_v^{*2} \cdot \left(TW\ Narrow^2 - bm^2 + 2 \cdot bf \cdot TW\ Narrow - 2 \cdot TW\ Narrow^2\right)/2$$
$$= a \cdot u_v^{*2} \cdot \left(bf \cdot TW\ Narrow - \tfrac{1}{2} TW\ Narrow^2 - \tfrac{1}{2} bm^2\right)$$

$$\therefore \frac{F_b}{\rho \cdot l} = \lambda_b/8 \cdot a \cdot u_v^{*2} \cdot \left(bf \cdot TW\ Narrow - \tfrac{1}{2} TW\ Narrow^2 - \tfrac{1}{2} bm^2\right) \tag{116}$$

If there is **no sidewall**:

$$\frac{F_v}{\rho \cdot l} + \frac{F_b}{\rho \cdot l} = g \cdot D \cdot S \cdot (bf - bm) \tag{117}$$

From Equation (84):

$$\frac{F_v}{\rho \cdot l} = D \cdot u_v^{*2} \tag{84}$$

$$\therefore D \cdot u_v^{*2} + \lambda_b/8 \cdot a \cdot u_v^{*2} \cdot \left(bf \cdot TW\ Narrow - \tfrac{1}{2} TW\ Narrow^2 - \tfrac{1}{2} bm^2\right) = g \cdot D \cdot S \cdot (bf - bm) \tag{118}$$

$$\therefore u_v^{*2}\left[D + \lambda_b \cdot a \cdot \left(bf \cdot TW\ Narrow - \tfrac{1}{2} TW\ Narrow^2 - \tfrac{1}{2} bm^2\right)/8\right] = g \cdot D \cdot S \cdot (bf - bm) \tag{119}$$

$$\therefore u_v^{*} = \sqrt{\frac{g \cdot D \cdot S \cdot (bf - bm)}{D + \lambda_b \cdot a \cdot \left(2 \cdot bf \cdot TW\ Narrow - TW\ Narrow^2 - bm^2\right)/16}} \tag{120}$$

From the definition of a (Equation 108):

$$\therefore u_v^* = \sqrt{\frac{g \cdot D \cdot S \cdot (bf - bm)}{D + \frac{K^2 \cdot h_T \cdot \lambda_b \cdot a \cdot (2 \cdot bf \cdot TW\ Narrow - TW\ Narrow^2 - bm^2)}{16 \cdot R_v \cdot bm \cdot [\log(V_{max}/V_{VegZone})]^2}}} \qquad (121)$$

This is the required expression for the apparent shear velocity of the vegetation interface without a sidewall. In laboratory experiments, this condition would apply where there is vegetation on both sides of the non-vegetated zone being considered.

With a sidewall:

$$\frac{F_v}{\rho \cdot l} + \frac{F_b}{\rho \cdot l} + \frac{F_w}{\rho \cdot l} = g \cdot D \cdot S \cdot (bf - bm) \qquad (122)$$

Where: F_w is the shear force on the wall.

Assume that the wall has the same friction factor as the bed. Also assume that V_{max} is the average velocity in the vicinity of the wall to which the wall shear stress is related. Then the shear stress on the wall (τ_w) is:

$$\tau_w = \frac{\rho \cdot \lambda_b}{8} \cdot V_{max}^2 \qquad (123)$$

$$\therefore F_w / \rho \cdot l = \tau_w \cdot D / \rho = \lambda_b \cdot V_{max}^2 \cdot D/8 \qquad (124)$$

Again: $\frac{F_v}{\rho \cdot l} = D \cdot u_v^{*2}$ (84)

Substitute Equations (84), (116) and (124) into Equation (122):

$$D \cdot u_v^{*2} + \lambda_b \cdot a \cdot u_v^{*2} \cdot \left(bf \cdot TW\ Narrow - \tfrac{1}{2} TW\ Narrow^2 - \tfrac{1}{2} bm^2\right)/8 + \lambda_b \cdot V_{max}^2 \cdot D/8 = g \cdot D \cdot S \cdot (bf - bm) \qquad (125)$$

$$\therefore u_v^{*2}\left[D + \lambda_b \cdot a \cdot \left(bf \cdot TW\ Narrow - \tfrac{1}{2} TW\ Narrow^2 - \tfrac{1}{2} bm^2\right)/8\right] = g \cdot D \cdot S \cdot (bf - bm) - \lambda_b \cdot V_{max}^2 \cdot D/8 \qquad (126)$$

$$= g \cdot D \cdot S \cdot \left[bf - bm - \lambda_b \cdot V_{max}^2 / (8 \cdot g \cdot S)\right] \qquad (127)$$

From Equation (81):

$$V_{\inf}^2 = 8 \cdot g \cdot D \cdot S / \lambda_b \qquad (128)$$

$$\therefore \lambda_b / (8 \cdot g \cdot S) = D / V_{\inf}^2 \qquad (129)$$

$$\therefore u_v^* = \sqrt{\frac{g \cdot D \cdot S \cdot \left[bf - bm - D \cdot (V_{\max}/V_{\inf})^2\right]}{D + \lambda_b \cdot a \cdot \left(bf \cdot TW\ Narrow - \frac{1}{2} TW\ Narrow^2 - \frac{1}{2} bm^2\right)/8}} \qquad (130)$$

Substituting the definition of a (Equation 108):

$$\boxed{\therefore u_v^* = \sqrt{\frac{g \cdot D \cdot S \cdot \left[bf - bm - D \cdot (V_{\max}/V_{\inf})^2\right]}{D + \dfrac{K^2 \cdot h_T \cdot \lambda_b \cdot \left(2 \cdot bf \cdot TW\ Narrow - TW\ Narrow^2 - bm^2\right)}{16 \cdot R_v \cdot bm \cdot \left[\log(V_{\max}/V_{VegZone})\right]^2}}}} \qquad (131)$$

which is the required expression for the apparent shear velocity of the vegetation interface with a sidewall on one side of the non-vegetated zone.

8.5.4 Narrow Channel Transition Width Equations

From Equation (112):

$$\sqrt{a \cdot TW\ Narrow} \cdot u_v^* = V_{\max} \qquad (112)$$

$$\therefore TW\ Narrow = \frac{V_{\max}^2}{a \cdot u_v^{*2}} = \frac{V_{\max}^2 \cdot R_v \cdot bm \cdot \left[\log(V_{\max}/V_{VegZone})\right]^2}{K^2 \cdot h_T \cdot u_v^{*2}} \qquad (132)$$

$$\boxed{\therefore TW\ Narrow = \frac{R_v \cdot bm}{h_T} \cdot \left[\frac{V_{\max} \cdot \log(V_{\max}/V_{VegZone})}{K \cdot u_v^*}\right]^2} \qquad (133)$$

Because equations (121), (131) and (133) express TW Narrow and u_v* each in terms of the other, there is no direct solution. Instead, these equations have to be solved iteratively. The suggested procedure is to guess an initial value of TW Narrow and to then calculate u_v* using equation (121) or (131) as appropriate. A new value of TW narrow can then be calculated using equation (133). This value may be used for the subsequent iteration.

8.5.5 Will Transverse Velocity Profiles Always Level Off?

Equations (121) and (131) assume that the non-vegetated zone (half) width bf is greater than the transition width TW Narrow. If this is not the case, the velocity is expected to continue to increase all the way across the non-vegetated zone. In this case, a different expression is needed for the interface shear velocity (u_v^*):

Consider a force balance:

$$\frac{F_v}{\rho \cdot l} + \frac{F_b}{\rho \cdot l} = g \cdot D \cdot S \cdot (bf - bm) \tag{134}$$

Compared with equation (115), the upper limit of the integration must be changed:

$$\frac{F_b}{\rho \cdot l} = \frac{\lambda_b}{8} \int_{bm}^{bf} V^2 \, dy \tag{135}$$

$$V = \frac{K \cdot u_v^*}{\log\left(V_{\max} / V_{VegZone}\right)} \cdot \sqrt{\frac{h_T}{R_v}} \cdot \sqrt{\frac{y}{bm}} \tag{136}$$

$$\begin{aligned} \therefore \frac{F_b}{\rho \cdot l} &= \frac{\lambda_b}{8} \cdot \frac{K^2 \cdot h_T \cdot u_v^{*2}}{R_v \cdot bm \cdot \left[\log\left(V_{\max} / V_{VegZone}\right)\right]^2} \cdot \int_{bm}^{bf} y \, dy \\ &= \frac{\lambda_b}{16} \cdot \frac{K^2 \cdot h_T \cdot u_v^{*2} \cdot \left(bf^2 - bm^2\right)}{R_v \cdot bm \cdot \left[\log\left(V_{\max} / V_{VegZone}\right)\right]^2} \end{aligned} \tag{137}$$

Also: $\frac{F_v}{\rho \cdot l} = D \cdot u_v^{*2}$ (84)

Subs (134):

$$D \cdot u_v^{*2} + \frac{\lambda_b \cdot K^2 \cdot h_T \cdot \left(bf^2 - bm^2\right)}{16 \cdot R_v \cdot bm \cdot \left[\log\left(V_{\max} / V_{VegZone}\right)\right]^2} \cdot u_v^{*2} = g \cdot D \cdot S \cdot (bf - bm) \tag{138}$$

$$\therefore u_v^* = \sqrt{\frac{g \cdot D \cdot S \cdot (bf - bm)}{1 + \frac{\lambda_b \cdot K^2 \cdot h_T \cdot (bf^2 - bm^2)}{16 \cdot R_v \cdot bm \cdot \left[\log\left(V_{\max} / V_{VegZone}\right)\right]^2}}} \quad (139)$$

$$\boxed{u_v^* = \sqrt{\frac{g \cdot S \cdot (bf - bm)}{1 + \frac{\lambda_b \cdot K^2 (bf^2 - bm^2)}{16D \cdot \left[\log\left(V_{\max} / V_{VegZone}\right)\right]}}}} \quad (140)$$

However, for the experimental data analysed, this condition was found never to apply. The reason is that, as the non-vegetated zone decreases, the predicted maximum velocity also decreases. The predicted maximum velocity was always found to decrease to a value which would be attained within the zone width (bf). Equation (140) therefore never needed to be applied. In the narrow channel experiments of James et al. (2001), there is also no test where the measured velocities can be seen to continue to increase all the way to the centre or edge of the non-vegetated zone. (In some tests, it is clear that the velocity profile levels off at a certain maximum velocity, while in others, the number of velocity measurements is not sufficient to state definitely whether the profile levels off.) A future theoretical analysis could consider whether there might be situations in which velocity would continue to increase all the way across the channel, or whether the transverse velocity profiles will always level off.

8.6 Selection of Methods

While the velocity distribution method of Nuding (1991, 1994) was found to be realistic, the following modifications can be recommended:

- Reduction of the maximum velocity in narrow channels as described in section 8.4. This has been shown to be a realistic method by which application of the equation of Nuding (1991, 1994) can be extended to narrow channels.
- Calculation of the interface shear velocity from a force balance for the non-vegetated zone as described in section 8.5. This method provides a better

theoretical basis for the estimation of shear on the vegetation interface, which is needed for the prediction of velocity profiles.

Note that these two methods are designed to be applied in combination with each other. The combination of both methods will be tested against laboratory data in Chapter 9.

The other two methods attempted were less successful, and are not recommended:

- The incorporation of bed shear into the velocity distribution does not improve the fit of the predicted velocity distribution to measured data. Furthermore, the typical shape of the velocity profiles was not correctly predicted with the incorporation of bed shear.
- The superposition methods discussed in section 8.3 generally over predict velocity, and thus do not take sufficient account of the interaction between the vegetation zones on each side. They also fail to predict any interaction for non-vegetated zone widths only slightly wider than the transition width.

9 Comparison of Proposed Lateral Velocity Distribution with Laboratory Data

9.1 Method

The velocity distribution method described in Chapter 8 was tested against all available laboratory data listed in Table 5-1on page 48 and Table 6-1 on page 55. Conditions for all experiments are detailed in Appendix A.

In order to determine a measured velocity profile, the measured velocities had to be interpolated with respect to lateral distance. (In some cases, the profile also had to be extrapolated to the vegetation interface.) Interpolation was performed by means of the following functions: For those velocity profiles where only three velocities were measured, a quadratic function was fitted to the measured velocity-distance pairs. For those velocity profiles for which five or more velocities were measured, a cubic spline was fitted to the measured velocity-distance pairs. The computer software CurveExpert version 1.3 (Hyams, 2001) was used to fit the cubic spline, and to solve the resulting functions for defined velocities and distances. Both of these curves have the following properties:

- They pass exactly through each measured velocity value.
- The slopes (dV/dy) are matched at each measured point.
- The curvature (d^2V/dy^2) is matched at each measured point.

The aim of the proposed method is to predict lateral velocity profiles, and hence to predict the velocity at particular positions.

9.2 Results

- While the shape and limits of the lateral velocity profiles are important, in the final instance, it is velocity which we need to predict. Results will therefore first be compared in terms of the velocities predicted at particular positions. A graph plotting each measured velocity against velocity predicted at the same position is given in Figure 9-1. A total of 787 velocities were measured.

- Next, individual profiles are compared graphically. Predicted and measured lateral velocity profiles for each test are plotted in Appendix C. In order to demonstrate the performance of this method, example profiles have been selected and compared to measured profiles and to predictions using the methods of Nuding (1991, 1994), Ikeda et al. (1991, 1994) and Tsujimoto and Kitamura (1994). In order to illustrate the performance over a range of non-vegetated zone widths, a profile was selected for each of the following ranges:
    - o bfo <0.1m in Figure 9-2,
    - o 0.1 m < bfo < 0.2m in Figure 9-3,
    - o 0.2m < bfo < 0.4m in Figure,
    - o 0.4m < bfo < 0.8m in Figure 9-5,
    - o 0.8m < bfo < 1.6m in Figure 9-6 and
    - o bfo >1.6m in Figure 9-7.

- The lateral velocity profiles are scaled in terms of the maximum velocity (V_{max}) and the transition width (TW), and comparison of these scales is important for evaluation of the method. Since predictions for maximum velocity were compared to laboratory data in section 8.4, only predicted and measured values of the distance to the maximum velocity (TW) will be compared here. A graph of the predicted vs. measured distance to the maximum velocity (TW) for each profile is included in Figure 9-8. Note that for some experiments, more than one profile was measured (since these experiments featured more than one interface), giving a total of 100 comparisons. The average absolute prediction error was 0.060m for an average measured transition width (TW) of 0.176m.

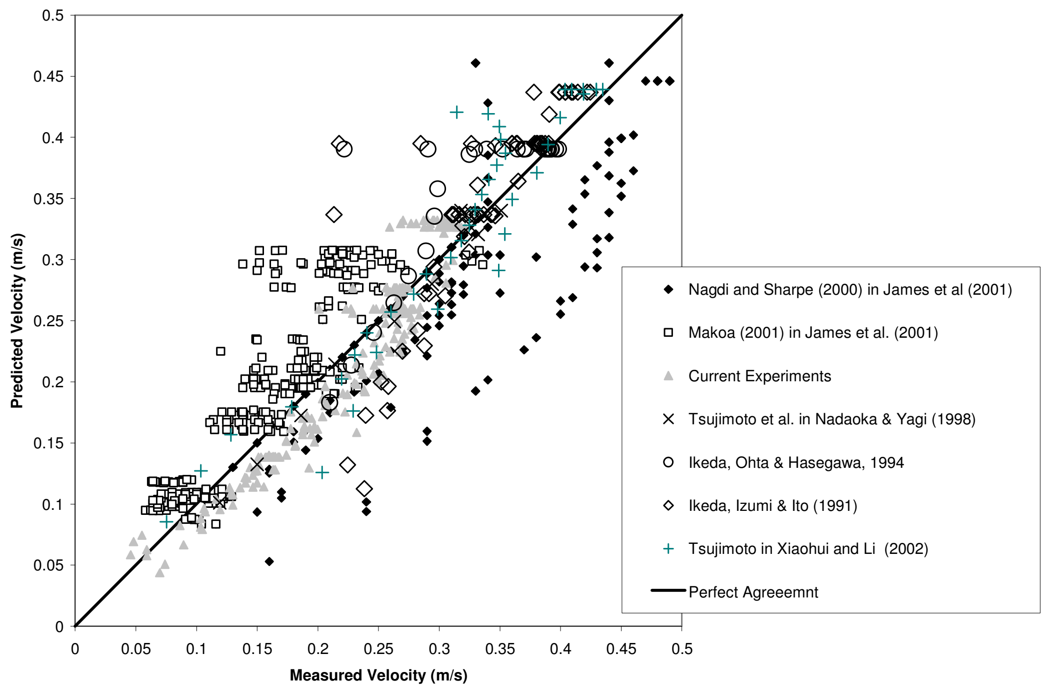

Figure 9-1: Comparison of all Predicted and Measured Velocities

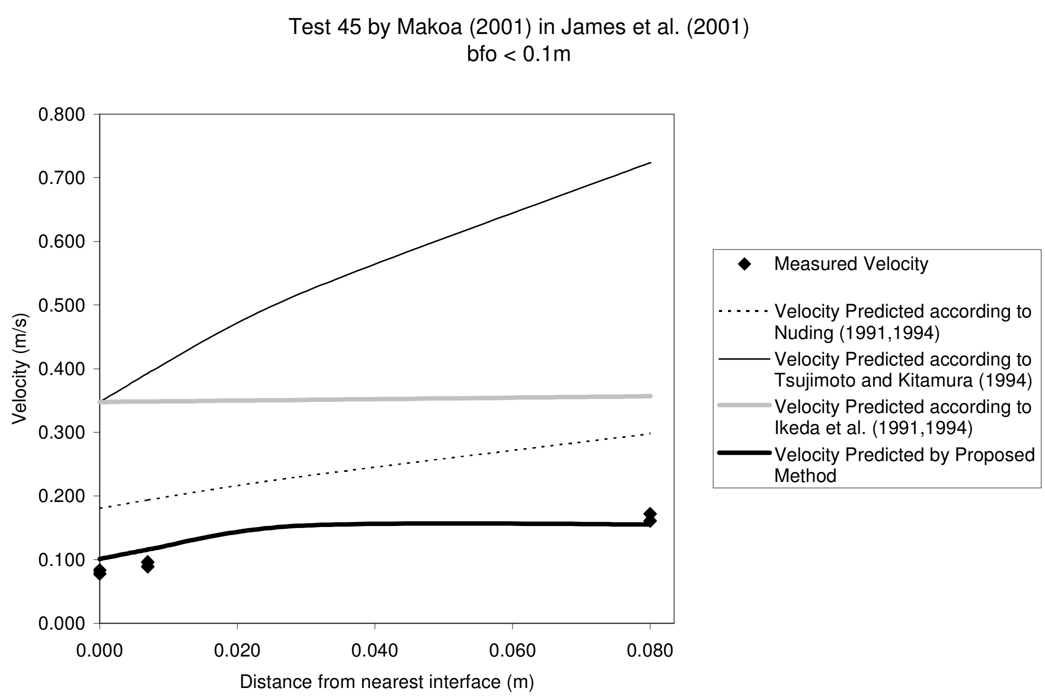

Figure 9-2: Performance of Proposed Velocity Prediction for a Test with bfo < 0.1m

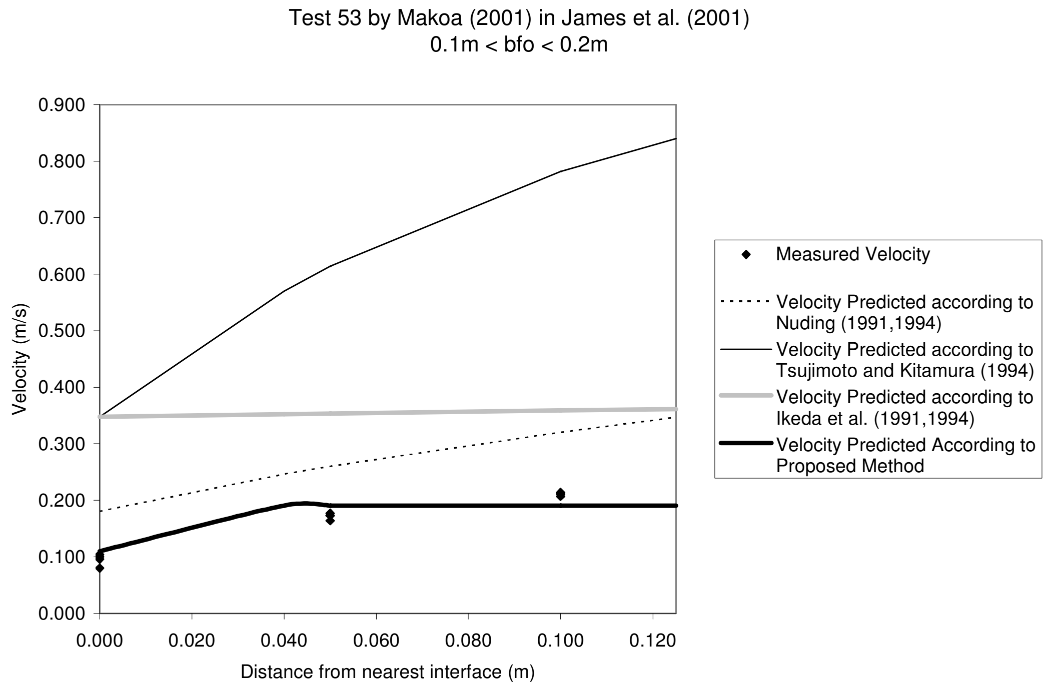

Figure 9-3: Performance of Proposed Velocity Prediction for a Test with 0.1m < bfo < 0.2m

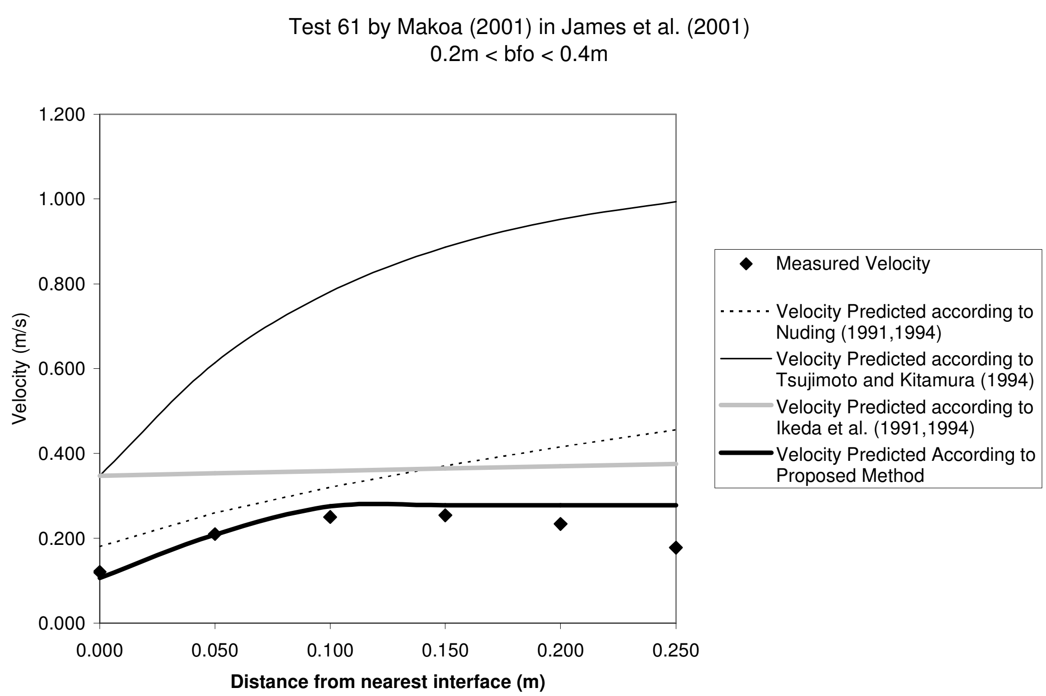

Figure 9-4: Performance of Proposed Velocity Prediction for a Test with 0.2m < bfo < 0.4m

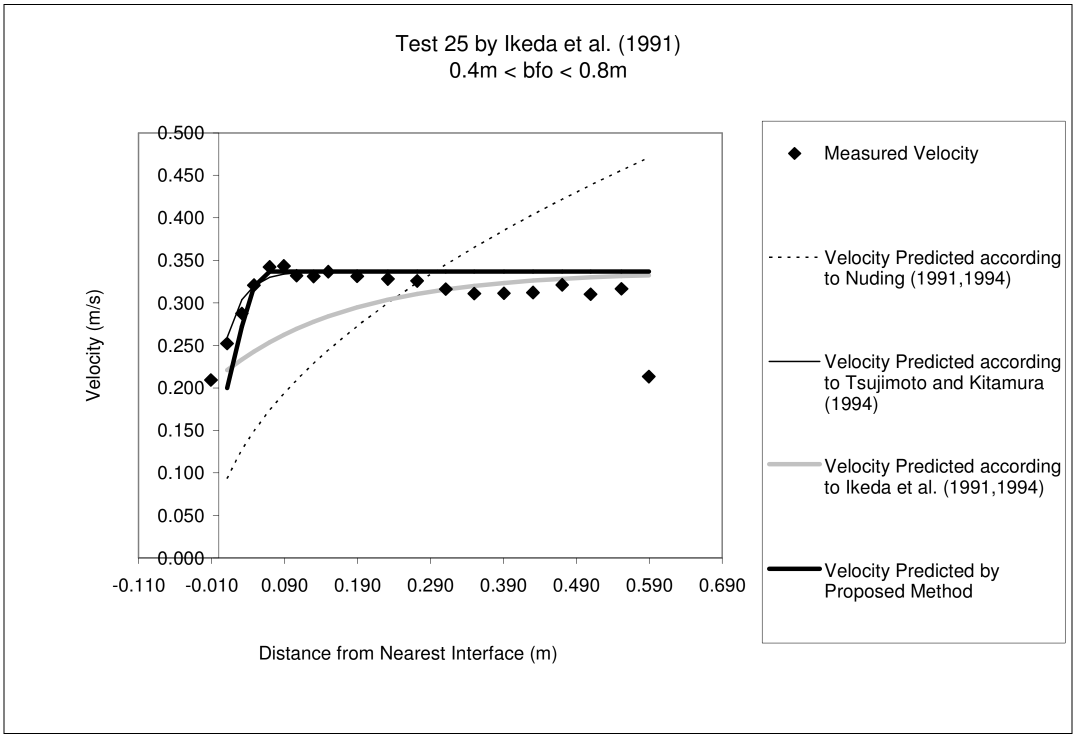

Figure 9-5: Performance of Proposed Velocity Prediction for a Test with 0.4m < bfo < 0.8m

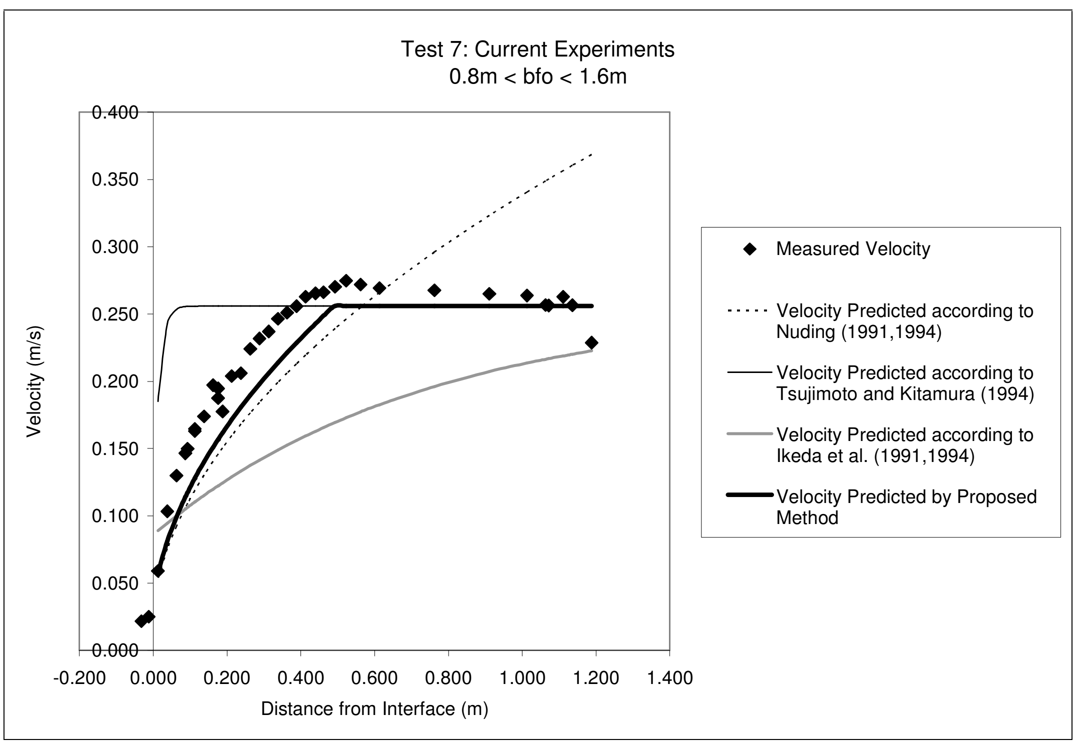

Figure 9-6: Performance of Proposed Velocity Prediction for a Test with 0.8m < bfo < 1.6m

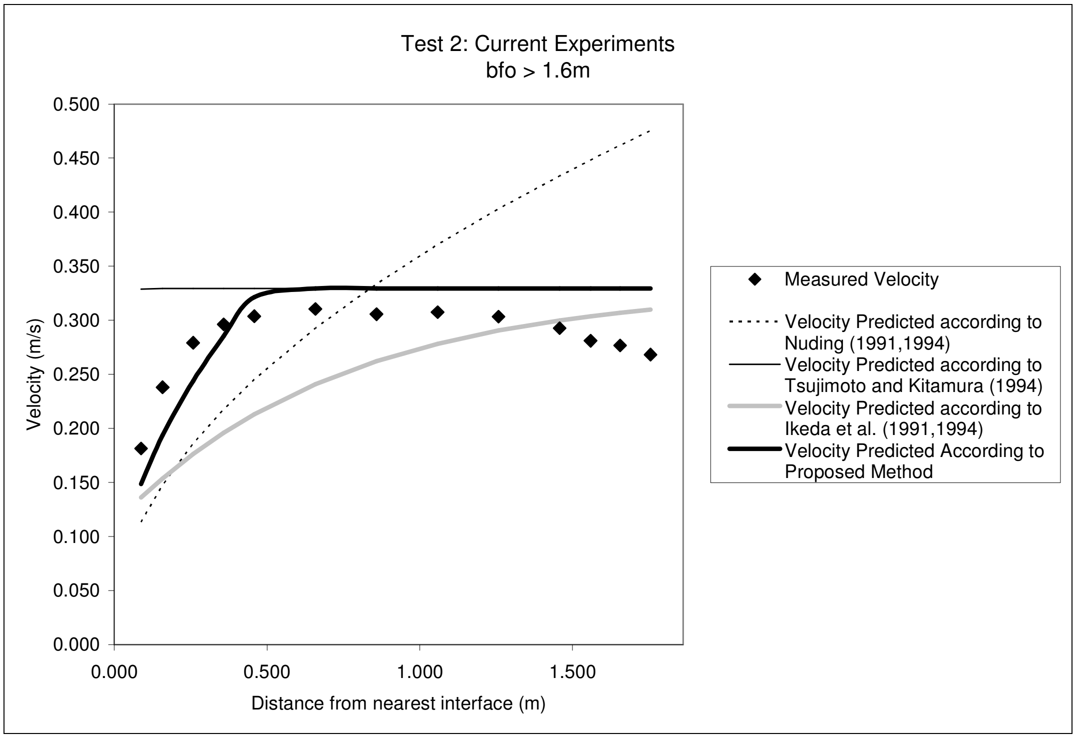

Figure 9-7: Performance of Proposed Velocity Prediction for a Test with bfo > 1.6m

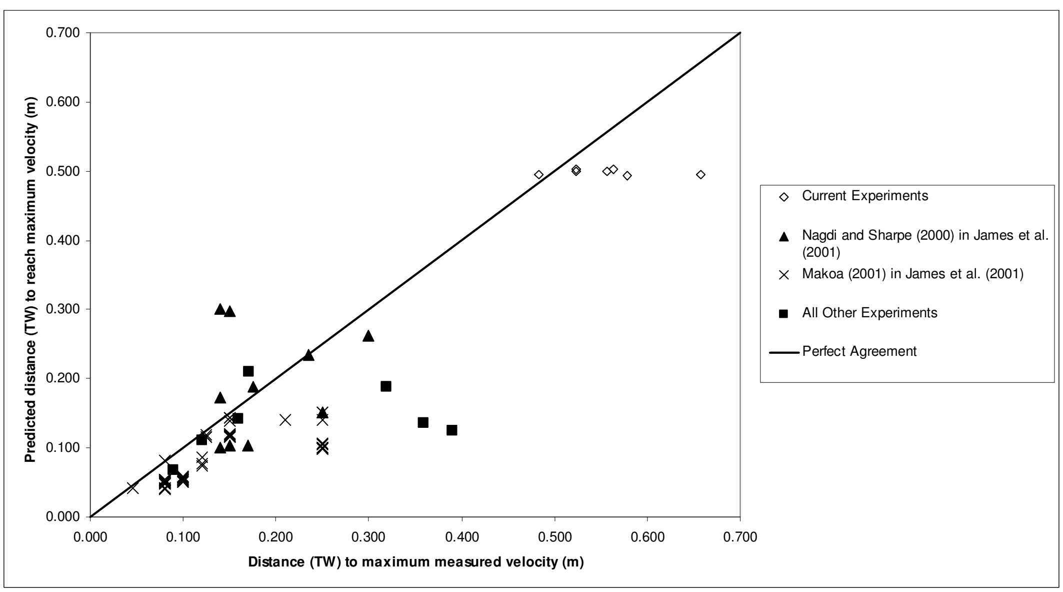

Figure 9-8: Predicted and Measured Transition Widths

9.3 Discussion

9.3.1 Velocity Values

The proposed method produces a reasonably accurate prediction of actual measured velocities, as indicated in Figure 9-1. (The root means square prediction error of 24% is a smaller error than the width of all of the biologically suitable velocity ranges suggested in Table 2-1. This accuracy should therefore be acceptable in many ecological studies. The maximum percentage errors generally occur close to the vegetation interface, an effect which will be discussed below. The average absolute error is 0.034m/s, which is of the same order of magnitude as the accuracy of many flowmeters. (For example, USBR (2001) suggests typical accuracies for ultrasonic transit time flowmeters of 0.03 to 0.09m/s, depending on the type of system used.)

Consideration of Figure 9-1 suggests that some errors may be related directly to the conditions of certain experiments.

Velocities measured during the experiments error of Nagdi and Sharpe (2000) in James et al. (2001) displayed the largest errors (in terms average and root mean square absolute error and root mean square percentage error). It is clear from Figure 9-1 that almost all velocities for this series of experiments were higher than the predicted values. This was probably due to an inconsistency in velocity measurement between the velocities used as inputs to the prediction method and the actual measured profiles. The extreme velocities V_{inf} and $V_{VegZone}$ were calculated from previous stage-discharge measurements using a V-notch weir. However, the velocity profiles were determined using a pitot-static tube. (Also, $V_{VegZone}$ was measured in a narrower flume.) The difference between these instruments is likely to have caused a corresponding difference between measured and predicted velocity profiles.

Also, the effect of the sidewall on the measured velocities was not taken into account (except in calculating the apparent shear stress on the vegetation interface). In many of the experiments, velocities were clearly reduced in the vicinity of the sidewall, so that these particular measurements were over-predicted. On Figure 9-1, this effect appears as a horizontal row of measurement points leading to the left of the graph. The right-most point represents the maximum measured velocity away from the influence of the sidewall. This is usually closest to the line of perfect agreement. The measurements to the left indicate the decreasing measured velocity closer to the sidewall.

In view of the fact that the errors have been shown to be relatively insignificant, and that several of the errors appear to have clear causes, the prediction method is acceptable.

9.3.2 Examination of Lateral Velocity Profiles

The velocity profiles illustrated in Figure 9-2 to Figure 9-7 show very good agreement with the measured data. It is also clear from these figures that the proposed prediction method is clearly an improvement over previous methods. Examination of the predictions presented in Appendix C indicates that good predictions are also achieved for the other experiments.

Predictions are generally least accurate close to the vegetation interface. Velocities measured at (or extrapolated to) the vegetation interface fall within a wider range (0.020 to 0.24m/s) than the predicted range of velocities at this position (0.034 to 0.15 m/s. The large variability in measured velocities may be indicative of local effects not taken into account. Local patterns of turbulence and velocity are set up around each vegetation stem. The velocity measured close to the vegetation interface will therefore depend on the measurement position relative to these patterns. These local effects are unknown, and cannot in any case be taken into account in a method aiming to predict the velocity distribution across the entire non-vegetated zone width. A better understanding of these velocities would depend on an understanding of the small-scale flow patterns within the vegetation. This would in turn have to be based on experiments designed to measure these patterns.

9.3.3 Distance Scale (TW)

Predictions for the distance scale of the transverse velocity distribution (TW) are clearly less accurate than predictions of velocity. These distances are expected to be related to the distance scales of the turbulence structures produced. These are in turn expected to be affected by the detailed geometry, as well as by hydraulic conditions, particularly Reynolds number. Nevertheless, the distance scales predicted are of the correct order of magnitude, and represent the correct general trend, as shown in Figure 9-8. This suggests that some of the applicable factors determining these distance scales have been taken into account in a suitable way. The suggested method can therefore be recommended for the prediction trends and approximate values of these distance scales. Future research may determine how other factors affecting the length scales may be taken into account.

One particular geometric feature affecting distance scales deserves to be mentioned. In the velocity distribution equation of Nuding (1991, 1994) (Equation 28 on page 62), longitudinal spacing is taken into account in two ways: Firstly, the longitudinal spacing of the vegetation influences the velocity predicted within a fully vegetated channel ($V_{VegZone}$). This effect will depend on the method used for the prediction of this velocity. Secondly, in the calculation of the transition width bm, the longitudinal spacing may be used in certain cases, depending on its magnitude relative to the flow depth and the transverse spacing. (See section 4.4.5.) However, Helmiö (2004) noted that longitudinal spacing also has a more direct influence on the transfer of momentum between the vegetation and non-vegetated zones. "The method of Nuding (1991) does not take into account that the density of vegetation dampens the momentum exchange." Helmiö (2004) performed a laboratory investigation of the effect of longitudinal spacing of living spruce saplings on resistance in a channel with a longitudinal strip of vegetation. She found one value of longitudinal spacing for which the resistance was a maximum over a range of flowrates. However, no general method could be suggested to quantify the effect of longitudinal spacing. This can therefore not be taken into account. The future investigation of the effect of longitudinal spacing would be valuable. In applying the methods recommended in this chapter, it is important to be aware that different longitudinal spacings may have an additional effect which has not been considered.

9.4 Conclusion

The proposed method produces an accurate prediction of the maximum velocity occurring in the channel and a good approximation to the shape of the lateral profile. Specific velocity measurements are predicted with reasonable accuracy. It is less accurate close to the vegetation interface, and the distance over which the vegetation affects the velocity is predicted only approximately. The proposed method is thus an improvement over previous methods for the prediction of lateral velocity profiles adjacent to strips of vegetation, and is recommended for application. Finally, a procedure for its application will be described in Chapter 10.

10 Proposed Procedure for Prediction of Lateral Velocity Distributions Adjacent to Vegetation Strips

1. Assume a water surface elevation and energy slope (S).

2. Estimate the average velocity with bed resistance only (V_{inf}) using any appropriate method.

3. Estimate the average velocity within a fully vegetated channel using any appropriate method, such as the method of Jordanova et al. (2006) for reeds, the method of Järvelä (2004) for woody vegetation or the method of Freeman et al. (2002) for trees and bushes.

4. Calculate the contributing width bm as the greater of:

- 0.15 times the flow depth at the interface

  or

- the smallest of :
  - The lateral spacing of the vegetation ay as indicted in Figure 4-3.
  - The wake width a_{NB}, which is calculated as $3.2\sqrt{a_x \cdot d_p}$ (23)

    where a_x is the longitudinal spacing of the vegetation and d_p is the vegetation diameter.
  - The actual thickness of the vegetation strip

5. Calculate the wide channel transition width TW Wide according to:

$$TW\ wide = bm + \sqrt{\frac{2 \cdot bm \cdot R_v}{h_T \cdot g \cdot S}} \cdot \frac{V_{\inf}}{K} \cdot \log\left(\frac{V_{\inf}}{V_{VegZone}}\right) \quad (103)$$

6. Calculate the ratio bf / TW Wide where bf is the non-vegetated zone (half) width (bfo) as shown in Figure 4-2 on page 33 plus the contributing width (bm).

7. Calculate the dimensionless maximum velocity according to:

$$V_{DL}\,max = \begin{cases} 0.674\ bf / TW\ Wide + 0.132 & : bf / TW\ Wide \le 1.29 \\ 1 & : bf / TW\ Wide \ge 1.29. \end{cases} \qquad (107)$$

   and classify the non-vegetated zone as narrow or wide, depending which of these conditions applies.

8. Calculate the maximum velocity according to:

$$V_{\max} = V_{VegZone} + V_{DL\max}\left(V_{\inf} - V_{VegZone}\right) \qquad (141)$$

If the non-vegetated zone is wide:

9. Calculate the apparent shear velocity on the vegetation interface (u_v*) according to:

$$u_v^* = \sqrt{\frac{TW\ wide - bm}{\dfrac{1}{g \cdot S} + \dfrac{K^2\left(TW\ wide^2 - bm^2\right)}{2 \cdot V_{\inf}^2 \cdot bm \cdot \log\left(\dfrac{V_{\inf}}{V_{VegZone}}\right)^2}}} \qquad (94)$$

Where: K is a constant equal to 2.2

If the non-vegetated zone is narrow:

9. Guess a transition width (TW Narrow) over which the velocity change takes place.
10. Calculate the apparent shear velocity on the vegetation interface (u_v*) according to:

$$u_v^* = \sqrt{\frac{g \cdot D \cdot S \cdot \left(TW\ Narrow - bm\right)}{D + \dfrac{K^2 \cdot \lambda_b \cdot \left(2 \cdot bf \cdot TW\ Narrow - TW\ Narrow^2 - bm^2\right)}{16 \cdot bm \cdot \left[\log\left(V_{\max} / V_{VegZone}\right)\right]^2}}} \qquad (121)$$

Where D is the flow depth.

(Note that an alternative equation is provided if the effect of a sidewall has to be taken into account.)

11. Calculate a new transition width (TW Narrow) according to:

$$TW\ \ Narrow = bm\left[\frac{V_{\max}\cdot\log\left(V_{\max}\big/V_{VegZone}\right)}{K\cdot u_v^*}\right]^2 \tag{133}$$

12. Iterate steps 10 and 11 until the calculated values of TW Narrow and u_v* no longer change significantly.

For both wide and narrow non-vegetated zones:

13. Calculate the velocity (V) at various lateral positions (y, as defined in Figure 5-1 on page 50) as required according to:

$$V(y) = \text{The smaller of :}\begin{cases} 2.2\cdot \mathrm{u}_\mathrm{v}^* \big/ \log\left(V_{\max}/V_{VegZone}\right)\times\sqrt{h_T/R_v}\times\sqrt{y/bm} \\ V_{\max}\end{cases} \tag{108}$$

Where: h_T is the depth at the vegetation interface

R_v is the hydraulic radius of the vegetation zone.

These velocities form the velocity profile. Note that the profile will be less accurate close to the vegetation interface.

14. Predicted velocities can be combined with depth information (derived from the difference between bed and water surface elevations) to predict the presence of defined habitats as specified for a particular ecological study.

PART IV: Numerical Modelling of Stage and Velocity in Partially Vegetated Channels of Complex Geometry

11 Using River2D Software to Model Vegetation

11.1 Aim

The equations presented thus far provide methods for the estimation of lateral velocity distributions and resistance for the case of longitudinal strips of vegetation which are long enough so that changes with longitudinal position are negligible. Furthermore, changes in flow depth and bed resistance across the non-vegetated zones are not taken into account. Commonly, vegetation patches are irregular in shape and distribution. The shape of the channel cross-section is frequently irregular, and the bed resistance may change within the transition width. In all of these cases, the simple procedures suggested in Parts II and III of this report will not be directly applicable. In these cases, no analytical solutions are available. The flow patterns produced by more complex geometries (particularly vegetation patches) can be predicted only by two- or three-dimensional numerical hydraulic models.

In this section, the two dimensional hydraulic model River2D is set up to provide predictions of the effect of vegetation on uniform flow depth (or conveyance) and transverse velocity distributions. Initially, the setup of the current laboratory experiment (Test 7) described in Chapter 6 will be reproduced, in order to test and guide the application of the numerical model. Next the response of a model to changing width of the non-vegetated zone will be investigated. Finally, having verified the models in these two situations, the model will be applied to reproduce predictions of uniform flow depth for selected vegetation patch patterns for which resistance data was measured in the laboratory by James et al. (2001).

This section thus aims to suggest how vegetation influenced flow should be modelled using River2D.

11.2 Introduction to River2D

11.2.1 General Description

River2D is a two-dimensional finite element hydraulic and habitat simulation model suitable for low flows. As a two-dimensional hydraulic model, River2D predicts spatial distributions of hydraulic parameters. Tools for the interpretation of modelled depths and velocities in terms of habitat suitability are also provided, but these will not be discussed here.

River2D is primarily an analysis tool, since it predicts values of hydraulic parameters such as depth and velocity in a spatially explicit way. River2D is designed for both steady and unsteady flow analysis. Only steady flow analysis will be applied here. The numerical solution in River2D is obtained using finite element methods, which are explained in the River2D manual (Steffler and Blackburn, 2002).

River2D is a highly accessible program. All software and documentation is available free of charge for download from website http://www.river2d.ualberta.ca/. It has been completely developed with a user-friendly menu-driven interface. River2D uses metric units. The program is, however, not entirely stable, and will usually freeze or shut down if there is some error in the input. Furthermore, there is no undo function within any of the modules. Frequent saving is therefore strongly recommended.

River2D consists of three modules, each of which is run separately. Specific information on the use of each module is included in a manual for each module:

- *R2D_bed*: for editing bed topography,
- *R2D_mesh* for generating a triangular finite element mesh
- *River2D* for flow and habitat analysis and mesh editing or refinement.

There is a separate module for ice cover information, but this is not relevant to prediction of the influence of vegetation.

11.2.2 Hydraulic Capabilities and Limitations

River2D is able to handle wetting and drying by utilizing a continuous water surface, which may be above or below the bed level. Flow below a user specified depth is analysed as groundwater flow with user-specified porosity and hydraulic conductivity. These parameters are specified as constants for the entire model. Vegetation can therefore not be modelled as a porous area with different characteristics to the bed. Vegetation through which flow occurs will therefore have to be treated either as part of the bed, or as a channel flow area with increased roughness, neither of which is ideal. Although the transition between wet and dry areas is handled well, calculated velocities at the water's edge may be un-realistic. (It is possible that this may be corrected by appropriate selection of model parameters.)

The model is able to handle localized super-critical flows and transitions between sub-critical and super-critical flows, provided that flow through the model boundaries is always sub-critical. This should not be a problem for low flows in rivers, where super-critical flows are usually localized. However, it does require care in the placement of model boundaries. The model has a capability of nesting scales. An area of the model (bounded by two streamlines and two flow boundaries) can be extracted and modelled in further detail using the results of the full model as boundary conditions. This allows additional accuracy in areas where this is needed. Inserting the remodelled section back into the parent mesh allows a comparison of the results.

11.2.3 Hydraulic Parameters

River2D makes use of the following hydraulic parameters, which must be input by the user:

- Equivalent Sand Grain Roughness k_s: This is used to calculate the Chézy resistance coefficient according to the relation:

If D/ks < 0.616 then $C = 2.5\sqrt{g} + 30D\sqrt{g}/e^2\ ks$ else $C = 5.75\sqrt{g}\log(12D/ks)$ (142)

Note that according to this formulation, the minimum value of C is $7.83m^{1/2}/s$.

- Transition depth from surface to groundwater equations (Default value: 0.01m).
- Substrate storativity, which is equivalent to dimensionless porosity. This parameter value should not make any difference to steady flow analyses. (Default value: 1)
- Substrate transmissivity (T), which is equivalent to the Darcy permeability. (Default value $0.1m^2/s$)

11.2.4 Eddy Viscosity

River2D also requires the selection of eddy viscosity parameters ε_1, ε_2 and ε_3, which are used to calculate a horizontal eddy viscosity (ε_T) according to:

$$\varepsilon_T = \varepsilon_1 + \varepsilon_2 \left(D\sqrt{g} \cdot \sqrt{vx^2 + vy^2} \middle/ C \right) + \varepsilon_3^2 \cdot D^2 \sqrt{2\frac{\partial vx}{\partial x} + \left(\frac{\partial vx}{\partial y} + \frac{\partial vy}{\partial x} \right)^2 + 2\frac{\partial vy}{\partial y}} \qquad (143)$$

Where: ε_T is the depth averaged horizontal eddy viscosity
vx and vy are the local depth average velocities in the x and y directions respectively.

An expression for eddy viscosity in terms of velocity gradient may be derived using expressions presented in the derivation of the Nuding's (1991, 1994) velocity distribution equation. Substituting expressions given by Nuding (1994), the following expression for eddy viscosity results:

$$\varepsilon_T = \left[2 \cdot bm \cdot \log \frac{V_{\inf}}{V_{VegZone}} \middle/ K \right]^2 \frac{h_T}{R_V} \cdot \left| \frac{dV}{dy} \right| \qquad (144)$$

Where: K is a constant, of value 2.2.
h_T is the depth at the interface
R_V is the hydraulic radius of the vegetated zone.

For a vegetated zone of constant depth, $h_T=R_V$, so the term h_T/R_V may be neglected.

Comparing this with equation (143) above, taking (for uniform flow) $\partial u/\partial x = \partial v/\partial x = \partial v/\partial y = 0$, and substituting V_{max} for V_{inf}, we obtain an expression by which Nuding's (1991, 1994) eddy viscosity relation, as modified for maximum velocity, can be represented in River2D:

$$\varepsilon_3 = \frac{2bm}{K \cdot D}\sqrt{\frac{h_T}{R_v}}\log\left(\frac{V_{max}}{V_{VegZone}}\right); \quad \varepsilon_1 = \varepsilon_2 = 0 \qquad (145)$$

Where: bm is the contributing width, calculated as described in Chapter 10.

K is a constant equal to 2.2.

D is the flow depth

h_T is the depth at the vegetation interface

R_v is the hydraulic radius of the vegetated zone

V_{max} is the maximum velocity predicted

$V_{VegZone}$ is the average velocity within a fully vegetated channel

An alternative formulation of eddy viscosity was used in the derivation of the lateral velocity profile of Ikeda et al. (1991, 1994) and Tsujimoto and Kitamura (1994). Manipulation of the relations given by Tsujimoto and Kitamura (1994) shows that the constant kinematic eddy viscosity is given by:

$$\varepsilon_T = V_{inf} \cdot f \cdot \left(1 - J^2\right) \cdot \left(Bm + Bs\right) \qquad (146)$$

Where: Bm is and Bs are transition widths as described in section 7.4 starting on page 64.

$$J = \sqrt{\frac{V_{VegZone}}{V_{inf}}} \qquad (35)$$

Eddy viscosity calculated according to this formula is constant, and can therefore be used directly as ε_1 in River2D. Note that (as stated on page 69) the two methods differ in the calculation of the mixing coefficient (f). According to Ikeda et al. (1991, 1994):

$$f = 0.035e^{-2.95e^{-3.8J^2}} \qquad (36)$$

According to Tsujimoto and Kitamura (1994):

$$f = 0.03e^{-4e^{-6J^2}} \qquad (37)$$

The dependence of the eddy viscosity calculated using this equation on depth and other experimental conditions is shown in Figure 11-1.

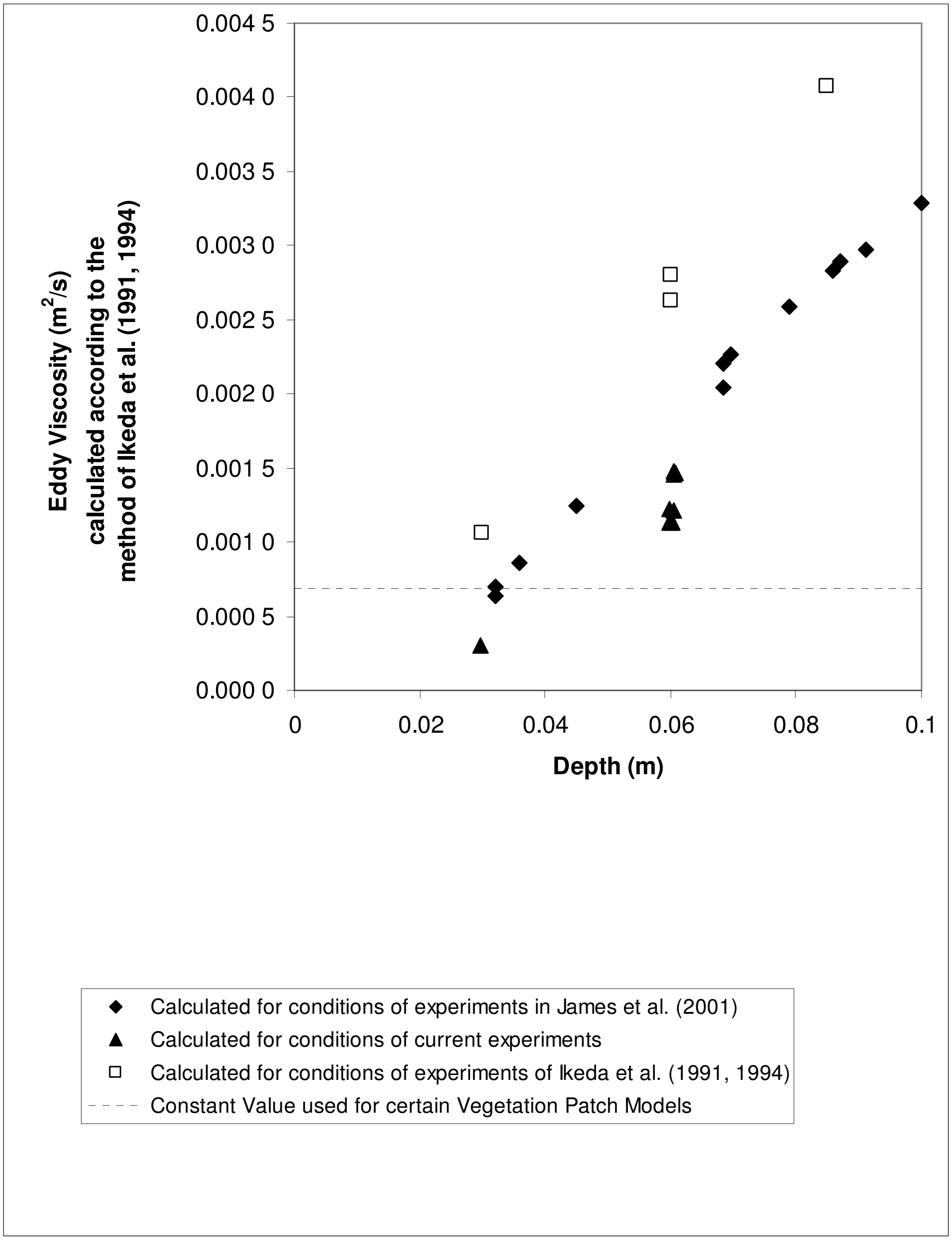

Figure 11-1: Dependence of Eddy Viscosity Predicted by the method of Ikeda et al. (1991, 1994) on Depth and Experimental Conditions

11.2.5 Outputs

Maps of various parameters can be produced and their display can be customised. These include: topographic data(bed elevation, bed roughness and channel index), hydraulic variables (depth, velocity magnitude, shear velocity magnitude, velocity vectors, unit width discharge vectors, water surface elevation, Froude Number, stream function and unit width discharge in x and y directions) and habitat suitability (depth suitability, velocity suitability, substrate suitability and combined suitability). For unsteady analyses, these maps can be combined into a video output.

Only one parameter can be displayed at a time. It is therefore not possible to map classes which combine two or more parameters, such as velocity-depth classes.

Values of any parameters can be output as a text file. This may include outputs at all or selected mesh nodes, or along a specified section, or on a grid. This capability allows the data to be analysed or presented using other programs. In this chapter outputs of water surface elevation and velocity are analysed and plotted using Microsoft Excel.

11.3 Modelling Flow through Vegetation as Groundwater Flow

11.3.1 Motivation for Treating Vegetation as Groundwater

James et al. (2001), based on a theoretical analysis of flow through vegetation, present the following equation for the average velocity in a fully vegetated region ($V_{VegZone}$):

$$V_{VegZone} = \frac{1}{F}\sqrt{S} \qquad (147)$$

Where: F is a resistance parameter, which is expected to be approximately constant with changing flow depth

S is the energy slope.

This equation may be compared with the one-dimensional Darcy Equation for flow through a permeable medium, such as soil:

$$V = K_d \sqrt{\frac{dH}{dx}} \qquad (148)$$

Where: K_d is the permeability of the medium

H is the total Head.

x is the distance in the direction of flow.

Substituting $F = 1/K_d$ and $dH/dx = S$, we see that these equations are identical. This should be no surprise, since vegetation is, in fact a porous medium, which may be defined as “a solid structure with interconnected voids,” Arunn, 2006.

In view of this similarity, de Lemos and da Silva (2002), modelled flow through the vegetation in a partially vegetated channel as flow through a porous material. As stated above, River2D includes groundwater equations for flow in dry areas, or where the depth is below a user-specified value. Following the approach of de Lemos and da Silva (2002), an attempt was made to model flow through and adjacent to a vegetation strip as groundwater flow in River2D. The bed at the vegetation was raised to above the water level, so that the groundwater flow equations would automatically be implemented in this region.

11.3.2 Setup

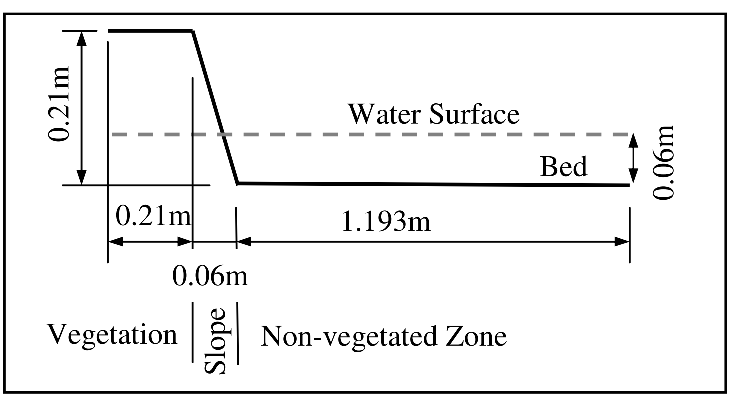

Figure 11-2: Cross-section Diagram of Model of Vegetation Strip As Groundwater Flow

The setup modelled was that used for test 8 of the current experiments. In order to replicate the topography of the laboratory experiments, a rectangular flume was set up 12m long and 1.463m wide. The topography was extended 0.1m upstream and downstream of the flume ends for interpolation at the boundaries. A slope of 0.0054m in 12.2m was set. A vegetation strip 0.24m wide was distinguished from the non-vegetated channel by being raised 0.3m above the level of the non-vegetated portion, as shown in Figure 11-2. A 0.06m wide transition zone was provided between the levels of the vegetation and non-vegetated zones.

Breaklines were specified at each side of this transition zone. These would ensure that the topography was correctly interpolated longitudinally along the flume. They also ensured that all cells of the computational mesh ended at the top and bottom of the short lateral slope indicated in Figure 11-2. This in turn ensured that for the purpose of hydraulic calculation, the high-level vegetation strip, the non-vegetated zone and the slope in between would be separated exactly at the locations specified.

A mesh of size approximately 0.15m was set up over most of the non-vegetated zone. This mesh was refined over the slope and vegetation zones, and between longitudinal distances 8 to 11m (close to the section at longitudinal distance 10m where velocity data were extracted).

Boundary conditions were set as a constant inflow of 0.017 7m^3/s at the upstream end and a constant water surface elevation of 0.059 6m at the downstream end. In the first model, the downstream boundary extended over the entire flume width. However, in this case, the total outflow calculated (which excludes flow through the vegetation zone) was too low, indicating that the flow through the vegetation was too high. For subsequent models, the downstream boundary extended only across the non-vegetated zone.

11.3.3 Procedure

Various runs were conducted with different parameter values. The parameters varied were: Bed roughness ks, Groundwater Transmissivity T, and Eddy Viscosity parameters E2 and E3. (E1 was set to zero.) These parameters are as defined in section 11.2.3. A summary is presented in Table 11-1.

For each run, a water surface elevation profile was defined by extracting a point every 1m along the flume centreline. The best fit straight line to these points was taken as the water surface slope, and is included in Table 11-1. This is the major indication of the changing overall flow resistance in response to changing input parameters.

For runs S1 to S7, S16 and S17, a transverse velocity profile at longitudinal position 10m from the upstream end of the flume was also extracted.

Table 11-1: Model Parameters and Resulting Water Surface Slopes for River2D Model of Vegetation Strip as Groundwater Flow

Model Run	ks	E1	E2	E3	Transmissivity	Resulting Water Surface Slope
Units	(m)	(m^2/s)	(None)	($m^{-1/2}$)	(m^2/s)	(None)
S1	0.00001	0	0	0	0.39	0.000206
S2	0.00001	0	0	1	0.83	0.000534
S3	0.00001	0	1	0	0.054	0.004903
S4	0.00001	0	0.3	0	0.054	0.004851
S5	0.00001	0	0.1	0.3	0.054	0.004859
S6	0.00001	0	0.02	0.5	0.054	0.004886
S7	0.00001	0	0	0.5	0.054	0.004885
S8	100	0	0.5	0.5	0.054	0.00475
S9	100	0	0	0	0.054	0.004657
S10	0.00058	0	0	0	0.28	0.000476
S11	0.0002	0	0	0	0.31	0.000373
S12	0.00015	0	0	0	0.31	0.000373

Model Run	ks	E1	E2	E3	Transmissivity	Resulting Water Surface Slope
Units	(m)	(m^2/s)	(None)	($m^{-1/2}$)	(m^2/s)	(None)
S13	0.00001	0	0.05	0.5	0.15	0.004874
S14	0.00001	0	0.05	0.5	0.2	0.004836
S15	0.00001	0	0.05	0.5	0.3	0.004741
S16	0.00001	0	0.0005	0.5	0.97	0.000375
S17	0.1	0	0.0005	0.5	0.101	0.002495

11.3.4 Results and Discussion

Excessive flow was predicted through the vegetation zone close to the longitudinal centre of the flume, despite relatively low permeability values. (Close to the upstream and downstream boundaries, the flow through the vegetation was reduced by the presence of the non-permeable boundary.) It is possible that the way in which groundwater transmissivity is specified in River2D was not well understood, since this is not clearly explained in the user manual.

The use of a single value of groundwater transmissivity throughout the model is very inflexible, since this means that all vegetation would have to be treated as hydraulically identical. Furthermore other substrates above or close to the water surface (including solid bedrock or soil) would be treated as hydraulically equivalent to vegetation.

The velocity profiles produced were very sensitive to various parameters, particularly the Eddy Viscosity parameters and the groundwater transmissivity. As an example, the velocity profiles produced by three model runs are plotted in Figure 11-5, and compared to the measured velocity profile from the laboratory experiment.

Lastly, it is clear from Figure 11-5 that zero velocities were always predicted at the vegetation interface. Not only is this unrealistic in itself, but it also indicates that the model does not take account of momentum transfer across the vegetation interface. This is particularly important since this lateral interaction forms the subject of this project.

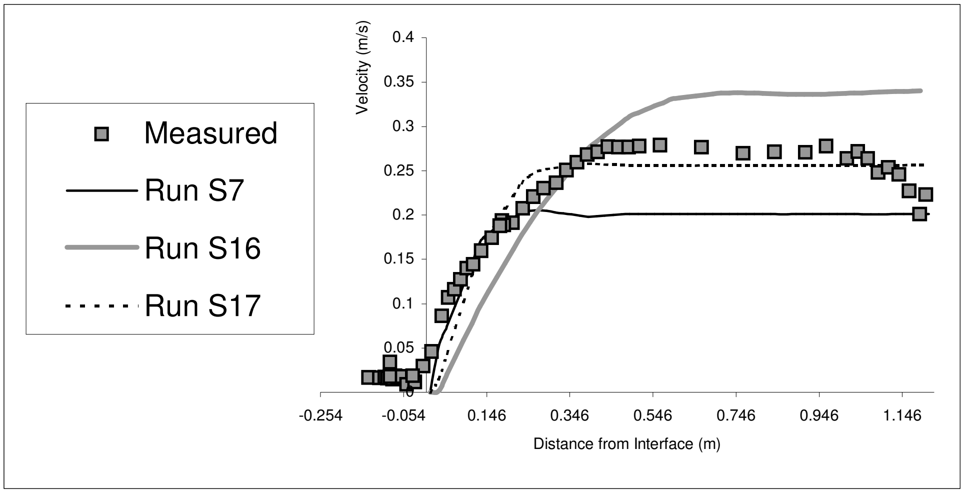

Figure 11-3: Outputs of River2D Model of Vegetation Strip as an Area where the Bed is Raised above the Water Level

11.3.5 Conclusion

The representation of vegetation in River2D as groundwater flow is unsatisfactory because:

- Models produced in this way do not take account of the lateral transfer of momentum across the vegetation interface.
- The use of a constant value of groundwater transmissivity throughout the model is a severe limitation on the flexibility of the models produced.
- A zero velocity is assumed at the interface, which is unrealistic
- It is unclear how transmissivity values can be selected to produce realistic rates of flow through the vegetation.

- There are three main hydraulic parameters which have to be selected: resistance in terms of ks, eddy viscosity and groundwater transmissivity Results are highly sensitive to all three parameters.

An alternative method was therefore attempted.

11.4 Vegetation Strips as Increased Roughness

The alternative way to represent vegetation in River2D is by specifying an increased value of the bed roughness ks in the vegetation zone. This is probably a more conventional method of representing vegetation in hydraulic models.

11.4.1 Setup

The vegetation used in the laboratory experiments was very dense, and hence had a very high flow resistance. As stated previously, there is a limit on the maximum resistance that can be specified in the program, which is equal to a minimum Chézy C resistance co-efficient value of $7.83m^{1/2}/s$. This value can be specified by specifying any high value of bed roughness ks. Since the estimated Chézy C co-efficient for flow through the vegetation under the experimental conditions is $2.7m^{1/2}/s$, this resistance cannot be specified. The best that could be achieved was therefore to specify a high but arbitrary value of bed roughness ks =31m, which the program would recognise as equivalent to the maximum resistance given above. (In one run (K1), a value of 1000m was used instead.) It was therefore expected that flow and velocity through the vegetation would be over-estimated. However, it was hoped that this would make a negligible difference to velocity estimation in the clear channel and to the estimation of overall resistance.

The topography of the laboratory experiments was again replicated, as described for the previous model. However, instead of specifying a different bed elevation for the vegetation strip, a different bed roughness (ks) was specified. A 0.06m wide transition zone (analogous to the slope used in the previous model setup) was incorporated, with breaklines on either side. For the non-vegetated zone, a bed roughness value of ks=0.000 58m was used, except for the first two runs, where a value of 0.001m was used instead. The value of 0.000 58m was calculated based on the water surface or energy slope measured in the flume with no vegetation.

The same mesh described for the previous model was again used.

Boundary conditions were set as a constant inflow at the upstream end and a constant water surface elevation of 0.0596m at the downstream end. Since the velocity profile is sensitive to discharge, two discharges were used. For some runs, a discharge of 0.020m^3/s was used. This is the discharge measured according to a V-notch downstream of the flume. For other runs, a discharge of 0.017 7m^3/s was used. This was the discharge calculated from the velocity measurements using the velocity area method. In retrospect, the discharge using the velocity area method is more appropriate for comparison of velocity measurements, regardless of accuracy. This is because any error of velocity measurement would be reproduced for both the velocity and discharge, so the measured and modelled results would remain comparable.

11.4.2 Procedure

Various runs were conducted with different values of the three eddy viscosity parameters. These parameters are as defined in section 11.2.3. Some runs were also performed with either the default values, or arbitrary values of certain of these eddy viscosity parameters. A summary of these parameter values is presented in Table 11-3. Values for these eddy viscosities were also determined for the various velocity profile methods as discussed in section 11.2.4 on page 130, and are included in Table 11-2 for comparison. The last three runs in Table 11-3 (runs K28, K29 and K30) used these values of eddy viscosity, together with the flowrate calculated using the velocity area method.

As for the model of vegetation flow as groundwater flow, for each run, a water surface elevation profile was extracted by extracting a point every 1m along the flume centreline. The best fit straight line to these points was taken as the water surface slope, and is included in Table 11-3. For each run (except runs K8, K14, K15, K17, K18 and K19), a velocity profile at longitudinal position 10m was also extracted by extracting a point every 0.05m across the flume.

Table 11-2: Calculated Eddy Viscosity Parameters for the Conditions of Test 7

Source	**River 2D Eddy Viscosity Parameters**		
	E1	E2	E3
	(m^2/s)		($m^{-1/2}$)
Nuding (1991, 1994)	0	0	0.211
Ikeda et al. (1991, 1994)	$87x10^{-6}$	0	0
Tsujimoto and Kitamura (1994)	$34x10^{-6}$	0	0

Table 11-3: Parameter Values and Resulting Water Surface Slopes for River2D Model of Vegetation Strips Modelled as Increased Bed Roughness ks

Run	**bed slope**	**ks No Veg.**	**ks Veg.**	**Q**	**E1**	**E2**	**E3**	**Resulting Water Surface slope**
Units	None	m	m	m^3/s	m^2/s	None	$m^{-1/2}$	None
K1	0.00044	0.00058	31	0.02	0	0	0	0.000 444
K2	0.00044	0.00058	31	0.02	0	0	1	0.000 573
K3	0.00044	0.00058	31	0.02	0	0.0005	1	0.000 573
K4	0.00044	0.00058	31	0.02	0	0.5	1	0.000 583
K5	0.00044	0.0001	31	0.02	0	0.5	1	0.000 457
K5a	0.00044	0.0001	31	0.02	0	0.5	1	0.000 46
K6	0.00044	0.0001	1000	0.02	0	0.5	1	0.000 466
K7	0.00044	0.0001	31	0.02	0	0.5	0.5	0.000 398
K8	0.00044	0.0001	31	0.02	0	0.5	0.3	0.000 369
K9	0.00044	0.0001	31	0.02	0	0.5	0.25	0.000 362
K10	0.00044	0.00058	31	0.017	0	0.5	0.25	0.000 366
K11	0.00044	0.00058	31	0.0177	0	0.5	0.25	0.000 395
K12	0.00044	0.00058	31	0.0177	0.00445	0	0	0.000 537
K13	0.00044	0.00058	31	0.0177	0.001	0	0	0.000 435
K14	0.00044	0.00058	31	0.0177	0.000445	0	0	0.000 406
K15	0.00044	0.00058	31	0.0177	0.000045	0	0	0.000 381

Run	bed slope	ks No Veg.	ks Veg.	Q	E1	E2	E3	Resulting Water Surface slope
Units	None	m	m	m^3/s	m^2/s	None	$m^{-1/2}$	None
K16	0.00044	0.00058	31	0.0177	4.5E-06	0	0	0.000 377
K17	0.00044	0.00058	31	0.0177	0	0.5	0.15	0.000 403
K18	0.00044	0.00058	31	0.0177	0	0.5	0.05	0.000 399
K19	0.00044	0.00058	31	0.0177	0	0.5	0.05	0.000 398
K20	0.00044	0.00058	31	0.0177	7.02E-07	0	0	0.000 35
K21	0.00044	0.00058	31	0.02	9.95E-06	0	0	0.000 449
K22	0.00044	0.00058	31	0.0177	9.95E-06	0	0	0.000 353
K23	0.00044	0.00058	31	0.0177	0	0	0.487	0.000 402
K24	0.00044	0.00058	31	0.02	0	0	0.487	0.000 509
K25	0.00044	0.00058	31	0.0177	0.0964	0	0	0.001 148
K26	0.00044	0.00058	31	0.0177	0.000687	0	0	0.000 403
K27	0.00044	0.00058	31	0.02	0.000687	0	0	0.000 509
K28	0.00044	0.00083	31	0.0177	0.211	0	0	0.000 417
K29	0.00044	0.00083	31	0.0177	0	0	8.7×10^{-5}	0.000 415
K30	0.00044	0.00083	31	0.0177	0	0	3.4×10^{-5}	0 000 413

11.4.3 Results and Discussion

The velocity profiles produced were sensitive to both discharge and eddy viscosity. This sensitivity is indicated by the differences in predicted water surface slopes, as indicated in Table 11-3. The effect of eddy viscosity on the predicted lateral velocity distribution is shown in Figure 11-4. This graph shows lateral velocity profiles for three runs which differ only in the value specified for the constant eddy viscosity parameter E1.

In Figure 11-5, velocity profiles predicted using the calculated values of eddy viscosity and using the discharge calculated by the velocity-area method are plotted. They are also compared to the measured velocity profile from the laboratory experiment, as well as to the velocity profiles produced by the various velocity distribution equations. It is clear that reasonable predictions for the velocity profile within the non-vegetated zone (particularly close to the vegetation interface) can be attained using eddy viscosities calculated by any of the specified methods. Profiles predicted by the model using all three calculated eddy viscosities are very similar.

As expected, modelled velocities within the vegetation are higher than measured velocities, because of the limit on resistance. The predicted velocity profiles appear reasonably realistic, depending on the eddy viscosity and discharge selected. The transverse interaction between vegetated and non-vegetated zones is a turbulence phenomenon, and (unlike phenomena which are dominated by geometry rather than turbulence) predictions are therefore extremely sensitive to the specification of eddy viscosity.

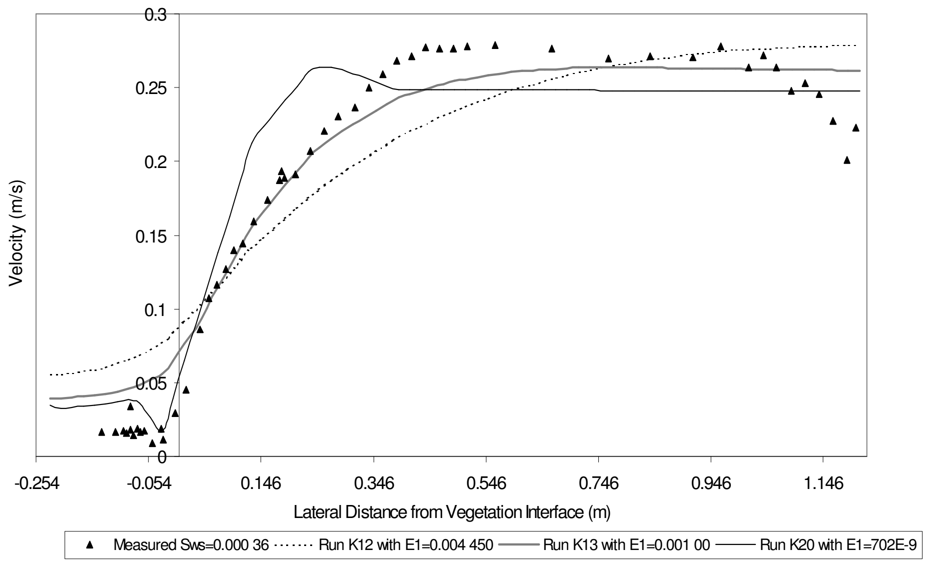

Figure 11-4: Effect of Eddy Viscosity on River2D predictions of lateral velocity profiles

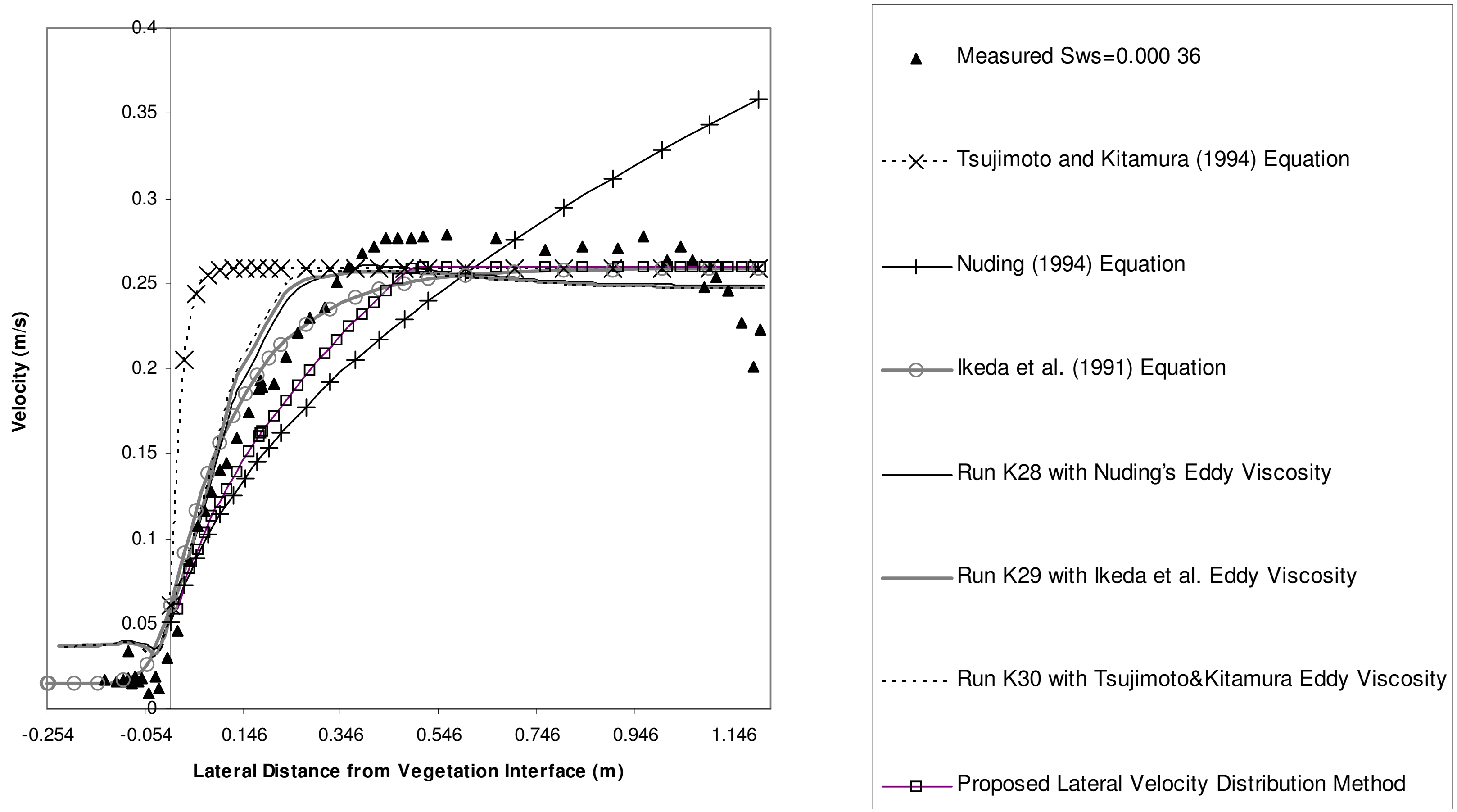

Figure 11-5: Results of River2D Model of Vegetation Strips with Vegetation Represented by Increased ks

11.4.4 Conclusion

In River2D, the use of an increased value of equivalent sand grain roughness (ks) to represent vegetation is better than representing flow through vegetation as groundwater flow. Reasonable predictions can be attained using one of the methods which have been proposed for the calculation of eddy viscosity in partially vegetated channels. The major limitation is that the maximum hydraulic resistance which can be specified corresponds to a Chézy C resistance co-efficient value of 7.83m$^{1/2}$/s. For very dense vegetation, this causes flow through the vegetation to be over-estimated. Further modelling of vegetation influenced flows will therefore represent the vegetation as increased roughness (ks), combined with calculated values of eddy viscosity.

11.5 Modelling the effect of Non-vegetated Zone Width

The effect of the width of the non-vegetated zone was the main factor investigated in Part III of this report. In evaluating the use of River2D to model partially vegetated channels, this effect also had to be considered. A model similar to that described in section 11.4 was set up for the conditions of test 40 by Makoa (2001) in James et al. (2001). The width of the non-vegetated zone in the model was changed, and the effect on predicted lateral velocity profiles and uniform depth was observed. Note that a new computational mesh had to be generated for each run.

The laboratory test used vegetation strips 0.25m wide on each side of a non-vegetated zone of total width 0.5m. The vegetation consisted of a staggered pattern with dp = 0.005m, ax=0.25m and ay=0.0125m, as indicated in Figure 4-3 on page 33. The bed roughness value (ks = 0.368mm) was derived from stage-discharge measurements in an empty flume. The vegetation roughness was arbitrarily taken as (ks=100m). A 40mm wide transition between these two values of ks was implemented. The depth at the downstream boundary was set at the measured depth of 62mm. In each run, discharge was adjusted until a uniform depth (for a slope of 0.00107) was achieved. Conditions for each run are given in Table 11-4.

In each case, eddy viscosity was calculated using Equation (145) on page 131. Since the maximum velocity could not be known before modelling, the velocity with bed resistance only (V_{inf} = 0.485m/s) was used in this equation. Where the maximum velocity predicted by the model was significantly less than this, the eddy viscosity was re-calculated with the predicted maximum velocity, and the model was re-run with this eddy viscosity. These re-runs will be referred to as iterated runs, and will be used to give some indication of when such iteration is necessary.

Table 11-4: Inputs for River2D model runs with changing non-vegetated zone width

Non-vegetated Zone Half Width (bf)	bf / TW Wide	Uniform Depth	Q	ε_3 Based on	ε_3
(m)		(m)	(m3/s)		($m^{-1/2}$)
0.10	0.26	0.064	0.002 6	Vinf	0.155
0.10	0.26	0.064	0.002 6	Vmax (iterative)	0.045
0.25	0.65	0.062	0.011 4	Vinf	0.155
0.25	0.65	0.062	0.011 6	Vmax (iterative)	0.140
0.50	1.30	0.062	0.019 0	Vinf	0.155
0.75	1.94	0.062	0.019 0	Vinf	0.155
1.00	2.59	0.062	0.053 5	Vinf	0.155
2.00	5.18	0.064	0.124 3	Vinf	0.155

Two sets of results will be considered: maximum velocity predictions and lateral velocity profiles.

Maximum velocities predicted using the River2D model have been added to the graph originally shown in Figure 8-10. (This graph showed the measured maximum velocity and that predicted by the proposed equations for different widths.) The result is presented as Figure 11-6. Predicted velocities at the channel centre have also been added. These give an indication of which predicted maximum velocities are local maxima, and which continue across to the channel centre.

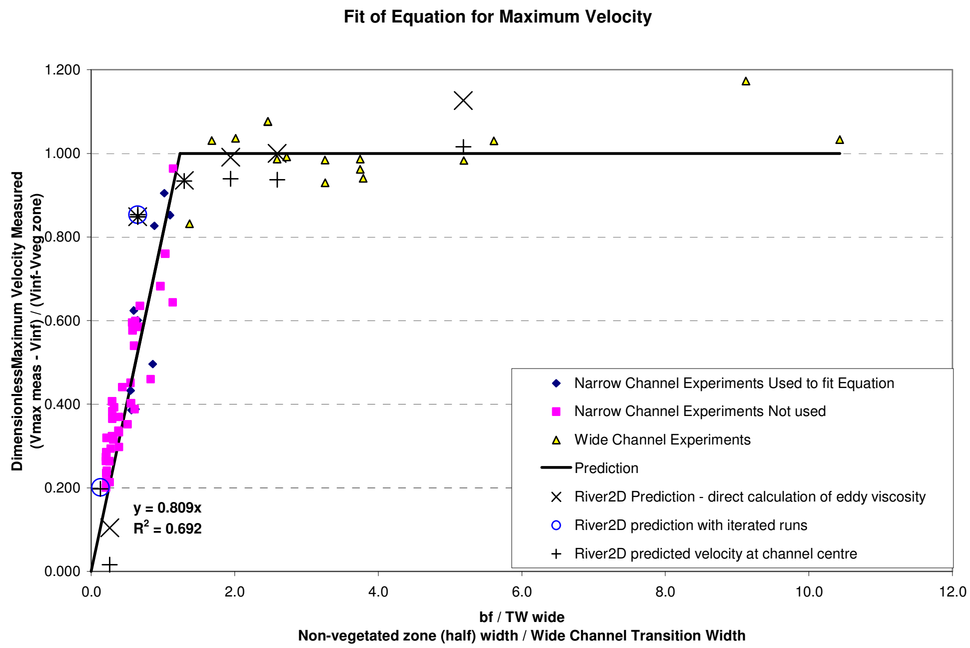

Figure 11-6: Maximum Velocity Predicted by River2D

For intermediate widths (1 < bf /TW Wide < 3), the maximum velocity is close to the velocity with bed resistance only (V_{inf}), and is well predicted by River2D. However, the maximum velocity is over-predicted for the widest non-vegetated zone. It is not clear why velocities significantly higher than that with bed resistance only are predicted in this case, but a plot of the predicted transverse velocity profile (Figure 11-7) indicates that this is a local effect only, and the predicted velocity at the channel centre is close to V_{inf}. For the narrowest non-vegetated zone, the maximum velocity is initially under-predicted. However, iteration (by recalculating eddy viscosity based on the predicted maximum velocity) allows a maximum velocity to be predicted which is the same as that measured and that predicted using the proposed equation. In the second narrowest test, the maximum velocity is close enough to that with bed resistance so that iteration for eddy viscosity makes no noticeable difference. However, for this width, the maximum velocity is over-predicted.

Transverse velocity distributions predicted by the River2D model for different non-vegetated zone half-widths (bfo) are plotted in Figure 11-7. Measured velocities for bfo = 250mm are also plotted for comparison. For the narrower channels (bfo=100, 250 or 500mm), a smooth transition from the vegetation zone to the maximum velocity is predicted. However, the wider channel predictions suggest a local maximum velocity some distance away from the vegetation interface, which decreases towards the channel centre. Such local maxima were observed in laboratory test number 25 by Ikeda et al. (1991). However, it was shown in section 6.5 that for the current experiments, local maxima were an effect of flume entrance conditions. The comparison with the measured profile for a

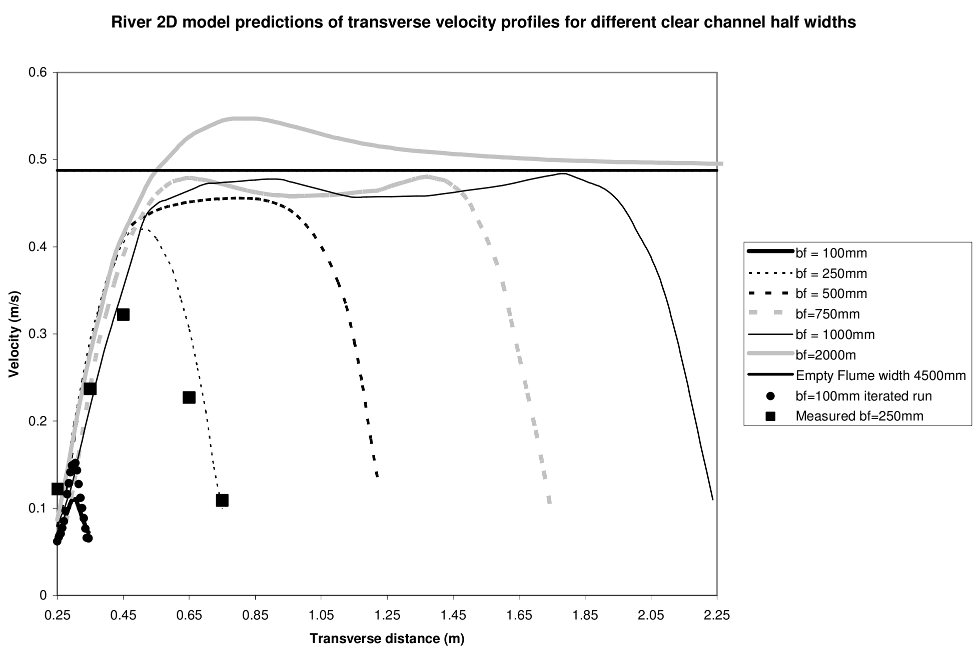

Figure 11-7: Transverse Velocity Profiles Predicted by River2D for changing non-vegetated zone width

250mm non-vegetated zone half-width suggests that the modelled profile has the correct shape and that the correct velocity is predicted at the vegetation interface, but that the maximum velocity is significantly over-predicted. The width over which the transition occurs also appears to be approximately correct.

In conclusion, although River2D does predict that width reduction reduces maximum velocity, for certain non-vegetated zone widths (particularly for the measured case where bf / TW Wide = 0.65), the predicted maximum velocity remains too high. The distance over which the transition occurs appears to be approximately in agreement with the laboratory test data. River2D thus provides a reasonable, but not entirely accurate representation of this situation.

11.6 Resistance of Vegetation Patches

Having confirmed that, with the selection of appropriate parameters, velocity distributions adjacent to vegetation strips can be modelled using River2D; the next step was to address the more complex situation where the vegetation occurs in patches. As explained in section 11.1, this is the situation in which numerical modelling is actually required, since the layout is too complex to be represented symbolically. For the purpose of this comparison, two patch layouts were selected from those tested by James et al. (2001).

11.6.1 Setup

The vegetation patterns modelled were patterns 14 and 21 of James et al. (2001). These patterns are as illustrated in Figure 11-8 and Figure 11-9, which contain bed roughness plots from River2d.

As for the vegetation strip experiments described in sections 11.4 and 11.5, vegetation was modelled as an arbitrary but high value of ks=100m. The measured depth-discharge relation for the empty flume was plotted, and this was used to calculate an appropriate value of ks for the bed corresponding to each depth.

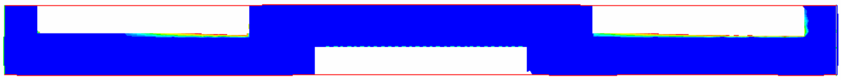

Figure 11-8: Pattern 14 Layout
(Vegetation in White)

Figure 11-9: Pattern 21 Layout
(Vegetation in Red)

In River2D, a single value of ks must be specified at each position. Any change in ks must therefore take place over a certain distance. If the distance over which this transition occurs is not specified explicitly, it will be interpolated. (Firstly, when the bed topography is triangulated, ks is interpolated linearly between adjacent topographic points. Then, when a mesh is generated, ks at each computational node is taken from the triangulated bed topography. In hydraulic calculations, a linear change over each element of the computational mesh is assumed, based on the values of ks previously calculated for each computational node.) These interpolations result in an irregular distribution of ks, depending on the topographic points input and on the local geometry of the computational mesh. In order to control the way in which ks was interpolated around each patch, a roughness transition zone around each vegetation patch was used. Within the transition region, ks changes linearly with distance. This transition was implemented in two ways as illustrated in Figure 11-10: either the transition region was half within and half outside the patch, or it was completely inside the patch. The resistance to flow is expected to be less with the transition inside, since the higher roughness extends over a smaller area.

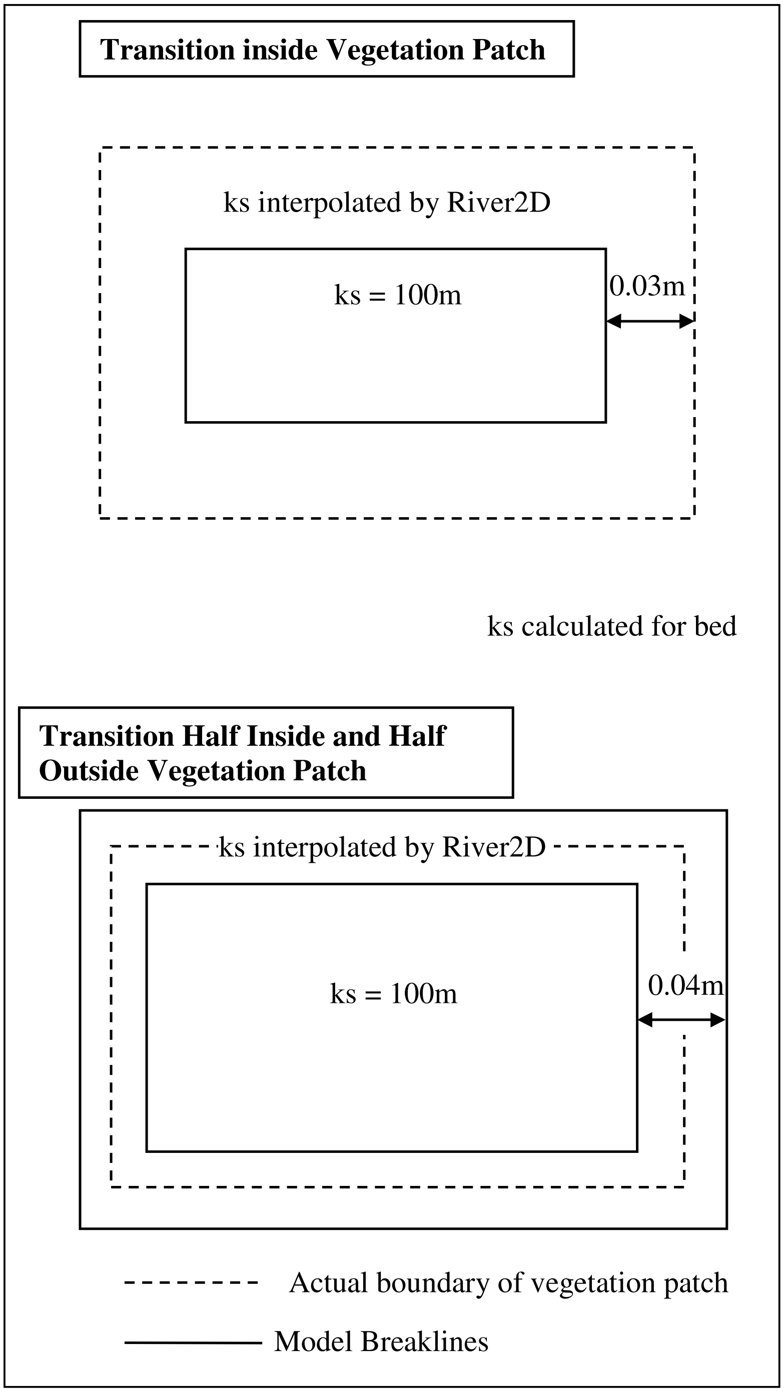

Figure 11-10: Patch boundaries and interpolation of roughness ks

The following topography of the laboratory experiments was replicated:

Total Width: 1m

Total Length: 12m

Bed Slope: 0.00107

The topography was extended by 0.01m all the way around the flume to allow for interpolation at the boundary.

In most experiments, the discharge was set at the value measured in the laboratory experiments. The downstream water surface elevation was adjusted to give approximately the uniform flow depth along the flume. (As an alternative for certain runs, the downstream water surface elevation was set at the measured depth. In this case, as for the previous models, a straight line fitted to the predicted water surface elevation yielded the average water surface slope.)

Eddy viscosity was calculated in three ways:

- A constant Eddy Viscosity of 0.000687m^2/s. was assumed for all runs. (ε_1= 0.000687, ε_2=ε_3=0). As can be seen from Figure 11-1 on page 132, this is approximately the eddy viscosity calculated for experiments using the same artificial vegetation for approximately the shallowest depth of 0.025 to 0.030 m. The calculated eddy viscosity would actually change with flow condition, including slope, depth and flume bed resistance. However, for simplicity, this value was used throughout. This would test whether acceptable results can be obtained without re-calculating eddy viscosity for every condition modelled.

- Eddy viscosity was calculated according to the equation of Tsujimoto and Kitamura (1994) for each run. (See Equation (146) on page 131, with f calculated according to equation (37).)

- Eddy viscosity was calculated according to the equation of Nuding (1991, 1994). (Equation (145) on page 131.)

Note that eddy viscosity calculated according to all of these methods is independent of width.

11.6.2 Results

Conditions for each run, as well as calculated prediction errors are included in Table 11-5. In this table, the column labelled BC indicates whether the downstream water surface elevation was set at the measured depth (WS) or the elevation was adjusted to produce a uniform depth (S). The column labelled R indicates whether the transition for ks was inside (I) or half inside and half outside the vegetation patch (H), as illustrated in Figure 11-10. The columns labelled E1 and E3 represent the values of the eddy viscosity parameters used in the model. Figure 11-11 and Figure 11-12 are graphs of the predicted and measured uniform flow depth for patterns 21 and 14 respectively. They indicate the differences between the different conditions selected (in terms of eddy viscosity calculation and the location of the roughness transition). A sample velocity plots for pattern 14 is included in Figure 11-13. A sample velocity plot for pattern 21 is included in Figure 11-14.

11.6.3 Discussion

Note in Figure 11-14 that high velocities close to the flume wall are predicted, because the wall was not included in the model. Slip was therefore allowed on the wall with no resulting wall shear stress. No reduction in velocity close to the wall would therefore be predicted. This would have resulted in a slight decrease in the uniform flow depth.

Table 11-5: Conditions and Prediction Errors for River2D models of Vegetation Patches

Pat-tern	Q (m^3/s)	BC	R	Water Sur-face slope	Mea-sured Depth (m)	Pre-dicted Depth (m)	Equation for Calculating Eddy Viscosity	E1 (m^2/s)	E3 ($m^{-1/2}$)	Manning's n (s / $m^{1/3}$) Predi cted	Meas ured	Error in Slope	Error in Uniform Depth (%)	(m)
14	0.005	WS	H	0.001 4	0.028	0.031	Constant	0.000687	0	0.023	0.017	35%		
14	0.005	S	H	0.001 1	0.028	0.041	Nuding (1991, 1994)	0	0.370	0.032	0.017		46%	0.013
14	0.005	S	I	0.001 1	0.028	0.040	Nuding (1991, 1994)	0	0.370	0.031	0.017		42%	0.012
14	0.005	S	I	0.001 2	0.028	0.040	Tsujimoto and Kitamura (1994)	5.80E-05	0	0.032	0.017		45%	0.013
14	0.010	WS	H	0.001 3	0.055	0.056	Constant	0.000687	0	0.029	0.026	20%		
14	0.010	S	H	0.001 2	0.055	0.066	Nuding (1991, 1994)	0	0.217	0.037	0.026		22%	0.012
14	0.010	S	I	0.001 0	0.055	0.065	Nuding (1991, 1994)	0	0.217	0.034	0.026		16%	0.009
14	0.010	S	I	0.001 1	0.055	0.066	Tsujimoto and Kitamura (1994)	8.40E-05	0	0.036	0.026		22%	0.012
14	0.015	WS	H	0.001 2	0.078	0.079	Constant	0.000687	0	0.034	0.031	14%		
14	0.015	S	H	0.001 1	0.078	0.091	Nuding (1991, 1994)	0	0.159	0.040	0.031		17%	0.013
14	0.015	S	I	0.001 1	0.078	0.086	Nuding (1991, 1994)	0	0.159	0.036	0.031		9%	0.007
14	0.015	S	I	0.001 1	0.078	0.090	Tsujimoto and Kitamura (1994)	1.09E-04	0	0.040	0.031		15%	0.012
14	0.020	WS	H	0.001 2	0.100	0.100	Constant	0.000687	0	0.037	0.035	11%		
14	0.020	S	H	0.001 1	0.100	0.111	Nuding (1991, 1994)	0	0.155	0.043	0.035		13%	0.012
14	0.020	S	I	0.001 1	0.100	0.106	Nuding (1991, 1994)	0	0.155	0.039	0.035		6%	0.006
14	0.020	S	I	0.001 1	0.100	0.111	Tsujimoto and Kitamura (1994)	1.15E-04	0	0.042	0.035		12%	0.012
21	0.005	WS	H	0.001 3	0.040	0.041	Constant	0.000687	0	0.035	0.030	18%		
21	0.005	WS	H	0.001 2	0.040	0.047	Nuding (1991, 1994)	0	0.292	0.042	0.030	11%		
21	0.005	S	H	0.001 1	0.040	0.047	Nuding (1991, 1994)	0	0.292	0.040	0.030		19%	0.008
21	0.005	S	I	0.001 1	0.040	0.043	Nuding (1991, 1994)	0	0.292	0.035	0.030		10%	0.004
21	0.005	S	I	0.001 1	0.040	0.049	Tsujimoto and Kitamura (1994)	6.17E-05	0	0.043	0.030		24%	0.010
21	0.008	WS	H	0.001 2	0.055	0.056	Constant	0.000687	0	0.038	0.035	14%		

Pat-tern	Q (m^3/s)	BC	R	Water Sur-face slope	Mea-sured Depth (m)	Pre-dicted Depth (m)	Equation for Calculating Eddy Viscosity	E1 (m^2/s)	E3 ($m^{-1/2}$)	Manning's n (s / $m^{1/3}$) Predi cted	Meas ured	Error in Slope	Error in Uniform Depth (%)	(m)
21	0.008	WS	H	0.001 2	0.055	0.062	Nuding (1991, 1994)	0	0.217	0.043	0.035	8%		
21	0.008	S	H	0.001 1	0.055	0.062	Nuding (1991, 1994)	0	0.217	0.043	0.035		14%	0.008
21	0.008	S	I	0.001 1	0.055	0.055	Nuding (1991, 1994)	0	0.217	0.035	0.035		1%	0.001
21	0.008	S	I	0.001 1	0.055	0.061	Tsujimoto and Kitamura (1994)	8.88E-05	0	0.042	0.035		13%	0.007
21	0.010	WS	H	0.001 0	0.075	0.074	Constant	0.000687	0	0.042	0.044	-7%		
21	0.010	WS	H	0.000 9	0.075	0.080	Nuding (1991, 1994)	0	0.166	0.045	0.044	-13%		
21	0.010	S	H	0.001 1	0.075	0.077	Nuding (1991, 1994)	0	0.166	0.045	0.044		2%	0.002
21	0.010	S	I	0.001 1	0.075	0.068	Nuding (1991, 1994)	0	0.166	0.037	0.044		-9%	-0.007
21	0.010	S	I	0.001 1	0.075	0.074	Tsujimoto and Kitamura (1994)	1.04E-04	0	0.044	0.044		0%	0.000
21	0.013	WS	H	0.001 1	0.086	0.085	Constant	0.000687	0	0.043	0.043	0%		
21	0.013	WS	H	0.001 0	0.086	0.091	Nuding (1991, 1994)	0	0.152	0.047	0.043	-6%		
21	0.013	S	H	0.001 1	0.086	0.089	Nuding (1991, 1994)	0	0.152	0.047	0.043		5%	0.004
21	0.013	S	I	0.001 1	0.086	0.079	Nuding (1991, 1994)	0	0.152	0.038	0.043		-7%	-0.006
21	0.013	S	I	0.001 1	0.086	0.089	Tsujimoto and Kitamura (1994)	1.08E-04	0	0.048	0.043		6%	0.005

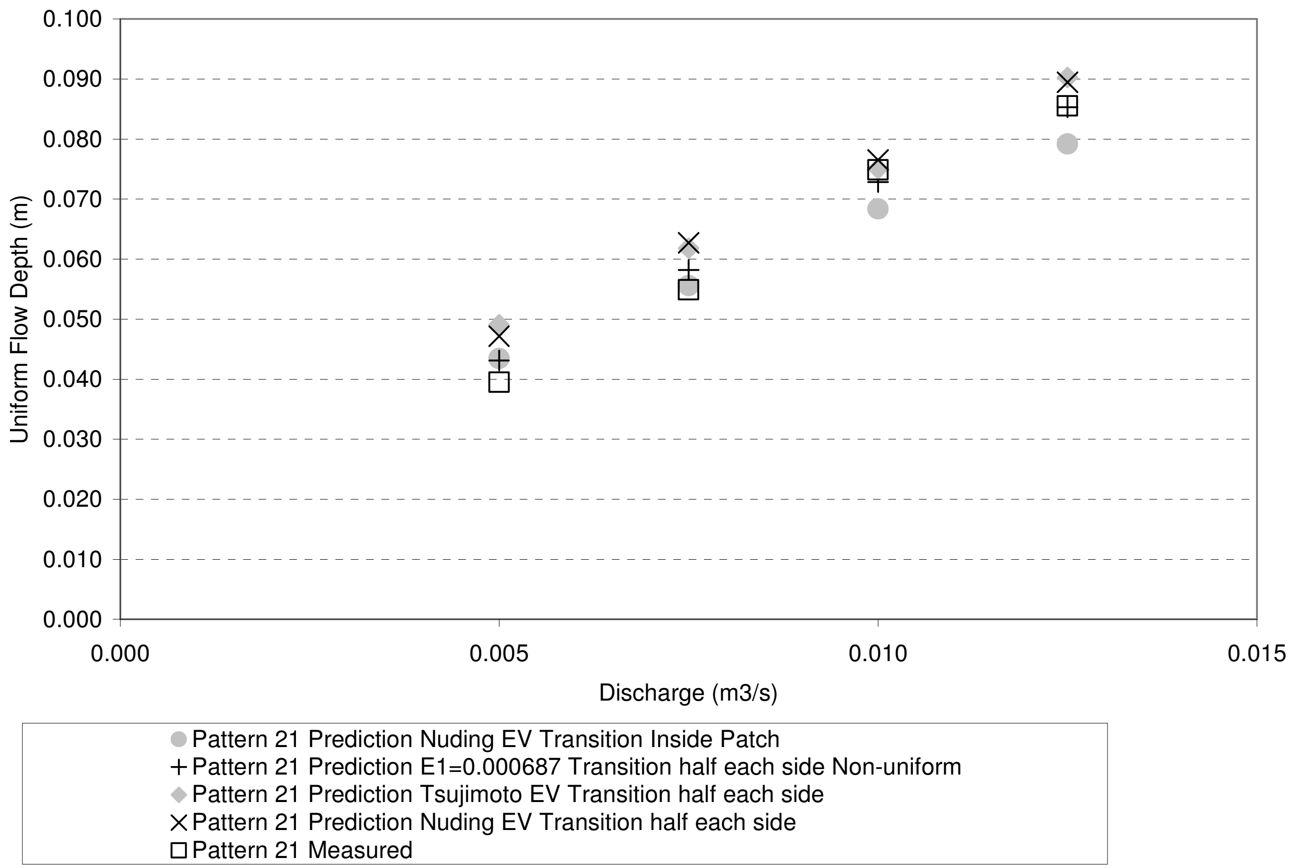

Figure 11-11: River2D Uniform Depth Predictions for Pattern 21

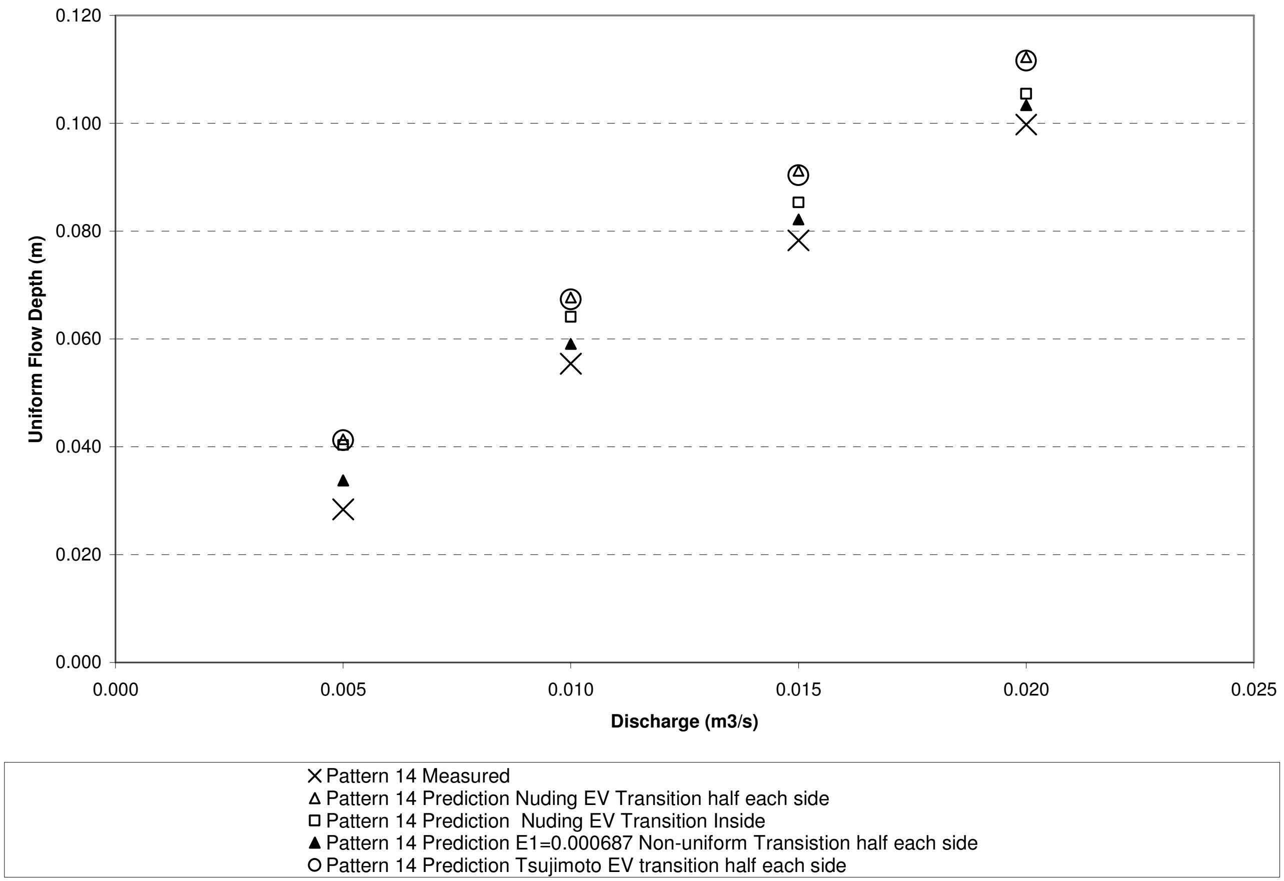

Figure 11-12: River2D Uniform Depth Predictions for Pattern 14

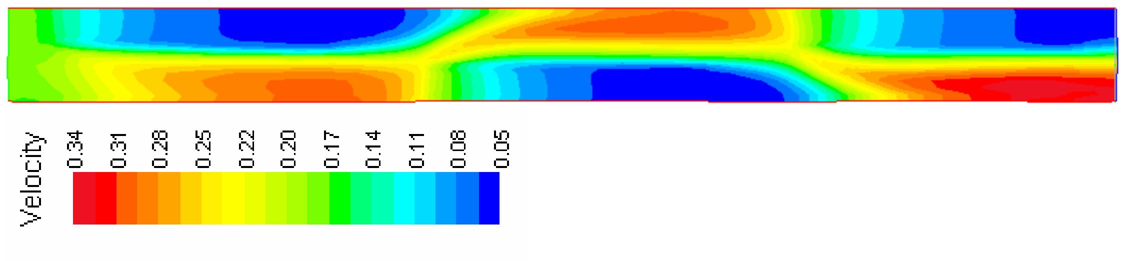

Figure 11-13: Velocities Predicted for Pattern 14 at a flow of 0.1m3/s

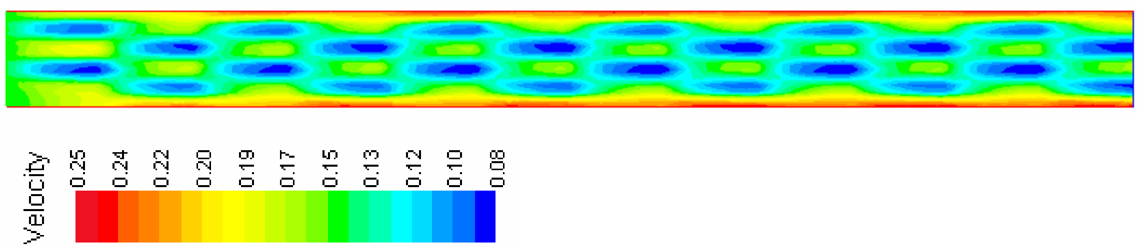

Figure 11-14: Velocities Predicted for Pattern 21 at a flow of 0.125m3/s

Note also that, as for the vegetation strips modelled in sections 11.4 and 11.5, the maximum value of hydraulic resistance which can be specified is less than the actual resistance of the vegetation. For these patterns, most of the channel is not vegetated, and the resulting increased flow through the vegetation is not significant. However, Jordanova et al. (in prep.) produced similar models of patterns in which up to 50% of the channel was covered by vegetation, and in some of these patterns, there was no clear flow path between the vegetation patches. In this case, the necessity of specifying a lower hydraulic resistance for the vegetation than that actually measured significantly decreases the overall hydraulic resistance and uniform flow depth.

It is clear from the results presented in Table 11-5 that uniform flow depth (or hydraulic resistance) is more accurately predicted for the higher discharges, and is over-predicted for lower discharges. (For the lowest discharge of 0.005m^3/s, errors in the prediction of uniform depth are 42-46% for Pattern 14 and 10-24% for pattern 21. For the highest discharges of 0.020m^3/s for Pattern 14, these errors are 6-13%. For the highest discharge of 0.013m^3/s for Pattern 21, these errors are all less than 7 %.) (This trend may be better specified in terms of flow depth relative to vegetation spacing i.e. the model runs with a flow depth of approximately four times the full transverse vegetation spacing yielded accurate predictions, whereas those with a uniform depth of less than double the full transverse vegetation spacing over-predicted the uniform flow depth.) The trend of increasing values of Manning's n with increasing discharge is, however, correctly predicted for both patterns. The difference in the magnitude of resistance (or uniform flow depth for the same discharge) between the two patterns is also correctly predicted.

Predicted stage and velocity information can be re-stated depending on the required habitat classification of a particular ecological study. This accuracy will be sufficient for prediction of most of the velocity ranges listed in Table 2-1on page 18.

In all cases, the most accurate predictions were achieved using the constant value of eddy viscosity. This gives a strong indication that it is not necessary to re-calculate eddy viscosity for different depths and patterns.

11.6.4 Conclusion

Resistance and velocity patterns produced by vegetation patches can only be estimated using numerical models, since analytical methods have not been developed. Jordanova et al. (in prep.) have shown that it is not possible to model very dense vegetation which covers half or more of the channel, because of the limitation on resistance values which can be specified in River2D. The analysis presented here has shown that resistance predictions using River2D also become less accurate for very low flows. Within these limitations, it would appear that River2D can be used to predict the resistance of vegetation patches within a 10 to 20% margin of error. A reasonable estimation of eddy viscosity is required, but this need not be re-calculated for each experimental run. River2D may therefore be selected as the final tool in the suite of methods presented in this report to predict of the effect of vegetation on resistance and laterally adjacent velocities in non-vegetated channel zones.

Part V: Conclusions and Recommendations

12 Conclusions

For emergent vegetation strips parallel to the flow direction, analytical methods have been proposed to predict:

- stage-discharge-energy slope relations via hydraulic resistance,
- maximum velocity attained, taking channel width into account and
- the lateral profile of depth-averaged velocity in the non-vegetated zone.

Limited testing of the hydraulic resistance relations against the data of James et al. (2001) has been conducted. Two alternative existing relations were found capable of reproducing the measured stage - discharge data.

The methods for the prediction of the lateral distribution of depth-averaged velocity have been tested against previously published and new experimental data. Velocity predictions are of limited accuracy close to the vegetation boundary, where velocities are irregular, but become more accurate further into the non-vegetated zone. Both the maximum velocity attained and the lateral distance over which a velocity profile is scaled can be predicted.

For more complex geometries, particularly where vegetation patches exist, two-dimensional numerical modelling is proposed in order to predict both stage-discharge-energy slope relations and the distribution of depth averaged velocity. The two-dimensional hydraulic and habitat simulation software River2D was shown to be capable of predicting the stage or slope measured by James et al. (2001) in a laboratory flume with vegetation patches. Because the flow in this situation is dominated by the turbulent transfer of momentum between vegetated and non-vegetated zones, the correct specification of eddy viscosity in the models is particularly important. Existing equations for eddy viscosity have therefore been tested and recommended.

In ecological studies, the way in which depth and velocity are specified is highly dependent on the particular situation being investigated. Predicted values of stage and depth-averaged velocity can be re-stated in terms of any ecological requirements, as specified for a particular study.

13 Research and Development Needs

The most important development required for practical application of the method proposed for the prediction of lateral velocity profiles stems directly from the main limitation of the development of this method. All experiments analysed were performed in rectangular channels with constant bed resistance. Furthermore, development of the equations for transition width and interface shear velocity used these same assumptions. Frequently, it will be desired to predict lateral velocity profiles in rivers which are more irregular in terms of their cross-section geometry and bed resistance. The proposed method for prediction of lateral velocity profiles needs to be extended to cover these conditions. This will greatly enhance the method's flexibility.

In this report, the following questions which require further research or development have also been specifically raised:

- As discussed in section 8.5.5, one aspect of the shape of the velocity profile remains unclear. The question remains: does the velocity profile in a rectangular non-vegetated zone always level off away from the vegetation, or will there be cases where the velocity continues to increase all the way to the centre (or far side) of the non-vegetated zone.

- Section 9.3.2 highlighted the need to investigate in more detail the flow patterns produced close to the vegetation interface.

- As discussed in section 9.3.3, the effect of the longitudinal spacing of vegetation has not been adequately taken into account. This effect will need to be investigated experimentally.

- A limitation on the maximum resistance which may be specified in River2D was explained in sections 11.2.3 and 11.4.1. In order to allow this program to better represent flow through vegetation, the formula used to calculate resistance for low flows should be modified to remove this limitation.

In addition, a few other points regarding future research deserve mention:

- In future experimental investigations, it is important to ensure that a broad range of non-vegetated zone widths (including both wide and narrow zones) is included. The fact that wide and narrow channel experiments have been conducted separately, under different conditions, makes the comparison between these conditions indirect.

- It would be useful to approximate the equations for narrow channel transition width and apparent shear velocity on the vegetation interface with relations which can be solved directly, and do not require iteration.

- This project focussed on predicting velocity profiles within the non-vegetated zone. Except for the presentation of the equation of Ikeda et al. (1991, 1994) and Tsujimoto and Kitamura (1994) in section 7.4, velocities within the vegetation zone were not discussed. Future research could investigate velocity profiles within the vegetation.

References

Arunn (2006) *Porous medium definition and examples*, INTERNET.http://www.arunn.net/scienceblog/2006/08/23/porous-medium-definition-and-examples/

Bertram, H.-U. (1985) *Über den Abfluß in Trapezgerinnen mit extremer Böschungsrauheit*, Report No. 86 of the Leightweiβ-Institut für Wasserbau, T.U. Braunschweig.

Biggs, B.J.F. (1996) Hydraulic Habitat of Plants in Streams*, Regulated Rivers: Research and Management* Vol. 12, Issue 2-3.

Bovee, K.D. (1996) Perspectives on Two-Dimensional River Habitat Models: The PHABSIM Experience, *Proceedings: Ecohydraulics 2000: 2nd International Symposium on Habitat Hydraulics*, Quebec, June 1996, Vol. B pp. B149-B162, INRS-Eau, Quebec, 1996.

Cambray, J., King, J. and Bruwer, C. (1998) Spawning Behaviour and Early Development of the Clanwilliam Yellowfish (Barbus Capensis Cypinidae), Linked to Experimental Dam Releases in the Olifants River, South Africa, Chapter 13 in Tharme, R.E. and King, J.M. (1998) *Development of the Building Block Methodology for Instream Flow Assessments and Supporting Research on the Effects of Different Magnitude Flows on Riverine Ecosystems*, WRC Report Number 576/1/98, Water Research Commission, Pretoria.

Chu, V.H., Wu, J.-H. and Khayat, R.E. (1991) Stability of transverse shear flows in shallow open channels, *Journal of Hydraulic Engineering*, Vol. 117, No. 10, October 1991, pp1370-1388.

Choi and Kang (2006) Numerical investigations of mean flow and turbulence structures of partly-vegetated open-channel flows using the Reynolds stress model, *Journal of Hydraulic Research*, Vol. 44, No. 2, pp203-217.

Darby, S.E. and Thorne, C.R. (1996) Predicting stage-discharge curves in channels with bank vegetation, *Journal of Hydraulic Engineering*, October 1996, pp583-586.

de Lemos, M.J.S. and da Silva, R.A. (2002) Simulation of Turbulent Flow in a Channel Partially Occupied by a Porous Layer Considering the Stress Jump at the Interface, *Proceedings of the 2002 ASME Joint U.S.-European Fluids Engineering Conference*, July 14-18, 2002, Montreal.

Desai, A.Y. and Chicktay, I. (2005) *Simulation of 2D velocity distribution associated with large obstructions in rivers by velocity defect superposition*, Final Year Investigation Project Report, Dept. Civil Engineering, University of the Witwatersrand, Johannesburg

Freeman, G.E., Rahmeyer, W.H. and Copeland, R.R. (2002) Development and Application of Methodology for Determination of Hydraulic Roughness for Vegetated Floodplains, *Conference: Hydraulic Measurements and Experimental Methods*, Jul-Aug 2002, Estes Park, CO, USA, ASCE.

Fukuoka, S. and Fujita, K. (1990) Flow Resistance due to Lateral Momentum Transport across Vegetation in the River Course, *International Conference on Physical Modelling of Transport and Dispersion*, Vol. 12B, pp25-30, American Society of Civil Engineers, New York, USA.

Gore, J.A. (1978) A Technique for Predicting In-stream Flow Requirements of Benthic Macroinvertebrates, *Freshwater Biology* Vol. 8, 1978, pp 141-151.

Gore, J.A., Layzer, J.B. and Mead, J. (2001) Macroinvertebrate Instream Flow Studies after 20 Years: A Role in Stream Management and Restoration, *Regulated Rivers Research and Management*, 17 (2001) pp 527-542.

Gore, J.A., Layzer, J.B. and Russel, I.A. (1992) Non-traditional Applications of Instream Flow Techniques for Conserving Habitat of Biota in the Sabie River of Southern Africa, Chapter 11 in Boon, P.J., Calow, P. and Petts, G.E. (Eds) *River Conservation and Management,* John Wiley and Sons, Chichester, England, 1992.

Harris, E.L., Babovic, V. and Falconer, R.A. (2003) Velocity predictions in compound channels with vegetated floodplains using genetic programming, *International Journal of River Basin Management*, Vol. 1, No. 2, pp117-123.

Helmiö, T. (2002) Unsteady 1D flow model of compound channel with vegetated floodplains, *Journal of Hydrology*, 269, pp88-99, Elsevier Science B.V.

Helmiö, T. (2004) Flow resistance due to lateral momentum transfer in partially vegetated rivers, *Water Resources Research*, 40, W05206, American Geophysical Union.

Horton, R. E. (1933). Separate roughness coefficients for channel bottom and sides. *Engineering News Record*, III (22,) 652-653

Hyams (2001) *CurveExpert Version 1.38* Software available on INTERNET.http://curveexpert.webhop.net/

Ikeda, S., Izumi, N. and Ito, R. (1991) Effects of Pile Dikes on Flow Retardation and Sediment Transport, *Journal of Hydraulic Engineering*, v. 117, no. 11, Nov 1991, ASCE.

Ikeda, S., Ohta, K. and Hasegawa, H. (1994) Instability-induced Horizontal Vortices in Shallow Open-channel Flows with an Inflection Point in Skewed Velocity Profile*, Journal of Hydroscience and Hydraulic Engineering*, Vol. 12, No. 2, November 1994, 69-84, Japan Society of Civil Engineers.

James, C.S., Birkhead, A.L., Jordanova, A.A., Nicolson, C.R. and Makoa, M.J.(2001*) Interaction of Reeds, Hydraulics and River Morphology*, WRC Report Number 856/1/01, Water Research Commission, Pretoria.

James and Makoa (in press) *Conveyance Estimation for Channels with Emergent Vegetation Boundaries*

Järvelä (2004) Determination of Flood Resistance caused by non submerged body vegetation, *Journal of River Basin Management,* vol. 2, issue1, pp61-70.

Jordanova, A.A., James, C.S. and Birkhead, A.L. (2006) Practical Resistance Estimation for Flow through Emergent Vegetation, *Water Management*, 159, Issue WM3, September 2006, pp173-181. Institution of Civil Engineers, UK.

Jordanova, A.A. et al. (in preparation) Report on Water Research Commission Project K5/1405: Low flow hydraulics in rivers for environmental applications, Water Research Commission, Pretoria.

Kaiser, W. (1984) *Fließwiderstandsverhalten in Gerinnen mit durchströmten Ufergehölzzonen,* Wasserbau-Mitteilung der Technische Hochschule Darmstadt, Darmstadt, Germany, Vol. 23 in Nuding (1991)

Kan, K. and Nakai, M. (1993) Transversal sediment transport in straight sandy rivers with bank vegetation, *Proc. Sym. River Hydraul. & Environ.,* Japan Society of Civil Engineers, pp. 111-118 (in Japanese) in Tsujimoto and Shimizu (1994).

Kleynhans, C.J. (1999) The development of a fish index to assess the Biological Integrity of South African Rivers, *Water SA* Vol. 25 No. 3, July 1999, South Africa.

Kutija, V. and Hong, H.T.M. (1996) A numerical model for assessing the additional resistance to flow introduced by flexible vegetation, *Journal of Hydraulic Research*, Vol. 34, No. 1.

Lamouroux, N., Capra, H., Pouilly, M. and Souchon, Y. (1999) Fish Habitat Preferences in Large Streams of Southern France, *Freshwater Biology* 42 (1999) pp 673-687.

Makoa, M.J. (2001) Flow resistance in partially reeded channels. Research report for the degree of MSc in Engineering, University of the Witwatersrand, Johannesburg in James et al. (2001).

Masterman, R. and Thorne, C. R. (1994) Analytical Approach to Flow Resistance in Gravel-bed Channels with Vegetated Banks. In Kirkby, M.J. (Ed.) *Process Models and Theoretical Geomorphology,* John Wiley and Sons.

McCarthy, T.S. (1992) Physical and Biological Processes Controlling the Okavango Delta –A Review of Recent Research, *Botswana Notes and Records*, 24, 1992, pp57-86.

McCarthy, T.S. (personal communication) *Okavango River Data – Velocity Measurements.*

Mertens, W. (1989) Zur Frage hydraulischer Berechnungen naturnaher Flieβgewässer, *Wasserwirtschaft,* 79 (4) 170-179, ISSN 0043-0978 in Nuding (1991) and in Helmiö (2002)

Nadaoka, K. and Yagi, H. (1998) Shallow-water Turbulence Modelling and Horizontal Large-eddy Computation of River Flow, *Journal of Hydraulic Engineering*, May 1998, pp493-500.

Nagdi, F.I. and Sharpe, R. (2000) *The effect of bank vegetation on flow resistance in river channels*, Final Year Investigation Project Report, Dept. Civil Engineering, University of the Witwatersrand, Johannesburg in James et al. (2001).

Naot, D., Nezu, I. and Nakagawa, H. (1996) Hydrodynamic behaviour of partly vegetated open channels, *Journal of Hydraulic Engineering*, Nov 1996, pp625-633.

Nezu, I. and Onitsuka, K. (2001) Turbulent structures in partly vegetated open-channel flows with LDA and PIV measurements, *Journal of Hydraulic Research*, Vol. 39, No. 6, pp629-642.

Niehaus, B.H., Steyn, G.L. and Rall, J.L. (1997) Habitat Preference and Population Structure of the Rock Catfish (Austroglanis Sclateri) in the Sequnyane River, Lesotho, *Water SA*, Vol. 23 No. 4, October 1997, pp 405-410.

Nilsson, C. (1987) Distribution of Stream Edge Velocity along a Gradient of Current Velocity, *Journal of Ecology* (1987) 75 p513.

Nuding, A. (1991) *Fließwiderstandsverhalten in Gerinnen mit Ufergebüsch: Entwicklung eines Fließgesetzes für Fließgewässer mit und ohne Gehölzufer, unter besonderer Berücksichtigung von Ufergebüsch*, A PhD Thesis submitted to: Wasserbau-Mitteilung der Technische Hochschule Darmstadt, Darmstadt, Germany, Vol. 35 of 1991.

Nuding, A. (1994) Hydraulic Resistance of River Banks Covered with Trees and Brushwood, *2nd International Conference on River Flood Hydraulics*, 22-25 March 1994, York, England, Paper 37 pp 427-437, John Wiley and Sons.

Pasche, E., Rada,M., Töppel, M. and Kilic, A.(2004) *Fundamentals of Fluid Mechanics*, Wasserbau River and Coastal Engineering, Technische Universität Hamburg-Harburg, INTERNET. http://www.tu-harburg.de/wb/lmg/logo/pdflogo.gif

Pasche, E. and Rouvé, G. (1985) Overbank Flow with Vegetatively Roughened Flood Plains, *Journal of Hydraulic Engineering* Vol. 111 No. 9, September 1985.

Patel, V.C. (1965) Calibration of the Preston Tube and limitations on its use in pressure gradients, *Journal of Fluid Mechanics*, Vol. 23, Part 1, pp185-208.

Pavlovski, N.N. (1931) On a design formula for uniform flow movement in channels with non-homogeneous walls, *Transactions, All-union Scientific Research Institute of Hydraulic Engineering,* Leningrad, Vol. 3, pp 157-164 (In Russian).

Petryk, S., (1969), *Drag on cylinders in open channel flow*, PhD thesis, Colorado State University, Fort Collins, Colorado, USA in Desai and Chicktay (2005).

Rimkus and Vaikasas (2001) Model for Hydraulic Calculations on Naturalised Channels, *XXVIII IAHR Congress, Graz, Austria, Aug. 22-27, 1999.*

Rooseboom, A. (1992) *Sediment Transport in Rivers and Reservoirs – A Southern African Perspective*, WRC Report Number 297/1/92, Water Research Commission, Pretoria.

Sand-Jensen, K. and Pedersen, O. (1999) Velocity gradients and turbulence around macrophyte stands in streams, *Freshwater Biology*, 42, pp315-328.

Steffler, P. and Blackburn, J. (2002) *River 2D: Two-Dimensional Depth Averaged Model of River Hydrodynamics and Fish Habitat: Introduction to Depth Averaged Modelling and Users Manual* INTERNET.http://www.river2d.ualberta.ca/.

Stephan, U.C. (1993) *Ansätze zur Durchflussberechnung naturnaher Gerinne-Vergleichsutersuchungen*, Thesis, Inst. für Hydraul., Gewässerkunde und Wasserwirt., Tech. Univ. Wien, Vienna in Helmiö (2004).

Thornton, I., Abt, S.R., Morris, C.E. and Fischenich, J.C. (2000) Calculating shear stress at channel-overbank interfaces in straight channels with vegetated floodplains, *Journal of Hydraulic Engineering,* Dec 2000, pp929-936.

Tsujimoto, T. (undated) Unstable Phenomena Appearing in Open-channel Flows with Vegetation. In Wang, S.S.Y. (Ed.) *Advances in Hydro-Science and Engineering*, Volume 1, ISBN 0-937099-02-3.

Tsujimota, T. and Kitamura, T. (1992) *Experimental study on open-channel flow with vegetated zone along* sidewall, KHL progressive report '92, Hydr. Lab., Kanazawa University, Japan in Nadaoka and Yagi (1998) and Xiahoui and Li (2002).

Tsujimoto, T. and Kitamura, T. (1994) *Lateral Bed Load Transport Due to Organised Fluctuation of Flow in Open Channel with Vegetation Zone*, Unknown Source.

Tsujimoto, T. and Shimizu, Y. (1994) Flow and Suspended Sediment in a Compound Channel with Vegetation, *KHL Hydraulic Research '94*, Hydr. Lab, Kanazawa University, Japan.

Tsujimoto, T., Shimizu, Y. and Nakagawa, H. (1991) Turbulent flow an suspended sediment transport in vegetated sand bed channel, *Proc. XXIV IAHR Congress*, Madrid, Spain, pp81-88 in Tsujimoto, undated.

USBR (2001) Water Measurement Manual: A water resources technical publication, United States Department of the Interior, Bureau of Reclamation, Water Resources Research Laboratory, in co-operation with United States Department of Agriculture, INTERNET.http:///www.usbr.gov/pmts/hydraulics_lab/pubs/wmm/

Xiaohui, S. and Li, C.W. (2002) Large eddy simulation of free surface turbulent flow in partly vegetated open channels, *International Journal for Numerical Methods in Fluids*, 39, pp919-937, John Wiley and sons.

Yano, M., (1966), *Turbulent diffusion in a simulated vegetative cover*, PhD thesis, Colorado State University, Fort Collins, Colorado, USA in Desai and Chicktay (2005).